الجامعة الإسلامية العالمية ماليزيا
INTERNATIONAL ISLAMIC UNIVERSITY MALAYSIA
يونيورسيتي إسلام انتارابغسا ملايسيا

ANALYSIS OF SEMIACTIVE CONTROL POLICIES FOR PASSENGER VEHICLES

BY

SANY IZAN IHSAN

INTERNATIONAL ISLAMIC UNIVERSITY
MALAYSIA

2008

ANALYSIS OF SEMIACTIVE CONTROL POLICIES FOR PASSENGER VEHICLES

BY

SANY IZAN IHSAN

A thesis submitted in fulfilment of the requirements for the degree of Ph. D of Engineering

Kulliyyah of Engineering
International Islamic University
Malaysia

MAY 2008

ABSTRACT

Comprehensive comparison on quarter-car, half-car and full-car models were conducted to analyze the effect of using semiactive control policies, namely skyhook, groundhook and hybrid controls, in improving ride quality of passenger vehicle. Sprung mass acceleration, suspension deflection and tire deflection responses were analyzed for measurements of ride quality, rattle-space and road holding, respectively. Analyses in frequency-domain transfer function, time-domain transient state and time-domain steady state were conducted on each of the models. Peak-to-peak values in both time-domain analyses and settling time and steady state values in the transient state were compared to passive system. Results show that hybrid control policy gives significant improvements in most responses while at the same time it does not compromise road holding ability of vehicle. Skyhook control generally improves sprung mass responses while at the same time increases unsprung mass responses. On the other hand, groundhook control generally improves unsprung mass responses at the expense of sprung mass responses. Groundhook control also found to take longer time to settle in transient state response. Further quantitative comparison of responses on all three models shows that quarter-car model is unable to accurately represent responses in full-car model. Half-car model gives reasonable representation of full-car model in some of the states. Root mean square analysis is further conducted on a H-car 2-DOF system and the results show good agreement to the previous work on Q-car 2-DOF. As expected, the response exhibit similar behavior of the skyhook control.

ملخص البحث

تمت المقارنة الشاملة على موديل ربع سيارة، نصف سيارة، وسيارة كاملة في الدراسة لتحليل تأثيراستخدام طرق السيطرة شبه النشطة، مثل التعليق الفضائي، التعليق الأرضي والسيطرة الهجينة، في تحسين نوعية جلوس الركاب في مركبات نقل الأشخاص. تعجيل الكتلة النابضة، وانعكاس إنحراف التعليق وردود أفعال إنحراف الإطارات، كلها تم تحليلها لقياسات نوعية الركوب، وفضاء الحشرجة، وتحمل الطريق، بالتتابع. التحليل في مجال ميدان التردد، ومجال وقت حالة التغيير، ومجال وقت الحالة الثابتة، كلها تم العمل عليها لكل موديل. قيم الذروة في كل من تحليل تعميم الوقت ووقت الاستقرار وقيم الحالة المستقرة في حالة الحركة تم مقارنتها مع النظام السلبي. بينت النتائج بأنه طريقة السيطرة الهجينة تعطي تحسين ملحوظ في معظم ردود الأفعال بينما في نفس الوقت لم تعطي تسوية لقابلية تحمل الطريق للمركبة. بصورة عامة فإن مسيطر التعليق الفضائي قد حسّن ردود أفعال الكتلة النابضة بينما في نفس الوقت زاد ردود أفعال الكتلة غير النابضة. من جهة أخرى، فإن مسيطر التعليق الأرضي بصورة عامة قد حسّن ردود أفعال الكتلة غير النابضة على حساب ردود أفعال الكتلة النابضة. كما وجد أيضاً أن مسيطرالتعليق الأرضي بأخذ وقت أطول للاستقرار في رد فعل حالة الحركة. وأوضحت المقارنة الكمية لردود أفعال الموديلات الثلاثة أن موديل ربع مركبة كان غير قابلاً لتمثيل ردود الأفعال بصورة مضبوطة كما هو الحال في المركبة الكاملة. موديل نصف المركبة أعطى تمثيل معقول لموديل المركبة الكاملة في بعض الحالات. كما تم تحليل المعدل التربيعي الجذري على نظام نصف مركبة 2- دوف والنتائج أوضحت توافقاً مع النتائج السابقة على ربع مركبة 2- دوف. وكما متوقع، فإن ردود الأفعال أعطت نفس التصرف لمسيطر التعليق الفضائي.

APPROVAL PAGE

The dissertation of Sany Izan Ihsan has been approved by the following:

_____
Waleed Fekry Faris
Supervisor

_____
Ahmed Aly Ibrahim Shaaban Ashour
Co-Supervisor

_____
Mehdi Ahmadian
Co-Supervisor

_____
Mohammed Ataur Rahman
Internal Examiner

_____
Mohd Jailani Mohd Nor
External Examiner

_____
Hishamuddin Jamaluddin
External Examiner

_____
Nasr Eldin Ibrahim Ahmed
Chairman

DECLARATION

I hereby declare that this dissertation is the result of my own investigations, except where otherwise stated. I also declare that it has not been previously or concurrently submitted as a whole for any other degrees at IIUM or other institutions.

Sany Izan Ihsan

Signature …… Date ……..

INTERNATIONAL ISLAMIC UNIVERSITY MALAYSIA

DECLARATION OF COPYRIGHT AND AFFIRMATION OF FAIR USE OF UNPUBLISHED RESEARCH

ANALYSIS OF SEMIACTIVE CONTROL POLICIES FOR PASSENGER VEHICLES

Affirmed by Sany Izan Ihsan.

……. ……..
Signature Date

To my beloved wife, Suriza Ahmad Zabidi,

My lovely children, Muhammad, Zubair, Muaz and Sofwan,

For their love and company

To my father, Ihsan Hj Awang and mother, Chong Kee Yin @ Aisah Abdullah

May Allah bless and grant upon them mercy

In this world and hereafter…

ACKNOWLEDGEMENTS

First and foremost, gratitude and appreciation is for Allah, the Most Merciful and Most Compassionate for granting me a precious opportunity to complete this work and granted me health and strength for the realization of this endeavor.

I would like to gratefully thank my supervisor, Dr. Waleed Fekry Faris for his scholarly guidance and tireless effort in assisting me in this very work. Truly this work shall not be completed without his continuous encouragement and support.

I would also like to thank to my co-supervisor, Prof. Dr. Ahmed Ali Shaaban Ashour for his motivation and guidance in keeping me going with the work and always making himself available for any assistance.

My sincere thank to my co-supervisor, Prof. Dr. Mehdi Ahmadian for his guidance and support, especially while hosting me as a visiting scholar at the Virginia Tech. Indeed the short visit was very valuable to this work and a big portion of it was as the outcome of the visit. Of course I will never forget the warm reception and helpful assistance from colleagues at the Virginia Tech. throughout the four months visit. Among all are Emmanuel Blanchard, Florin, Benny, Mohammed, Brendan and many more.

Not to forget also my colleagues at the Kulliyyah of Engineering, IIUM especially Fadly Jashy Darsivan for offering to hear and share all problems and challenges of PhD student. Also to all others, whether academic and non-academic staff for assistance and for keeping asking me on my completion of study.

This work would not be possible without the scholarship provided by the Government of Malaysia and International Islamic University Malaysia throughout the study period. Also I must mention about the special fund granted by IIUM for me to visit the Virginia Tech.

Of course, I owe the greatest debt of gratitude to my beloved wife, Suriza Ahmad Zabidi, for her patience, support, understanding, assistance and prayer throughout my study. It would surely be impossible for me to complete this work without her contribution. Also gratitude to my sons – Muhammad, Zubair, Muaz and Sofwan for making my life very exciting and lively. Not to forget my deepest gratitude to my beloved mother, Aisah Abdullah and father, Ihsan Hj. Awang for their love and prayers.

TABLE OF CONTENTS

LIST OF TABLES

LIST OF FIGURES

LIST OF ABREVIATION

CG	Center of gravity
cpm	Cycle-per-minute
-DOF	Degree-of-freedom
ER	Electro-rheological
ERF	Electro-rheological fluid
F-car	Full-car
H-car	Half-car
ISO	International Organization for Standardization
LTI	Linear time invariant
MR	Magneto-rheological
MRF	Magneto-rheological fluid
m_s	Sprung mass
m_{us}	Unsprung mass
PSD	Power spectral density
PTP	Peak-to-Peak
Q-car	Quarter-car
RMS	Root mean square
SAE	Society of Automotive Engineers
t_s	Settling time

LIST OF SYMBOLS

ζ_s	Damping Ratio
r_k	Spring Ratio
ω_n	Natural Frequency

CHAPTER ONE

INTRODUCTION

1.1 OVERVIEW

By definition, Ride Quality is degree to which the whole subjective experience (including the motion environment and associated factors) of a journey or ensemble of journeys by vehicle is perceived and rated as favorable or unfavorable by passengers or operators (International Organization for Standardization [ISO] 5805, 1997). Its primary concern is on sensation or feel of driver or passenger in the environment of a moving vehicle. In a simple word, ride is considered as comfort when the occupant is comfortable riding the vehicle. Vehicle ride quality is strongly related to the pitch and vertical motions of the vehicle.

Vehicles traveling at high speed usually experience a broad spectrum of vibrations. These vibrations are transmitted to passengers either by tactile, visual or aural paths (Gillespie, 1992). Ride is usually dealing with the tactile and visual vibrations, while the aural vibration is categorized as noise. Alternatively, spectrum of vibrations may be categorized by frequency range and specified as ride for frequency range of 0 to 25 Hz and noise between 25 to 20000 Hz.

Ride quality is affected by various designs and operating parameters in a highly complex manner, including high frequency vibrations, body booming, body roll and pitch motion, vertical motion by spring in the suspension system and frequency vibration transmitted from the road input excitations. Other factors include high frequency vibrations or noise induced by aerodynamic forces as well as the engine and driveline. Ride quality can also be influenced by vehicle interior design

such as seat comfort, temperature, ventilation, location of features etc. Among these factors, the major source of vibration of a vehicle that affects ride quality is the road irregularities which are transferred to the passenger through the tires and suspension system.

Generally vibrations affecting ride quality can be categorized into two parts; low frequency vibrations and high frequency vibrations. The range differs from one researcher to another, but is generally agreed that the low frequency is less than around 25 Hz. High frequency vibrations may be excited by either impacts originating at the wheels and transmitted through the suspension, or alternating forces by unbalanced rotating masses in the engine (Janeway, 1948). This vibration may be eliminated by having proper cushioning of impact and accurate balancing of high speed rotating parts. However, low frequency vibrations, which mainly due to the road irregularities posed more significant effect on the ride quality of vehicle. This is due to it being close to the natural frequencies of vehicle. Generally the natural frequency of sprung mass (mass of the vehicle, excluding the tire and its components) is about 1 Hz, the natural frequency of unsprung mass (mass of the tire and its components) is between 8 to 10 Hz and there exist an intermediate natural frequency between 6 to 20 Hz (Janeway, 1948).

To eliminate this low frequency vibrations effect on passenger, there are several components of interest that become the focus of improvement; tire, suspension and passenger seat. Tire technology has come to its relative stagnant, as not much improvement can be made as far as ride quality is concerned. Limited improvements can be made on the seat but at the expense that the vehicle as a whole having to face the vibrations, which could cause some components failure. The focus of most researchers in this area is thus looking towards improving the suspension system in

order to eliminate the vibrations. Several researchers have proposed the concept of active control system, which claimed to eliminate the inherent problem of passive suspension system – that is the conflicting parameters for ride and handling. However, this new system is by far still not free from any shortcomings.

1.2 RIDE QUALITY CRITERIA

Over the years, various researches were conducted to identify some generalized criteria in ride quality, which is commonly called as ride comfort criteria. Several approaches have been proposed. One of them is Janeway's comfort criterion, which is described in the *Ride and Vibration Data Manual J6a* of the Society of Automotive Engineers (SAE) (1965). Figure 1.1 defines the acceptable amplitude of vertical vibration as a function of frequency and it could be divided into three parts:

1. Frequency range of 1-6 Hz - peak jerk < 12.6 m/s^3 (496 $in./s^3$)
2. Frequency range of 6-20 Hz - peak acceleration < 0.33m/s^2 (13 $in./s^2$)
3. Frequency range of 20-60 Hz - peak velocity < 2.7mm/s (0.105 in./s)

It should be noted that this criterion is based on vertical sinusoidal vibration of a single frequency data. There is no established basis to evaluate the effect when two or more components of different frequencies are present. All data that were used to establish the boundaries were obtained with test subjects standing or seating on a hard seat (Wong, 2003).

ISO has developed and adopted a general guide for defining human tolerance to whole-body vibration, ISO 2631 (1997). This guide defines three distinct limits for whole-body vibration in the frequency range of 1-80 Hz, such as:

1. Exposure limits, which are related to the preservation of safety and should not be exceeded without special justification.

2. Fatigue or decreased proficiency boundaries, which are related to the preservation of working efficiency and are applied to such tasks as driving a road vehicle of a tractor.
3. Reduced comfort boundary, which are concerned with the preservation of comfort and are related to such functions as reading, writing and eating in a vehicle.

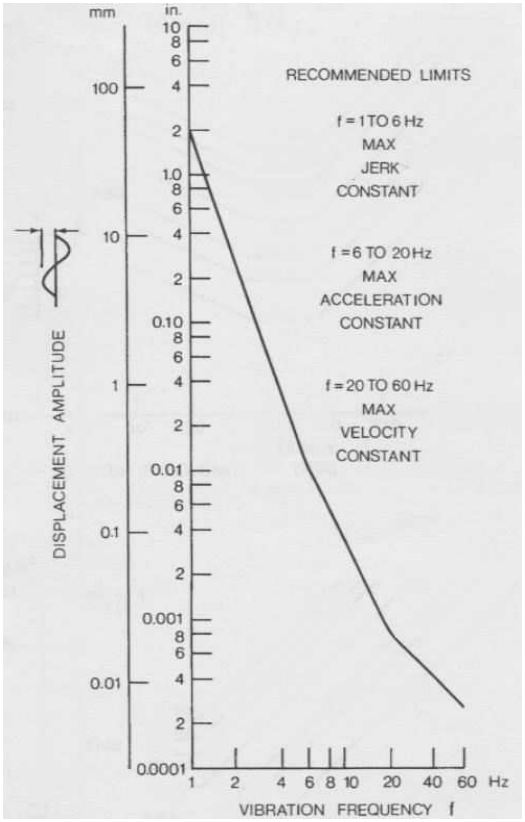

Fig. 1.1: Vertical vibration limits for passenger comfort proposed by Janeway (Wong, 2003).

Figure 1.2 shows the fatigue or decreased proficiency boundaries: (a) vertical vibration direction and (b) transverse or lateral direction which is defined in terms of root-mean-square values (RMS) of acceleration versus frequency for various exposure times. It can be observed that as exposure times increases, the boundary lowers.

Generally, the exposure limits for safety (or health) can be obtained by raising the boundaries by a factor of 2 and for the reduced comfort boundaries by a factor of 3.15.

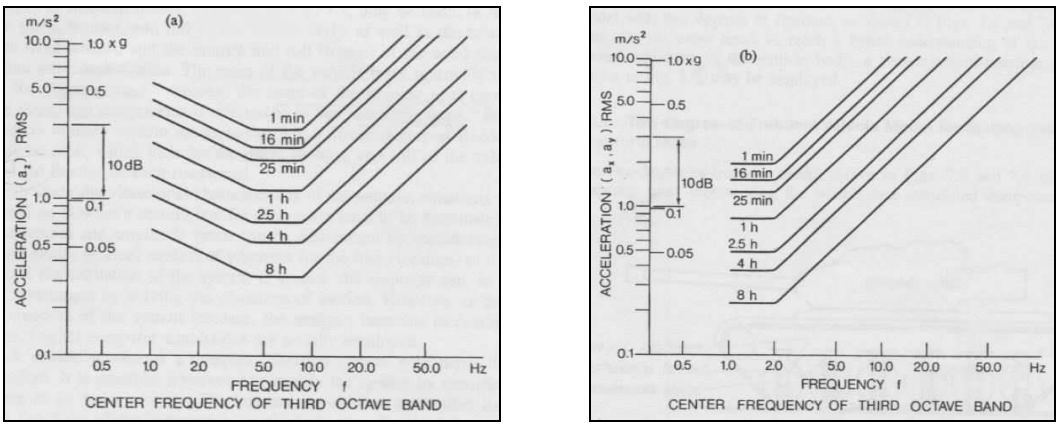

a) vertical direction b) transverse direction

Fig. 1.2: Limits of whole-body vibration for fatigue or decreased proficiency for various exposure times, as recommended by ISO (Wong, 2003).

As for motion sickness, ISO 2631 (1997) suggest that the percentage of people who may vomit is proportional to the Motion Sickness Dosage Value (MSDV). This value is calculated by the square root of the integral of the square of the frequency weighted z-axis acceleration. A severe discomfort boundary and a reduced comfort boundary for various exposure times in the frequency range of 0.1-1 Hz has been recommended by ISO.

Another proposed parameter in evaluating human response to vibration is the absorbed power, which is the product of vibration force and velocity transmitted to the whole body. It is basically a measure of the rate at which vibration energy is absorbed by human. This parameter has been used mainly in military vehicle research and it has been reported that the tolerance limit is defined as at 6 W absorbed power at the driver's position (Wong, 2003).

In short, extensive researches have been conducted to better understand on how to measure ride quality. However, they is no single, generally accepted approach. Several ride comfort criteria have been suggested but all are derived from various limitations in data and assumptions and far from the actual situation in vehicle vibration and motion.

1.3 VEHICLE SUSPENSION SYSTEM

Suspension system separates the axles from vehicle chassis, so that any road irregularities are not transmitted directly to the driver and the load on the vehicle. Suspension system affects both ride quality and handling performance of vehicle. As a matter of fact, ideal ride quality and handling performance pose a conflicting design requirement of vehicle suspension. While a lightly damped soft suspension yields good shock performance, hard suspension with high damping is desirable to achieved good handling. Active suspension system has been introduced as a promising alternative to overcome this traditional design limitation.

Suspension systems can be classified into passive system and active system, according to the existence of control input. The conventional passive suspension system consists of a typical spring and damper. It is the oldest system built by the principles outlined by Olley (1934) and gradually improved. Most vehicles used nowadays are using this system. Active suspension system can be further classified into two types – a semiactive system and a fully active system, according to the control input mechanism. While the fully active suspension system produces the control force through a separate hydraulic/pneumatic unit, the semiactive suspension system uses a varying damping force as control force (Hong *et al.*, 2002).

Semi-active and fully active systems are relatively new systems introduced as an attempt to overcome the shortcomings existed in the passive system. An optimal fully active suspension system is expected to be able to (Barak, 1992):

1. Optimize between ride comfort and road handling.
2. Control car attitude changes due to braking (dive), accelerating (lift) and cornering.
3. Maintain optimal system response independent of vehicle loads.
4. Faster system response time.

However, the improved performance is directly related with increased in hardware complexity, higher costs and diminished reliability. Semiactive suspension system was therefore introduced as a compromise between passive system and fully active system. In general, it improves ride without compromising the handling of vehicle as compared to passive system and at the same time less complexity and less costly than active system. Semiactive suspension system is the main focus in this work and the result is compared to the conventional passive system.

There are generally two types of semiactive damping system, namely electro-rheological (ER) damper or magneto-rheological (MR) damper. Magneto-rheological fluid (MRF) is used in MR damper. This MRF usually is a fluid such as hydrocarbon oil filled with randomly dispersed micron-sized magnetically polarizable iron. Additives usually are added to promote homogeneity and to prevent gravitational settling of the irons. This MRF exhibit a change in rheological properties from a free-flowing fluid state to a semi-solid state upon application of an external magnetic field. This change can be varied according to the strength of the applied magnetic field. The process is also reversible that upon removal of the magnetic field, the fluid will revert back to its original free-flowing state.

Similarly, ER damper uses electro-rheological fluid (ERF) with the same concept of the MR system. However, for automotive suspension system application, there are many drawbacks to ER fluids, including relatively small rheological changes and extreme property changes with temperature. Although power requirements are approximately the same (Carlson *et al.*, 1995) MR fluids require only small voltages and currents, while ER fluids require relatively larger voltages and very small currents.

The performance of a suspension system is usually characterized by the ride quality, the handling performance of the vehicle, the size of the rattle space or suspension working space and the dynamic tire force (Hong *et al.*, 2002).

1.4 SCOPE OF THE THESIS

Several works conducted by researchers at the Advanced Vehicle Dynamics Laboratory (AVDL), Virginia Tech. have shown that several variations of semiactive suspension systems provide some promising improvements to the ride quality without compromising vehicle handling (Ahmadian, 1997a & 1997b and Koo and Ahmadian, 2001).

However most of the work there as well as other places is limited to only the simpler quarter-car (Q-car) model and employing mostly frequency-domain transfer function response. There has been no attempt to extend the analysis using more complex full-car model and to use other analysis such as the time-domain steady state and transient state responses.

Q-car model, while being simpler to modeled and analyzed is limited to only being able to simulate vertical deflection of a car. Thus the effect of pitch and roll is absent and impossible to be analyzed, even though there are several attempts to

extrapolate the Q-car response to that effect, such as Blanchard (2003). It is therefore in the interest of the area of research to find out whether the response in simpler model is in good agreement with the more complex and accurate model.

Frequency domain analysis has been used in this area for so many years. Analyzing responses in this domain, which assume input signal as sinusoidal function with varying frequency, would provide information on how much power is transferred from the input to output over the span of input frequencies. However, analyzing response in time domain provides several other essential information on system performance. Transient state for example would show how fast the system response, how much it overshoot from the input value and how long it takes to reach steady state. An ideal system is to give response to an input fast, with low overshoot and takes short period of time to reach steady state condition. Steady state response to sinusoidal input would provide the peak to peak value of the steady state condition of the system. It would be important to identify this value when the system is at resonance, i.e. when the input frequency is at the same value as the natural frequency of the system.

Thus, this work is intended to fill in the hole to further analyze semiactive systems with half-car (H-car) and full-car (F-car) models and employing all frequency-domain and time-domain analyses. Furthermore, comparison of responses of various models - quarter-car (Q-car), H-car and F-car, can be conducted to analyze for any correlation.

Apart from that the laboratory was also working on analysis of total system response in the frequency span (Blanchard, 2003). The root-mean-square (RMS) value is analyzed with the assumption that reducing RMS of a system would increase the ride quality of the vehicle. The initial results based on Q-car model shows satisfactory

improvement in using semiactive control policies when compared to passive. Thus this work intended to extend the work to H-car model.

1.4.1 Research Objectives

The objectives of the study are:

1. To simulate and analyze several variations of semiactive suspension system models – skyhook, groundhook and hybrid, using various analyses – transient state, steady state and transfer function responses.
2. To use a set of performance criteria to compare between the different semiactive control policies and passive system.
3. To compare between several vehicle models – from a simple Q-car 2 degree-of-freedom (DOF) to a more complex F-car 7-DOF.
4. To analyze a H-car 2-DOF semiactive model using RMS value analysis.

1.4.2 Research Methodology

The research begins with literature survey on related works. Generally the works can be categorized into three areas – human response to vibration, vehicle response to excitations and ride quality testing. The main purpose of this review is to get the whole picture of research activities in the area.

In human response to excitation area, extensive review on existing study is conducted. Generally these work consist of three major activities, that is subjective testing works, which employs human subject as to rate the response to certain comfort level criteria, objective testing works, which uses theoretical analysis and mathematical model of vehicle and human, and related them to a certain ride quality criteria, and the last one is a combination of subjective and objective testing.

In vehicle response to excitations area, existing mathematical models proposed by various researchers are reviewed. The models can generally be categorized in three ways; the degree-of-freedom (DOF) of the model, whether it is a quarter-car one-dimensional (1-D), half-car two-dimensional (2-D) or full-car 3-dimension (3-D) model, and the system used, whether the conventional passive system or active control system. Focus is given to the work on passive system and semiactive control policies.

From the literature review, the work proceeds with detail discussion on the models and systems to be used for analysis. As will be shown, this work involves all model types – Q-car, H-car and F-car. The performance of semiactive control policies – skyhook, groundhook and hybrid of each model type are compared to the conventional passive system. Extensive comparison study on the responses between these passive system and semiactive control policies, both in time-domain (transient state and steady state) and frequency-domain is presented.

Additionally, an almost a separate analysis from the others altogether is conducted on H-car 2-DOF model. This RMS analysis is actually a direct continuation from a work done at the Virginia Tech., USA.

1.4.3 Layout Of The Thesis

In chapter 2, related literature review is presented. The review is grouped into three parts, namely human response to vibrations, vehicle response to excitations, and ride quality testing as already explained before.

In chapter 3, general concept of modeling analysis is presented. A typical Q-car passive system and semiactive control policies are derived and presented. Then, models of Q-car, H-car and F-car to be used in Chapters 4 to 7 are presented and their

equations of motion are derived. Detail discussion on the types of analyses and performance criteria is also presented.

In chapters 4, 5 and 6, comparison of results between all models is presented for frequency domain, transient state and steady state responses, respectively. Sprung mass vertical acceleration, suspension and tire deflections responses are compared between all models. The pitch angular acceleration response is also compared between the H-car and F-car model. Comparisons are made between passive system, which is considered as reference, and the various semiactive control policies for all three models, model type as well as input types.

In chapter 7, an analysis on RMS values for H-car 2-DOF system is presented in details. This can be considered as a stand alone chapter since the analysis and approach used is totally different from the previous chapters.

Finally, conclusion and recommendation for future work is presented in chapter 8.

CHAPTER TWO

LITERATURE REVIEW

2.1 INTRODUCTION

Researches in ride quality can generally be categorized into three main areas, namely human response to vibration, vehicle response to excitation, and ways of testing and evaluating ride quality. Another area that directly related is road profile since road irregularities are considered as the main source of excitation to vehicle. Literature review presented here however focuses only on the first two areas. It is interesting to note that while passenger cars are one of the fastest growing industries, no single review on ride quality to this category of vehicles is currently exists. Articulated vehicles for example were surveyed by ElMadany *et al.* (1979) while review on ride quality for heavy vehicles was conducted by Jiang *et al.* (2001).

2.2 HUMAN RESPONSE TO VIBRATIONS

In general, human response to vibrations is quite complex. For example, frequency in the range of 30 to 50 cpm (less than 1 Hz) has been reported to produce motion sickness, the visceral region of the body objects to frequencies between 300 and 400 cpm (5 to 7 Hz) and the head and neck regions are especially sensitive to vibrations of 1000 to 1200 cpm (18 to 20 Hz) (Riley, 2002). Furthermore, the response varies from one individual to another. This is mainly due to the distinctive features of every human being and the different in sensitivity.

Although various research findings show variation in the exact value, it is found that vibration frequency and magnitude play the most important criteria in ride

quality. For example in vertical acceleration, an increase in the human sensitivity is observed in the frequency range of 4 to 6 Hz (Jiang *et al.*, 2001). Research in this area had started longtime back and still growing, which opens the way to more active and creative research.

Goldman (1948) divided the human response level into three thresholds:

1. Threshold of perception (level 1) – detectable using sensory measurement.
2. Threshold of discomfort (level 2) – Stimulus is intense enough so that the subject feels a tinge of discomfort or unpleasantness due to pain, muscular effort or any other source.
3. Threshold of tolerance (level 3) – the subject is unwilling to tolerate the stimulus further due to pain, extreme discomfort or merely lack of desire to cooperate.

Several tests were conducted with the subjects were either standing, seated or lying down on a vibrating body with the direction of vibration along any of the three principal body axes for the duration of exposure of five to ten minutes. Results showed that differences due to direction of application of the vibration were smaller than statistical variations which therefore are not significant. Therefore data were grouped without directional factor with the assumption that direction was secondary importance.

Pradko (1965) intended to develop a technique to identify and measure whole body human response to vibration and to describe properly the performance potential of man in vibrational environment and to predict his response. The work proposed that human vibration must be defined in terms of several factors:

1. the nature of the forcing function,
2. the source of vibratory energy,

3. the path between the source, the human, and the posture,
4. and characteristics of the receiver (subject)

The hypothesis of the research was that measurable changes in human equilibrium are caused by input vibration and such changes may appear in physical performance capabilities – ability to concentrate, ability to communicate and visual acuity. Subjects were evaluated from eight different experimental positions – standing (erect and knee bent), seated (relaxed and braced), reclining and walking (normal walk, fast walk and running). The experiments lead to several conclusions:

1. pitch vibration affects human tolerance significantly more than do roll and vertical vibration,
2. pitch tolerance does not change appreciably with increased frequency,
3. whole body tolerance of random vibration in the vertical mode is significantly greater than sinusoidal tolerance,
4. whole body vibration endurance is greatly increased for vertical motion when space orientation is removed
5. when the vibratory path is applied completely or partially to the head, the vibration tolerance is decreased to a minimum level,
6. acceleration tolerance is greatly influenced by the direction and duration of the force vector and the measurement technique employed to record effects.

Pradko *et al.* (1966) discussed whole body human response to mechanical vibration below 60 Hz. The response was determined through measurement of input condition using the concept of absorbed power introduced by Pradko and Lee (1966) and further discussed by Lee and Pradko (1968). The work concluded that

1. human response displays linear characteristics to vibration under physical equilibrium,
2. transfer function statements accurately describe human response to random vibration, and
3. absorbed power describes human response qualitatively and is sensitive to time.

Corbridge and Griffin (1986) provided fundamental data of seated subjects exposed to vertical and lateral vibration in the frequency range of 0.5 to 5.0 Hz. Three experiments were conducted. The first one was to determine equivalent comfort contours for male and female subjects using sinusoidal vertical vibration in the range 0.5 to 5.0 Hz. Results showed that female are more sensitive to vibration at 3.15, 4.0 and 5.0 Hz for 0.75ms^{-2} RMS reference and at 5.0 Hz for 0.25 ms^{-2} RMS reference, and increasing sensitivity to vibration acceleration at frequencies above 2 Hz.

The second experiment involved the determination of a comfort contour using octave bands of random vibrations centered on 0.5, 1.0, 2.0 and 4.0 Hz. The results indicated that subjects are more sensitive to random motion than sinusoidal motion, but not very significant different with an average of 7% lower.

The last experiment was to determine equivalent comfort contours for lateral vibration using sinusoidal vibration in the range of 0.5 to 5.0. The results showed that the maximum sensitivity to lateral vibration occurred in the range 1.25 – 2.0 Hz.

Corbridge and Griffin (1991) were concerned with the effect of vertical vibration on writing and holding cup ability, simulating the passengers of railway trains activities. The reference motion used was an octave band of random motion centered on 1 Hz, magnitude of 0.63 m/s^2 rms and duration of 20.5 s. Each test motions consisted of the same octave bandwidth but with an added sinusoidal

vibration component. From the test it was concluded that by adding sinusoidal vibration of duration 10s and frequency range of 3.15 to 8 Hz, significant increase in writing difficulty and writing performance were observed. This is fairly consistent with the frequency weightings defined by ISO 2631 and BS 6841 which indicate maximum sensitivity to vibration acceleration in the frequency range of 4 to 8 Hz. Furthermore, adding sinusoidal vibration especially from 3.15 to 5 Hz produce considerable difficulty in holding a cup of liquid with 4 Hz gives the most sensitive to vertical vibration.

Demic *et al.* (2002) attempted to investigate human behavior under random vibrations and observed that:

1. In the vertical vibration, subjects are very sensitive to low-frequency random vibration (less than 1 Hz), less sensitive to narrowband random vibration (1.25 Hz to 5 Hz) and least sensitive to frequency above 5 Hz,
2. in the fore and aft vibration, subjects are very sensitive to vibration below 0.8 Hz, less sensitive to the frequency range of 1 – 5 Hz and least sensitive to frequency above 5 Hz, and
3. subjects are more sensitive to random, multi-directional vibration than one-directional and equivalent comfort curves for multi-directional random vibrations are 15 to 20 percent lower than for one-directional vibrations.

Other works worth mentioning are by Donati *et al* (1983) which developed an experimental technique known as the *floating reference* to compare the subjective response of seated subjects to sinusoidal vibrations in the range 1 to 10 Hz, and Fairley and Griffin (1988) which introduced a function relating horizontal ($\boldsymbol{H}$) and vertical ($\boldsymbol{V}$) components of vibration in the form of $\left(\boldsymbol{H}^{\boldsymbol{n}}+\boldsymbol{V}^{\boldsymbol{n}}\right)^{1/\boldsymbol{n}}$, to predict the

discomfort produced by vibration in the fore-and-aft, lateral and vertical axis directions.

Guignard and Irving (1979) have shown that vibration affect human activities such as visual ability and in making precise movements. At low frequencies, the eye reflex and compensating movement of the head can reduce the effect of the vibration. However, it is found that pursuit eye movement is attenuated at frequencies greater than 2 Hz and compensating movement of the head at frequencies greater that 3 Hz.

Ride comfort is generally decreases with the magnitude of vibration. Jones and Saunders (1972) showed that when the magnitude of vibration was less than 3 m/s^2, there was no significant change in the equivalent comfort contours. As the magnitude increases, the test subjects were concerned about effects such as loss of control and dangerous vibration. The test also has found that random vibration signal produced slightly greater discomfort than harmonic motion.

In studying the effects of shock and vibration to human health, Guignard and McCauley (1982) have found that a group of drivers experienced an increment in heart rate variability when drove continuously for more than 5 hours. It was also found that human balance was impaired during and after exposure to vibration at frequencies below 1 Hz or above 15 Hz. In studying the effect of long-term exposure of whole-body vibration, results of work from Rakheja and Boileau (1993) have shown that the most frequently reported disorders related to vibration exposure are back problems, digestive and reproductive disorders and nervous disorders.

2.3 VEHICLE RESPONSE TO EXCITATIONS

Research in vehicle response can be conducted either experimentally or through model simulation using computer and software packages.

Stone and Demetriou (2000) have described a detail derivation of a F-car vehicle model with 6-DOF using the Newtonian approach. This model is able to simulate the effect of suspension (ride) as well as braking and steering (handling) in all three translational motions (vertical, forward and side), pitch, roll and yaw (heave) directions. General assumptions in deriving the model, which are common assumptions, are provided, that are: the vehicle mass may be lumped into a single mass which is referred to as the sprung mass, m_s, the vehicle center of gravity is located above the roll and pitch centers, the vehicle suspension springs will not be allowed to *top out* during maneuvering; the suspension springs will always be in compression, aerodynamic lift and drag force, and tire rolling resistance are neglected, the vehicle remains grounded at all times, i.e. the four tires never loose contact with the ground, and the deflections in the pitch and roll planes are small, and may be simplified with small angle approximation.

Gillespie and Karamihas (2000) studied Q-car model under effect of road roughness and found that Q-car models to be adequate for discriminating the roughness of the road on a scale that correlates well to the public judgment of its severity.

Soliman *et al.* (2001) aimed at introducing a solution of the vehicle dynamics problem by studying the effect of various types of suspension element on the vehicle suspension system performance. Mathematical model of conventional Q-car model, Q-car model with twin spring system, Q-car fully active system and H-car conventional model were derived. Objective testing experiment was conducted using a test rig to verify the theoretical analysis. It can be concluded that:

1. load carrying capacity of a vehicle rear suspension can be solved using stiff suspension spring system or a twin spring suspension system,

2. a fully active suspension system can improve the vehicle performance criteria significantly but at a high cost,
3. the tire damping has a very small effect on the vehicle ride comfort,
4. when the tire stiffness parameter is increased, the systems have higher wheel resonance peaks in the dynamic tire load response,
5. the predicted values of the suspension working space and vertical acceleration were 8 – 10% lower than the measured, and
6. the peak resonance for the body acceleration and suspension working space at a certain frequency was similar to that obtained theoretically.

Several works involving semiactive damper are reviewed and presented here. Barak (1989) conducted analytical and numerical comparison study on passive, on-off semiactive and active linear feedback suspension systems. Three models were used for the comparison, which are Q-car one degree-of-freedom (DOF), Q-car 2-DOF, and F-car 7-DOF. Both transient state time-domain and frequency domain (root mean square (RMS) and peak values) are presented. The ride design criteria for the analyses were the passenger seat acceleration response, the suspension space requirement and the road holding. To meet these criteria, Performance Index (PI) was introduced for full vehicle model.

$$\mathrm{PI} = E\left[r_{ps} \sum_{i=1}^{4} \Delta_{ps_i}^2 + r_{ss} \sum_{i=1}^{4} \Delta_{ss_i}^2 + r_p a_p{}^2 + r_u \sum_{i=1}^{4} F_{tss_i}^2 \right] \tag{2.1}$$

where r_{ps} is the weighting factor for primary suspension deflection, Δ_{ps} which is the deflection of the unsprung mass, m_{us} relative to the road input, r_{ss} is the weighting factor for secondary suspension deflection, Δ_{ss} which is the deflection of the unsprung mass relative to the sprung mass deflection, r_p is the weighting factor for passenger

seat acceleration, a_p, and r_u is the weighting penalty factor related to the total force, F_{tss} acting at secondary suspension.

The results indicated significant improvements obtained in both active and semiactive dampers in the sprung mass acceleration. However significant increases in the suspension and tire deflections were observed in both active and semiactive.

Sun, Zhang and Barak (2002) investigate the effect of so-called dynamic index in pitch (DIP), $k^2/a \cdot b$, mass ratio, m/m_u, weight distribution, W_F/W_R and flat ride tuning, k_{SR}/k_{SF} on ride quality of a 4-DOF model. k is the radius of gyration in pitch, a and b are the longitudinal distance from vehicle center of gravity (CG) to the front wheel center and rear wheel center respectively, m and m_u are the sprung mass and unsprung mass, respectively, W_F is the front part vehicle weight, W_R is the rear part vehicle weight, k_{SR} and k_{SF} are the front and rear suspension stiffness, respectively.

Lagrange's method is used to derive the equations of motion of the model. Step input is used to obtain transient state, time-domain responses for all performance criteria, which are the sprung mass bounce and pitch motion (displacement and acceleration), front secondary suspension force, front shock absorber force, and front and rear wheel hop frequencies. The work concluded that the optimized ride is obtained when the dynamic index in pitch equal 1.0, the mass ratio equal 10 and weight distribution equal 1. The rear suspension stiffness should be higher than the front to reduce pitch motion of vehicle body, which was said to be more disturbing to passenger than the bounce motion.

Barak *et al.* (2004) further investigated the effect of Chassis Design Factor (CDF) on ride quality of a full-car 7-DOF vehicle model. This CDF includes stabilizer

bars, suspension stiffness, Dynamic Index in Pitch (DIP) and mass ratio. Again, transient state, time-domain response of step input function is used in the analysis. Each of the CDF is varied to observe its effect to the sprung mass (bounce, pitch and roll) acceleration and displacement responses. The work concludes that anti-roll bar has no significant effect on the ride characteristics. The work recommends the spring stiffness values to be chosen such that the natural frequencies of the system are within the *comfort range,* which is 1 to 1.2 Hz for bounce, 1.2 to 1.5 for pitch and 1.5 to 2.0 for the roll motion. The DIP value is recommended to be around 1.0 and mass ratio to be about 9 to 10 so that the wheels hop frequencies to be in the range of 10 to 12 Hz, which is within the road holding range.

Ahmadian *et al.* (1997) studies the behavior of semiactive suspensions subjected to pure-tone input. A Q-car 1-DOF model is used to compare the response of conventional passive and optimal passive dampers to two different types of semiactive dampers, namely on-off (bang-bang) and continuously variable semiactive dampers. This model can effectively analyze the effectiveness of semiactive dampers at cab and seat suspensions of heavy on-highway vehicle. The on-off semiactive control policy, which commonly known as *skyhook* policy basically assume a damper with its damping can be switched between low-state and high-state. The control policy is based on:

$$\begin{aligned} v_1 \times v_{12} \geq 0 &\rightarrow \textit{high-state} \\ v_1 \times v_{12} \leq 0 &\rightarrow \textit{low-state} \end{aligned} \tag{2.2}$$

where v_1 represents the absolute velocity of the sprung mass and v_{12} is the relative velocity across the damper. The low-state damping is often selected to be one-tenth of the high sate damping. This equation implies that high-state damping is desired when the relative velocity across the damper and sprung mass velocity have the same sign.

Otherwise, a low-state damping is needed in order to provide a better compromise between the ride comfort and vehicle handling.

For continuous skyhook policy, as the name suggested, damping is adjusted within the allowable range according to the absolute velocity of the sprung mass. The control policy is based on:

$$\begin{aligned} v_1 \times v_{12} \geq 0 \ &\rightarrow \ F = C\, v_1 \\ v_1 \times v_{12} \leq 0 \ &\rightarrow \ F = C_{\min} v_1 \end{aligned} \tag{2.3}$$

The transmissibility ratio magnitude and phase for the four dampers are compared and analyzed. The results show that traditional performance compromise between controlling resonance peak and isolation at higher frequencies can be significantly improved by using semiactive dampers.

Ahmadian (1997b) further analyzes semiactive control schemes for multi degree of freedom system, namely H-car 2-DOF and Q-car 2-DOF. Three different on-off semiactive schemes which are skyhook, groundhook and hybrid, were introduced and analyzed against the conventional passive system by comparing the transmissibility ratio of the displacement and acceleration. Similar control policy was used as in the previous work (see Eq. 2.5). It is observed that skyhook scheme improve body resonance response but at the expense of increasing the wheelhop. On the other hand, groundhook scheme provide better control of wheelhop at the expense of increasing body resonance. A hybrid, which is actually a combination of both skyhook and groundhook schemes turns out to provide better control in all.

ElMadany and El-Tamimi (1990) analyzes several nonlinear passive and semiactive dampers and compare them with conventional passive of a Q-car model. Detail discussion on each system is presented in the paper. The nonlinear passive are varying bump to rebound (asymmetric damping), quadratic damping and acceleration

sensitive damping. An on-off semiactive system is used and the damper force laws are given as:

$$F_1 = \begin{cases} c_1\dot{x}_1 - c_{11}\dot{x}_2 & when\ F_1\left(\dot{x}_1 - \dot{x}_2\right) > 0 \\ 0 & when\ F_1\left(\dot{x}_1 - \dot{x}_2\right) \le 0 \end{cases} \tag{2.4}$$

and

$$F_2 = \begin{cases} c_2\dot{x}_3 - c_{22}\dot{x}_4 & when\ F_2\left(\dot{x}_3 - \dot{x}_4\right) > 0 \\ 0 & when\ F_2\left(\dot{x}_3 - \dot{x}_4\right) \le 0 \end{cases} \tag{2.5}$$

where c_1, c_{11}, c_2 and c_{22} are the feedback gains, $\dot{x}_1$ and $\dot{x}_3$ are the rear and front sprung mass vertical velocity, $\dot{x}_2$ and $\dot{x}_4$ are the rear and front unsprung mass velocity, respectively.

The input signal is modeled as a stationary Gaussian white noise. The performance criteria are defined in terms of ride comfort, suspension working space and road holding, thus the variables of interest are sprung mass acceleration, suspension travel and tire deflection. RMS values of each variable are obtained and compared among the dampers. The mean square response is calculated from:

$$\sigma_y^2 = \frac{2\alpha\upsilon\sigma^2}{\pi}\int_{\omega_1}^{\omega_2}\left|H_y\left(\omega\right)\right|^2 d\omega \tag{2.6}$$

where $\omega_1 = 0.2\pi\,\mathrm{sec}^{-1}$, $\omega_2 = 60\pi\,\mathrm{sec}^{-1}$, $\dfrac{2\alpha\upsilon\sigma^2}{\pi}$ is the spectral density of the white noise excitation, and $H_y\left(\omega\right)$ is the transfer function relating the response variable y to white noise input. The asymmetric damping is shown to be disadvantageous to ride quality, quadratic damper provides less effective vibration isolation than conventional linear viscous damper, and improvement in the acceleration sensitive damping is relatively insignificant. On the other hand, semiactive damper is found to significantly improve the performance criteria. They further conducted preliminary analysis on a H-

car 4-DOF vehicle model for semiactive dampers. The equations of motion are solved in time domain using step-by-step numerical integration technique. The results show that while RMS sprung mass acceleration is reduced, there are relatively smaller increased in RMS tire force and suspension deflection.

Yao *et al.* (2002) conducted a laboratory experiment on an MR damper to obtain its performance characteristics. Then, a non-parametric model is constructed and parameter estimation is done based on the experimental results using a Bouc-Wen mathematical model. A half-scale Q-car model which includes the MR damper model is then set up to demonstrate the application of this type of damper in vibration control of vehicle suspension system. Semiactive control strategy, specifically on-off skyhook control, which is similar to Eq. 2.5 is used to control the suspension vibration. The work concludes that the MR damper has a very broad changeable damping force range and its property can be described with the Bouc-Wen model. The simulation results show that semiactive control can effectively improve sprung mass acceleration, tire and suspension deflections around body resonance.

Miller (1988) investigated the tuning of the damping for passive, semiactive and active suspensions of a Q-car model. The tuning typically involves changes in the specification of spring and damper characteristics, and in this work the effect of changing the damping ratio is investigated. Both on-off and continuously variable semiactive control schemes are analyzed. The control algorithm used for the on-off semiactive control is:

$$\begin{aligned} \dot{x}_1\left(\dot{x}_1 - \dot{x}_2\right) > 0 \;&\rightarrow\; F_d = C_{on}\left(\dot{x}_1 - \dot{x}_2\right) \\ \dot{x}_1\left(\dot{x}_1 - \dot{x}_2\right) < 0 \;&\rightarrow\; F_d = C_{off}\left(\dot{x}_1 - \dot{x}_2\right) \end{aligned} \tag{2.7}$$

where C_{on} is the on-state damping coefficient and C_{off} is the off-state damping coefficient. The continuously variable semiactive control policy is very similar to the on-off with only a slight variation and given as:

$$\begin{aligned} \dot{x}_1\left(\dot{x}_1 - \dot{x}_2\right) > 0 \;&\rightarrow\; F_d = C_{on}\dot{x}_1 + C_{off}\left(\dot{x}_1 - \dot{x}_2\right) \\ \dot{x}_1\left(\dot{x}_1 - \dot{x}_2\right) < 0 \;&\rightarrow\; F_d = C_{off}\left(\dot{x}_1 - \dot{x}_2\right) \end{aligned} \tag{2.8}$$

RMS values of sprung mass acceleration for ride comfort, body motion for sprung mass pitch and roll motion, tire deflection for road holding and suspension deflection for suspension travel are investigated based on random input velocity. The results show that both semiactive schemes and active dampers provide significant improvements in ride comfort, body motion and suspension travel while maintaining almost the same road holding capability as in passive suspension. The trade-offs between ride comfort, body motion, road holding and suspension travel are still apparent in all cases although semiactive and active systems offers more options in balancing these trade-offs. Generally, the continuously variable scheme gives superior performance than the on-off semiactive suspension.

Sharp and Hassan (1986) analyzes performance parameters related to ride comfort, suspension working space and tire load variability for passive, active and semiactive suspension systems for a Q-car representation. Two types of active suspension system are used, namely the full-state feedback and limited-state feedback. The semiactive systems studied also use the control laws based on the two active systems, but only limited to the ability to dissipate energy. There were three types of semiactive systems used, namely full-state feedback with no passive damper, limited-state feedback with passive damper, and limited-state feedback without passive damper. The control law used in semiactive system is equal to the one in the fully

active system, except that when the active system acts as an energy supplier, the semiactive system switches off. The control law of full-state feedback system used is:

$$u_{full-state} = k_{f1}\left(x_1 - x_0\right) + k_{f2}\left(x_2 - x_0\right) + k_{f3}\dot{x}_1 + k_{f4}\dot{x}_2 \tag{2.9}$$

where x_1 is the unsprung mass deflection, x_2 is the sprung mass deflection, k_{f1} and k_{f2} are the full-state spring stiffness, and k_{f3} and k_{f4} are the damping coefficient. The control law of the limited-state feedback system is:

$$u_{\text{limited-state}} = k_{l1}x_1 + k_{l2}x_2 + k_{l3}\dot{x}_1 + k_{l4}\dot{x}_2 \tag{2.10}$$

where k_{l1} and k_{l2} are the limited-state spring stiffness, and k_{l3} and k_{l4} are damping coefficients. The input used is displacement spectral density function defined as:

$$S\left(f\right) = \frac{3.14\times10^{-6}U^{1.5}}{f^{2.5}} \tag{2.11}$$

where $U = 20$ m/s and at any frequency, the output spectral density is equal to input spectral density multiplied by an appropriate frequency response function. The discomfort parameter, dynamic tire load and suspension spring stiffness are plotted against suspension working space parameter for analysis. The work concludes that as suspension working space is restricted, the active and semiactive systems becoming more substantially advantageous. It is observed also that limited-state feedback system performs almost as well as the full-state feedback system.

Ivers and Miller (1989) conducted laboratory experiments on a Q-car 2-DOF model apparatus to verify the existing simulation results. Passive, on-off semiactive and continuous semiactive suspensions were analyzed using a developed force controlled damper. The semiactive suspensions used basically emulates skyhook damper. The on-off control policy is given in Eq. 2.12, where positive absolute velocity is defined as sprung mass moving upward, positive relative velocity is

defined as sprung mass and unsprung mass separating, F is the force exerted by the damper, C_{on} is the damping coefficient for high damping state, and C_{off} is for the low damping state.

$$\begin{aligned} F &= C_{on} V_{rel} \quad if\ V_{abs} V_{rel} > 0 \\ F &= C_{off} V_{rel} \quad if\ V_{abs} V_{rel} < 0 \end{aligned} \tag{2.12}$$

The continuous semiactive control policy is given in Eq. 2.13. Note that the difference in this policy is that when absolute and relative velocities have the same sign, force produced is proportional to the absolute velocity, as oppose to relative velocity in the previous policy.

$$\begin{aligned} F &= C_{on} V_{abs} \quad if\ V_{abs} V_{rel} > 0 \\ F &= C_{off} V_{rel} \quad if\ V_{abs} V_{rel} < 0 \end{aligned} \tag{2.13}$$

Random excitation is used as an input to represent real road inputs and the results are compared to corresponding simulation results. The comparison are made on several responses: RMS sprung mass acceleration, RMS suspension travel, RMS tire contact force, and percent overshoot. Results indicated good agreement between the simulation and experimental results for passive system. However significant deviations were observed in semiactive policies.

2.4 RIDE QUALITY TESTING

von Eldik Thieme (1961) defined the term *traveling comfort* as the sum of all measures which maintain and improve the well-being of a person and reduce his fatigue during traveling. It consists of Riding Comfort – the comfort experienced in the road or rail vehicle itself, Local Comfort – the comfort experienced at stations, interchange points, and airports, and Organizational Comfort – such as good connections, reliability of service and custom clearance. The paper dealt only with the

Riding Comfort with focus only on the mechanical vibration problem in the frequency region of 0.1 to 100 cps (cycle per second).

There are generally two types of tests for comfort criteria, which are Objective and Subjective tests. Objective test is related to medical test in which human fatigue is considered as a criterion. Several investigations were discussed and can be concluded that it is very difficult to establish good relation between fatigue and the vibration characteristics of the vehicle.

Subjective test is widely used in comfort criteria and a reasonably good correlation has been established between comfort criteria and the vehicle‘s vibration characteristics. The test is generally to study the influence of the various vibrations on the human subject. Several criteria proposed by various researchers were discussed like Reiher-Meister Criteria, Jacklin-Liddel Criteria, Janeway Criteria, Sperling Criteria, Mauzin-Sperling Criteria, and Dieckmann Criteria. These criteria were compared carefully and modified classification of limits for different groups of vibrations were later introduced. However the limits are still disputable.

Janeway (1966) reviewed various ride instrumentation and give recommendations on measurement equipment which is relatively uncomplicated, economical, and commercially available and road testing procedures which facilitate the acquisition and processing of essential data. Some instrumentation commonly needed includes the strain gage accelerometer - its advantage includes readily calibrated on the job, covers the complete frequency range of interest, accurate, rugged and moderate in cost, and differential transformer – has the ability to measure jerk directly at the low frequencies, however, with d-c excitation, it has a very small output and therefore requires more powerful amplification.

Through available experimental evidences, the simple analogy of human body as a vibrating system over the entire ride frequency range is not accurate and the assumption seems to be correct for low frequency range (1-8 Hz) but beyond this range, the body does not seem to respond as a simple vibrating system. that Constant jerk and constant absorbed power are found to be synonymous.

Butkunas (1966) intended to present methods for analyzing and evaluating vibration measurements. He discussed in detail on Power Spectral Density (PSD) and provided examples of PSD calculation for periodic and random signals. The transfer function of a device is defined as the square root of the ratio of the response PSD to the excitation PSD. Only motion input in the range of 0.5 to 25 Hz were considered with the argument that at higher frequencies the perception of vibrational motion diminishes and gradually the perception of vibration as noise takes place.

Experiments to illustrate the integration of the seat cushion, the seat back and the floorpan to compute a single ride index were conducted. It was argued that although a single combined ride index is a good tool of comparing vehicles, it does not provide information on which part of the total system contribute what to the overall effect so that improvement can be focused on and for detail information, therefore, each input to the passenger must be individually analyzed for its frequency spectrum (or PSD for random vibration). This experimental approach is claimed to be advantageous since it is very flexible to handle either simple and direct input or even extensive and multi input problem. While the approach can provide a single number representation of the comfort achieve, it can also give a detailed comfort picture of the system, making it easier for product improvement.

Van Deusen (1968) defined *riding quality* as subjective experience resulting from whole body (or nearly whole body) vibration to which a person is subjected

when riding in a motor vehicle over an uneven course. The work focused on the stable ground roughness input with the objective to develop criteria for evaluating vehicle vibration, and ultimately to establish numeric scales for riding quality in terms of physical objective measurements made on the vehicle.

Cross modality technique was used in the work. This is a method of continuously monitoring the vibration sensation of a subject in an actual vehicle test, for subjective measurement, where subjects were required to adjust sound intensity relative to the ride discomfort experienced on the different surfaces. The match between loudness and vibration appears as:

$$L = BI^{0.6} = R = AX^{n} \tag{2.14}$$

where L is loudness, I refers to sound intensity, R is magnitude of vibration, X is measure of vibrational intensity, A and B are scale factors and the exponent n is characteristic of ride.

The result was then correlated with data obtained from objective measurement and showed that a single number, such as weighted acceleration variance is meaningful to quantify vibration level provided the spectral composition is fixed and vibration is in single direction. If the spectral composition is not fixed, it is probably necessary to tabulate several numbers that represent the acceleration variances in different frequency band. Direction of vibration essentially determine the ride quality. Thus, variance of acceleration in each frequency band and covariance between directions should be tabulated to quantify riding quality in actual vehicles.

Allen (1975) presented a technique for evaluating ride quality as a function of cab isolation parameters. SAE J1013 technique for the measurement of whole body vibration of the seated of agricultural equipment were used to evaluate the capability

of cab isolation systems for ride quality improvement of on-highway tractors. The work concludes that by modifying the suspension elements at the back of the cab, no improvement in the vertical ride can be obtained. Some improvement in the longitudinal ride can be obtained but at the expense of lost in vertical ride.

Dempsey *et al.* (1979) conducted experimental work to investigate the interactive effects of noise and vibration and further to develop criteria for ride quality prediction in a noise-vibration environment. Subjects are seated on an apparatus that resemble the interior of modern jet transport and asked to evaluate the comfort by comparing the test vibration to a reference vibration. The reference is a vertical 5 Hz vibration, sinusoidal at 0.074 g_{rms} and ambient noise of 65 dB and test vibration is 5Hz both sinusoidal and random, presented at 0.02, 0.042, 0.064, 0.085, 0.106 and 0.130 g_{rms}. The noises were octave bands of random noise centered at 500 or 200 Hz and presented at 65, 75, 85 and 95 dB, A-weighted noise level.

The work concludes that:

1. the addition of noise to the vibration environment generally increases the discomfort responses,
2. increasing acceleration at each noise level/octave band combination generally increasing discomfort level,
3. rating of discomfort level increases linearly with vibration acceleration when noise is absent, and loses its linearity as noise is increases, and
4. logarithmic value of the rating of discomfort level increases linearly with noise level.

Set of constant discomfort curves or criteria curves for human response to the combined environment were introduced.

CHAPTER THREE

MODELING AND PERFORMANCE CRITERIA

3.1 INTRODUCTION

In this chapter, general discussion on modeling is presented. Quarter-car 2-DOF model is used to discuss in details on equations of motion derivation, state-space technique transformation and control policies on various semiactive systems used in this work. Detail mathematical derivations are then presented for Q-car 2-DOF, H-car 4-DOF and F-car 7-DOF models. Finally performance criteria used in the analyses are presented.

3.2 MODELING IN VIBRATION ENGINEERING

A model basically represents only an approximation of the actual physical system and the same physical system can usually be modeled in several ways. However, a good model must retain all the essential dynamic characteristics of the system so that the behavior predicted by the model could satisfactorily match the observed behavior of the actual system.

Modeling in vibration engineering is usually categorized into two systems - lumped-parameter system (discrete system), and distributed-parameter system (continuous system). This work focuses on discrete modeling of system. Discrete modeling generally describes vehicle into a lumped mass system. Masses are concentrated at discrete points and connected together by massless elastic and damping elements. A set of ordinary differential equations can be obtained based on

this model. Fig. 3.1 show several examples of discrete modeling of vehicle, human and vehicle-human combination.

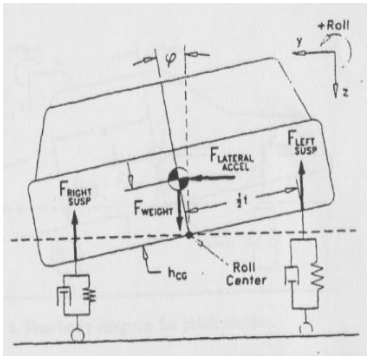

(a)

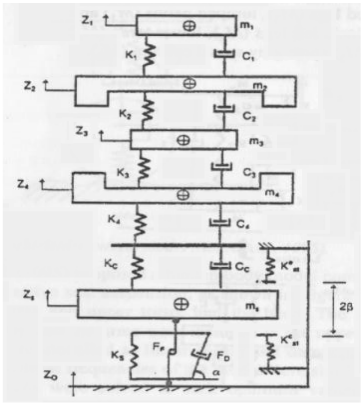

(b)

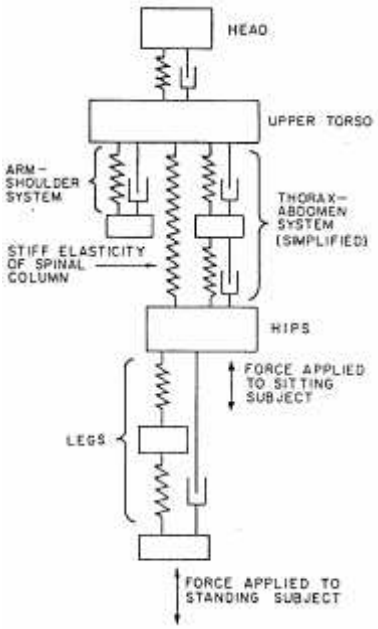

(c)

Fig. 3.1: Examples on discrete modeling; (a) half-car model (Stone and Demetriou, 2003), (b) human-with-seat model (Boileau *et al.*, 1997), and (c) human model (Brüel and Kjael Instruments).

For ride quality study, vehicle mass is usually separated into two parts: sprung mass, m_s and unsprung mass, m_{us}. Unsprung mass includes the mass of tires, brakes, suspension linkages and other components that move in unison with the wheels. These components are on the roadway side of the springs and therefore react to roadway irregularities with no damping, other than the pneumatic resilience of the tires (Gillespie, 1992). The rest of the mass, which is on the vehicle side of the springs, is called sprung mass. m_s is therefore isolated from the road by suspension system.

3.3 PASSIVE SYSTEM AND SEMIACTIVE CONTROL SCHEMES

Models for passive and semiactive control schemes that is used in this work are discussed before detail derivations are presented in the next sections. For the sake of simplicity, Q-car models which represented a single suspension from one of the four corners of vehicle are used.

3.3.1 Passive Suspension System

An example of a passive Q-car 2-DOF model is shown in Fig. 3.2. The variables and input are defined in Table 3.1.

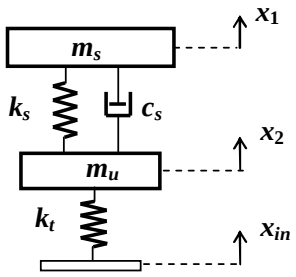

Fig. 3.2: Passive Quarter-car 2-DOF model.

Table 3.1: Passive Q-car 2-DOF variables and input description.

Symbol	Description	Units
m_s	Sprung mass	kg
m_u	Unsprung mass	kg
k_s	Suspension stiffness	N/m
k_t	Tire stiffness	N/m
c_s	Suspension damping coefficient	N s/m
x_1	Sprung mass vertical displacement	m
x_2	Unsprung mass vertical displacement	m
x_{in}	Displacement input	m

Input to the model is a displacement which represents a typical road profile. This input excites the unsprung mass, which represents the wheel, tire, and some suspension components through tire stiffness. The unsprung mass is connected to the sprung mass, representing the body of vehicle through primary suspension spring and damper. The equations of motion of the system can be derived as

$$m_s\ddot{x}_1 + c_s\dot{x}_1 - c_s\dot{x}_2 + k_s x_1 - k_s x_2 = 0$$
$$m_u\ddot{x}_2 - c_s\dot{x}_1 + c_s\dot{x}_2 - k_s x_1 + (k_s + k_t)x_2 = k_t x_{in}$$

and represented in matrix form as:

$$\begin{bmatrix} m_s & 0 \\ 0 & m_u \end{bmatrix}\begin{Bmatrix} \ddot{x}_1 \\ \ddot{x}_2 \end{Bmatrix} + \begin{bmatrix} c_s & -c_s \\ -c_s & c_s \end{bmatrix}\begin{Bmatrix} \dot{x}_1 \\ \dot{x}_2 \end{Bmatrix} + \begin{bmatrix} k_s & -k_s \\ -k_s & k_s + k_t \end{bmatrix}\begin{Bmatrix} x_1 \\ x_2 \end{Bmatrix} = \begin{bmatrix} 0 \\ k_t \end{bmatrix} x_{in} \tag{3.1}$$

This matrix form can be represented in a simplified relation,

$$[\mathbf{M}]\{\ddot{x}\} + [\mathbf{C}]\{\dot{x}\} + [\mathbf{K}]\{x\} = [\mathbf{U}]\{y\} \tag{3.2}$$

where $[\mathbf{M}]$, $[\mathbf{C}]$, $[\mathbf{K}]$ and $[\mathbf{U}]$ are the mass matrix, damping matrix, stiffness matrix and input matrix respectively, $\{\ddot{x}\}$, $\{\dot{x}\}$ and $\{x\}$ are the acceleration, velocity and displacement vectors respectively while $\{y\}$ is the external/input force vector, which in this particular case is road irregularities input.

State-space approach is used in this study to solve the differential equations. Second order differential equations are reduced to first order with the number of equations doubled by the following relationship:

$$z_1 = x_1,\ z_2 = x_2,\ z_3 = \dot{x}_1,\ z_4 = \dot{x}_2$$

So that the equations become:

$$\dot{z}_1 = \dot{x}_1 = z_3 \tag{3.3}$$

$$\dot{z}_2 = \dot{x}_2 = z_4 \tag{3.4}$$

$$\dot{z}_3 = \ddot{x}_1 = -\frac{k_s}{m_s} z_1 + \frac{k_s}{m_s} z_2 - \frac{c_s}{m_s} z_3 + \frac{c_s}{m_s} z_4 \tag{3.5}$$

$$\dot{z}_4 = \ddot{x}_2 = \frac{k_s}{m_u} z_1 - \frac{\left(k_s + k_t\right)}{m_u} z_2 + \frac{c_s}{m_u} z_3 - \frac{c_s}{m_u} z_4 \tag{3.6}$$

The system can be represented in state-space representation by compact general matrix notation of the state differential equation as:

$$\{\dot{x}\} = [\mathbf{A}]\{x\} + [\mathbf{B}]\{u\} \tag{3.7}$$

where $\{x\}$ is an $n \times 1$ real vector, $\{u\}$ is an $m \times 1$ real vector, $[\mathbf{A}]$ is an $n \times n$ square state matrix and $[\mathbf{B}]$ is an $n \times m$ input or control matrix. This state differential equation basically relates the rate of change of the state of the system to the state of the system and the input signals (Dorft and Bishop, 1995). For this particular model, state-space representation becomes:

$$\begin{Bmatrix} \dot{z}_1 \\ \dot{z}_2 \\ \dot{z}_3 \\ \dot{z}_4 \end{Bmatrix} = \begin{bmatrix} 0 & 0 & 1 & 0 \\ 0 & 0 & 0 & 1 \\ -k_s/m_s & k_s/m_s & -c_s/m_s & c_s/m_s \\ k_s/m_u & -\left(k_s + k_t\right)/m_u & c_s/m_u & -c_s/m_u \end{bmatrix} \begin{Bmatrix} z_1 \\ z_2 \\ z_3 \\ z_4 \end{Bmatrix} + \begin{bmatrix} 0 \\ 0 \\ 0 \\ k_t/m_u \end{bmatrix} \{x_{in}\} \tag{3.8}$$

The output or outputs of the system can then be related to state variables and input signals by:

$$y = [\mathbf{C}]\{x\} + [\mathbf{D}]\{u\} \tag{3.9}$$

where $[\mathbf{C}]$ is an $l \times n$ output matrix and $[\mathbf{D}]$ is an $l \times m$ direct transmission matrix. The output is basically depends on the interest of the user. For example if sprung mass deflection is of the interest, the output in this case becomes:

$$y = \begin{bmatrix} 1 & 0 & 0 & 0 \end{bmatrix}\{x\} + [0]\{u\} \tag{3.10}$$

If the matrix is expanded, the relation gives $y = z_1 = x_1$ which is the displacement of unsprung mass according to the model shown in Fig. 3.2. With the same argument, if sprung and unsprung mass accelerations are the outputs of interest, the output can then be given as:

$$\begin{Bmatrix} y_1 \\ y_2 \end{Bmatrix} = \begin{bmatrix} -k_s/m_s & k_s/m_s & -c_s/m_s & c_s/m_s \\ k_s/m_u & -(k_s+k_t)/m_u & c_s/m_u & -c_s/m_u \end{bmatrix} \{x\} + \begin{bmatrix} 0 \\ k_t/m_u \end{bmatrix} \{u\} \qquad (3.11)$$

where y_1 is m_s acceleration output and y_2 is m_{us} acceleration output. With the advancement of computing power and availability of numerous numerical computation softwares, finding the solutions for these equations are now tremendously simplified. MATLAB numerical computing software for example can be used to obtain the solution and plot the responses with relative ease. In some cases where symbolic computation is required, MATHEMATICA or MAPLE can be used.

3.3.2 Semiactive Control Scheme

This section discusses briefly on the concept of *on-off* control scheme semiactive systems that are used in this work. It is worth noted that there exist several variations in the *on-off* control policies introduced by various researchers. Several of the variations have already been presented in the literature review in the last chapter. This thesis uses only the control policy that has been extensively used for past works at the Advanced Vehicle Dynamics Laboratory (AVDL), Virginia Tech.

In *on-off* semiactive control scheme, damper in the suspension system is controlled by two damping values, referred to as high-state and low-state damping. The value used at any instance depends on the product of the relative velocity of the suspension, v_{12} and the absolute velocity of the sprung mass or vehicle body mass, v_1

that attached to the damper for skyhook scheme and the absolute velocity of the unsprung mass, v_2 for groundhook scheme.

3.3.2.1 Skyhook Control

An ideal skyhook configuration is quite similar to passive system except that instead of having the damper connected between sprung and unsprung mass, it is connected to an inertial reference in the '*sky*'as shown in Fig. 3.3.

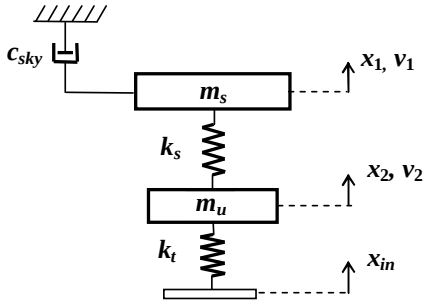

Fig. 3.3: Ideal skyhook configuration.

Since skyhook control focuses on the sprung mass, it is then expected that as c_{sky} increases, the sprung mass motion decreases. However, this improvement in sprung mass motion comes at the expense of an increase in the unsprung mass motion (Ahmadian, 1997a).

Also since the configuration is not possible in real automotive applications, a controllable damper is usually used to achieve similar response. This equivalent semiactive damper is shown in Fig. 3.4. Relating the two configurations, semiactive skyhook control policy can be summarized as having the following conditions (Ahmadian, 1997a):

$$\begin{aligned} v_1 v_{12} \geq 0 \quad & c_{sa} = c_{max} = c_{on} \quad (high\text{-}state\ damping) \\ v_1 v_{12} < 0 \quad & c_{sa} = c_{min} = c_{off} \quad (low\text{-}state\ damping) \end{aligned} \tag{3.12}$$

where relative velocity, v_{12} is defined as the velocity of the sprung mass, m_s relative to unsprung mass, m_u, i.e. $v_{12} = v_1 - v_2$.

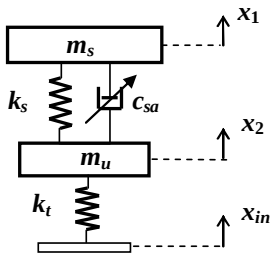

Fig. 3.4: Skyhook-equivalent semiactive model.

3.3.2.2 Groundhook Control

Groundhook configuration is similar the skyhook configuration except that the damper is connected from unsprung mass to an inertial reference on the '*ground*' as shown in Fig. 3.5. It can be said that the focus now is in controlling the unsprung mass, thus improvement in the unsprung motion is expect in using groundhook control. This again comes at the expense of increasing the sprung mass motion (Ahmadian, 1997a).

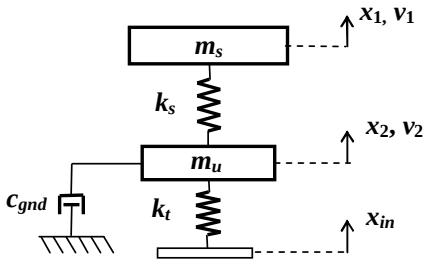

Fig. 3.5: Ideal Groundhook configuration.

Similarly, for automotive application, an equivalent semiactive damper shown in Fig. 3.4 can be used. The control policy for groundhook (Ahmadian, 1997a) is as follows:

$$
\begin{aligned}
&-v_2 v_{12} \geq 0 \quad c_{sa} = c_{max} = c_{on} \quad (high\text{-}state\ damping) \\
&-v_2 v_{12} < 0 \quad c_{sa} = c_{max} = c_{off} \quad (low\text{-}state\ damping)
\end{aligned}
\tag{3.13}
$$

3.3.2.3 Hybrid Control

Alternatively, the two configurations discussed above can be combined and this hybrid configuration has been shown to have the advantages of both policies (Ahmadian, 1997b). This configuration is shown in Fig. 3.6.

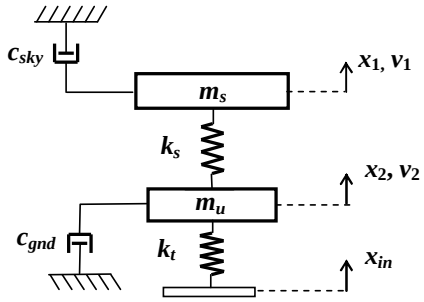

Fig. 3.6: Ideal Hybrid configuration

Semiactive hybrid control policy can be obtained by combining the two previous control policies, which becomes (Blanchard, 2003):

$$
\begin{aligned}
&\alpha v_1 v_{12} - (1-\alpha) v_2 v_{12} \geq 0 \qquad c_{sa} = c_{max} = c_{on} \\
&\alpha v_1 v_{12} - (1-\alpha) v_2 v_{12} < 0 \qquad c_{sa} = c_{min} = c_{off}
\end{aligned}
\tag{3.14}
$$

where α is the relative ratio between skyhook and groundhook control. From this configuration one can easily specify how closely the controller resembles either more towards skyhook control by setting the value of α closer to 1 or groundhook control by setting the value closer to 0.

Looking at the configurations of the skyhook, groundhook and hybrid semiactive (Figs. 3.3, 3.5 and 3.6), it should be realized that these figures basically assumed that c_{sa} of semiactive damper (as shown in Fig. 3.4) can be set to zero.

However in reality, it is not possible to completely eliminate any amount of damping in the suspension, and it is also undesirable (Ahmadian, 1999). To overcome this, an alternative configuration is proposed by the author and shown in Fig. 3.7.

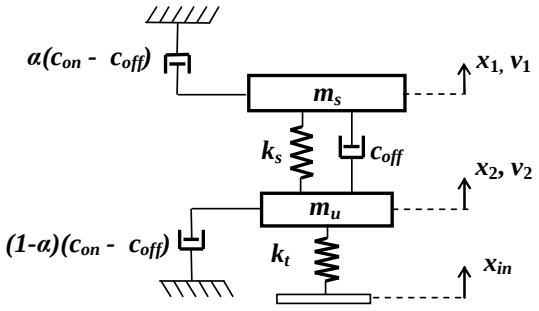

Fig. 3.7: Alternative representation of Hybrid Semiactive control.

The *off-state* damping c_{off} is just a small portion of the *on-state* damping c_{on} which typically is one-tenth of its value. This same model approach will be used in the subsequent section when the equations of motion for Q-car, H-car and F-car models are derived.

3.4 MODEL DERIVATIONS

In this section, complete derivation of each model to be used for analysis in the coming chapters is presented. Parameters used for each system and models are presented. Typical semiactive damping coefficients are chosen using the relationships of $c_{on} = 2.2c_s$ and $c_{off} = 0.2c_s$ (Blanchard, 2003). These relationships yield to $\left(c_{on} - c_{off}\right) = 2c_s$.

3.4.1 Quarter-car 2-DOF Model

The generalized Q-car model used in this work is similar to Fig. 3.7 and repeated below for convenient. x_1 is the sprung mass displacement, x_2 is the unsprung mass displacement and x_{in} is the displacement input.

Based on this configuration, skyhook and groundhook controls can be obtained by varying the value of α. The system becomes a skyhook when $\alpha = 1$ and groundhook when $\alpha = 0$. The system is said to be in hybrid control when the value of α is between these values. For the purpose of analysis in this work, hybrid control is taken as when $\alpha = 0.5$. Moreover, the equations of motion for passive system can be readily obtained from the same figure by letting $c_{off} = c_s$ and $c_{on} = c_s$.

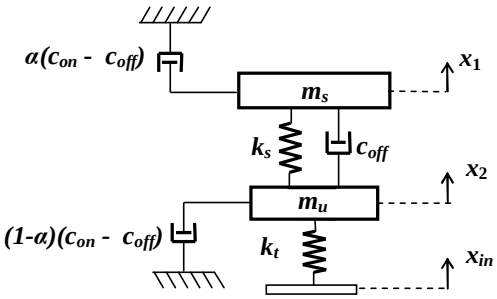

Fig. 3.8: Q-car 2-DOF generalized model.

The general equations of motion derived from the model are:

$$m_s\ddot{x}_1 + c_{off}(\dot{x}_1 - \dot{x}_2) + \alpha\left(c_{on} - c_{off}\right)\dot{x}_1 + k_s(x_1 - x_2) = 0 \tag{3.15}$$

$$m_u\ddot{x}_2 - c_{off}(\dot{x}_1 - \dot{x}_2) + (1-\alpha)\left(c_{on} - c_{off}\right)\dot{x}_2 - k_s(x_1 - x_2) + k_t x_2 = k_t x_{in} \tag{3.16}$$

These can be simplified in matrix form of as described in the previous section and the mass, damping, stiffness and input matrices, respectively are given as:

$$[\mathbf{M}] = \begin{bmatrix} m_s & 0 \\ 0 & m_u \end{bmatrix}$$

$$[\mathbf{C}] = \begin{bmatrix} c_{off} + \alpha\left(c_{on} - c_{off}\right) & -c_{off} \\ -c_{off} & c_{off} + (1-\alpha)\left(c_{on} - c_{off}\right) \end{bmatrix}$$

$$[\mathbf{K}] = \begin{bmatrix} k_s & -k_s \\ -k_s & k_s + k_t \end{bmatrix}$$

$$[\mathbf{U}] = \begin{bmatrix} 0 \\ k_t \end{bmatrix}$$

Transforming the equation into state-space representation, with the assumption that $z_1 = x_1$, $z_2 = x_2$, $z_3 = \dot{x}_1$, $z_4 = \dot{x}_2$, the equations can be simplified into the following form:

$$\dot{z}_1 = \dot{x}_1 = z_3 \tag{3.17}$$

$$\dot{z}_2 = \dot{x}_2 = z_4 \tag{3.18}$$

$$\dot{z}_3 = \ddot{x}_1 = -\frac{k_s}{m_s} z_1 + \frac{k_s}{m_s} z_2 - \frac{\left(c_{off} + \alpha\left(c_{on} - c_{off}\right)\right)}{m_s} z_3 + \frac{c_{off}}{m_s} z_4 \tag{3.19}$$

$$\dot{z}_4 = \ddot{x}_2 = \frac{k_s}{m_u} z_1 - \frac{\left(k_s + k_t\right)}{m_u} z_2 + \frac{c_{off}}{m_u} z_3 - \frac{\left(c_{off} + (1-\alpha)\left(c_{on} - c_{off}\right)\right)}{m_u} z_4 \tag{3.20}$$

or, in the matrix form, the corresponding matrices are:

$$[\mathbf{A}] = \begin{bmatrix} 0 & 0 & 1 & 0 \\ 0 & 0 & 0 & 1 \\ -\frac{k_s}{m_s} & \frac{k_s}{m_s} & -\frac{\left(c_{off} + \alpha\left(c_{on} - c_{off}\right)\right)}{m_s} & \frac{c_{off}}{m_s} \\ \frac{k_s}{m_u} & -\frac{\left(k_s + k_t\right)}{m_u} & \frac{c_{off}}{m_u} & -\frac{\left(c_{off} + (1-\alpha)\left(c_{on} - c_{off}\right)\right)}{m_u} \end{bmatrix}$$

$$[\mathbf{B}] = \begin{bmatrix} 0 \\ 0 \\ 0 \\ \frac{k_t}{m_u} \end{bmatrix}$$

The motion variables or states of interest are sprung mass acceleration ($\ddot{x}_1$), suspension deflection ($x_1 - x_2$), and tire deflection ($x_2 - x_{in}$). Thus the outputs in state space is given below where y_1, y_2 and y_3 are the sprung mass acceleration, suspension deflection and tire deflection outputs, respectively.

$$[\mathbf{Y}] = \begin{Bmatrix} y_1 \\ y_2 \\ y_3 \end{Bmatrix}$$

$$[\mathbf{C}] = \begin{bmatrix} -\frac{k_s}{m_s} & \frac{k_s}{m_s} & -\frac{\left(c_{off} + \alpha\left(c_{on} - c_{off}\right)\right)}{m_s} & \frac{c_{off}}{m_s} \\ 1 & -1 & 0 & 0 \\ 0 & 1 & 0 & 0 \end{bmatrix}$$

$$[\mathbf{D}] = \begin{bmatrix} 0 \\ 0 \\ -1 \end{bmatrix}$$

Numerical values of parameters used, which are typical for passenger vehicle are summarized in Table 3.2. Using built-in MATLAB command, natural frequencies of each system are obtained and shown in Table 3.3. These values are reasonably within the recommended values for passenger vehicle as suggested by Gillespie (1992) and Wong (2003). A good passenger vehicle should have the m_s natural frequency, ω_{n1} at around 10 Hz, while the m_{us} natural frequency, ω_{n2} should be within an order of magnitude higher.

Table 3.2: Q-car 2-DOF Model Parameters.

Symbol	Description	Units
m_s	Sprung mass	240 kg
m_u	Unsprung mass	36 kg
Cs	Suspension damping coefficient	980 N s/m
k_s	Suspension stiffness coefficient	16000 N/m
k_t	Tire stiffness coefficient	160000 N/m

Table 3.3: Natural frequencies of each Q-car system and control policy.

System	ω_{n1} (m_s natural frequency), rad/s	ω_{n2} (m_{us} natural frequency), rad/s
Passive	7.8581	69.2702
Skyhook	7.7801	69.9642
Groundhook	7.7813	69.9539
Hybrid	7.7840	69.9296

3.4.2 Half-car 4-DOF Model

The generalized H-car 4-DOF model is shown in Fig. 3.9 below. x_1 is the sprung mass vertical displacement, x_2 is sprung mass pitch angular displacement, x_3 and x_4 are front and rear unsprung mass displacements and x_{in1} and x_{in2} are front and rear displacement inputs, respectively.

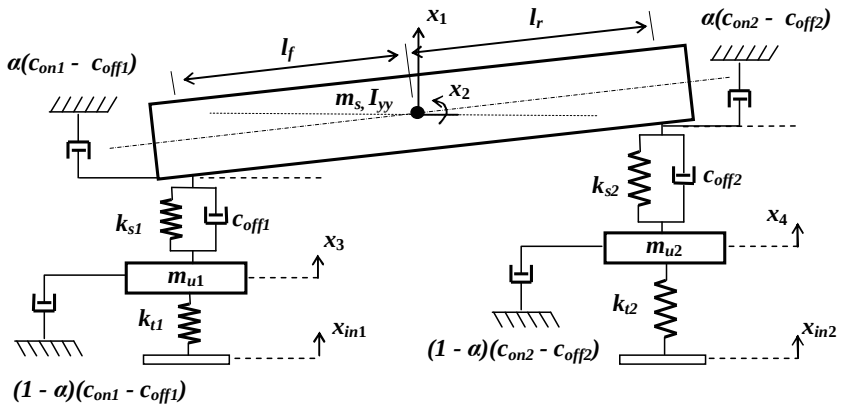

Fig. 3.9: H-car 4-DOF generalized model.

Similar to the Q-car model case, all passive and semiactive control policies can be obtained from this single model, which is by letting $\alpha = 1$, $\alpha = 0.5$ and $\alpha = 0$ to obtain skyhook, hybrid and groundhook control policies respectively, and letting $c_{off1} = c_{on1} = c_{s1}$ and $c_{off2} = c_{on2} = c_{s2}$ to obtain passive system. The equations of motion derived from the model are shown below:

$$m_s\ddot{x}_1 + k_{s1}Z_1 + k_{s2}Z_2 + c_{off1}\dot{Z}_1 + c_{off2}\dot{Z}_2 + \alpha(c_{on1} - c_{off1})(\dot{Z}_1 + x_3) + \alpha(c_{on2} - c_{off2})(\dot{Z}_2 + x_4) = 0 \quad (3.21)$$

$$I_{yy}\ddot{x}_2 - k_{s1}Z_1 l_f + k_{s2}Z_2 l_r - c_{off1}\dot{Z}_1 l_f + c_{off2}\dot{Z}_2 l_r - \alpha(c_{on1} - c_{off1})(\dot{Z}_1 + x_3) l_f + \alpha(c_{on2} - c_{off2})(\dot{Z}_2 + x_4) l_r = 0 \quad (3.22)$$

$$m_{u1}\ddot{x}_3 - k_{s1}Z_1 - c_{off1}\dot{Z}_1 + k_{t1}(x_3 - x_{in1}) + (1-\alpha)(c_{on1} - c_{off1})\dot{x}_3 = 0 \quad (3.23)$$

$$m_{u2}\ddot{x}_4 - k_{s2}Z_2 - c_{off2}\dot{Z}_2 + k_{t2}(x_4 - x_{in2}) + (1-\alpha)(c_{on2} - c_{off2})\dot{x}_4 = 0 \quad (3.24)$$

where,

$$Z_1 = x_1 - x_2 l_f - x_3$$

$$Z_2 = x_1 + x_2 l_r - x_4$$

In matrix form, the mass, damping, stiffness and input matrices, respectively are given as:

$$[\mathbf{M}] = \begin{bmatrix} m_s & 0 & 0 & 0 \\ 0 & I_{yy} & 0 & 0 \\ 0 & 0 & m_{u1} & 0 \\ 0 & 0 & 0 & m_{u2} \end{bmatrix}$$

$$[\mathbf{C}] = \begin{bmatrix} C_1 + C_2 & -C_1 l_f + C_2 l_r & -c_{off1} & -c_{off2} \\ -C_1 l_f + C_2 l_r & C_1 l_f{}^2 + C_2 l_r{}^2 & c_{off1} l_f & -c_{off2} l_r \\ -c_{off1} & c_{off1} l_f & c_{off1} + (1-\alpha)(c_{on1} - c_{off1}) & 0 \\ -c_{off2} & -c_{off2} l_r & 0 & c_{off2} + (1-\alpha)(c_{on2} - c_{off2}) \end{bmatrix}$$

$$[\mathbf{K}] = \begin{bmatrix} k_{s1}+k_{s2} & -k_{s1}l_f + k_{s2}l_r & -k_{s1} & -k_{s2} \\ -k_{s1}l_f + k_{s2}l_r & k_{s1}{l_f}^2 + k_{s2}{l_r}^2 & k_{s1}l_f & -k_{s2}l_r \\ -k_{s1} & k_{s1}l_f & k_{s1}+k_{t1} & 0 \\ -k_{s2} & -k_{s2}l_r & 0 & k_{s2}+k_{t2} \end{bmatrix}$$

$$[\mathbf{U}] = \begin{bmatrix} 0 \\ 0 \\ k_{t1} \\ k_{t2} \end{bmatrix}$$

where,

$$C_1 = c_{off\,1} + \alpha(c_{on1} - c_{off\,1})$$

$$C_2 = c_{off\,2} + \alpha(c_{on2} - c_{off\,2})$$

Letting $z_1 = x_1$, $z_2 = x_2$, $z_3 = x_3$, $z_4 = x_4$, $z_5 = \dot{x}_1$, $z_6 = \dot{x}_2$, $z_7 = \dot{x}_3$ and $z_8 = \dot{x}_4$, the state space representation of the equations as follows:

$$\dot{z}_1 = \dot{x}_1 = z_5 \tag{3.25}$$

$$\dot{z}_2 = \dot{x}_2 = z_6 \tag{3.26}$$

$$\dot{z}_3 = \dot{x}_3 = z_7 \tag{3.27}$$

$$\dot{z}_4 = \dot{x}_4 = z_8 \tag{3.28}$$

$$\dot{z}_5 = \ddot{x}_1 = -\frac{(k_{s1}+k_{s2})}{m_s} z_1 + \frac{(k_{s1}l_f - k_{s2}l_r)}{m_s} z_2 + \frac{k_{s1}}{m_s} z_3 + \frac{k_{s2}}{m_s} z_4$$

$$-\frac{(C_1+C_2)}{m_s} z_5 + \frac{(C_1l_f - C_2l_r)}{m_s} z_6 + \frac{c_{off\,1}}{m_s} z_7 + \frac{c_{off\,2}}{m_s} z_8 \tag{3.29}$$

$$\dot{z}_6 = \ddot{x}_2 = \frac{(k_{s1}l_f - k_{s2}l_r)}{I_{yy}} z_1 - \frac{(k_{s1}{l_f}^2 + k_{s2}{l_r}^2)}{I_{yy}} z_2 - \frac{(k_{s1}l_f)}{I_{yy}} z_3 + \frac{(k_{s2}l_r)}{I_{yy}} z_4$$

$$+\frac{(C_1l_f - C_2l_r)}{I_{yy}} z_5 - \frac{(C_1{l_f}^2 + C_2{l_r}^2)}{I_{yy}} z_6 - \frac{(c_{off\,1}l_f)}{I_{yy}} z_7 + \frac{(c_{off\,2}l_r)}{I_{yy}} z_8 \tag{3.30}$$

$$\dot{z}_7 = \ddot{x}_3 = \frac{k_{s1}}{m_{u1}} z_1 - \frac{k_{s1}l_f}{m_{u1}} z_2 - \frac{(k_{s1}+k_{t1})}{m_{u1}} z_3$$

$$+\frac{c_{off1}}{m_{u1}}z_5-\frac{c_{off1}l_f}{m_{u1}}z_6-\frac{c_{off1}+(1-\alpha)(c_{on1}-c_{off1})}{m_{u1}}z_7 \tag{3.31}$$

$$\dot{z}_8=\ddot{x}_4=\frac{k_{s2}}{m_{u2}}z_1+\frac{k_{s2}l_r}{m_{u2}}z_2-\frac{(k_{s2}+k_{t2})}{m_{u2}}z_4$$

$$+\frac{c_{off2}}{m_{u2}}z_5-\frac{c_{off2}l_r}{m_{u2}}z_6-\frac{c_{off2}+(1-\alpha)(c_{on2}-c_{off2})}{m_{u2}}z_8 \tag{3.32}$$

$$[\mathbf{B}]=\begin{bmatrix}0 & 0\\ \vdots & \vdots\\ \frac{k_{t1}}{m_{u1}} & 0\\ 0 & \frac{k_{t2}}{m_{u2}}\end{bmatrix}^{8\times 2}$$

where $[\mathbf{B}]$ is an 8 by 2 matrix. The states of interest are sprung mass vertical acceleration ($\ddot{x}_1$), sprung mass pitch angular acceleration ($\ddot{x}_2$), front suspension deflection ($x_1-x_2\cdot l_f-x_3$), rear suspension deflection ($x_1+x_2\cdot l_r-x_4$), front tire deflection (x_3-x_{in1}) and rear tire deflection (x_4-x_{in2}). Thus accordingly, output matrices $[\mathbf{Y}]$, $[\mathbf{C}]$ and $[\mathbf{D}]$ can be derived based on the motion variables of interest the same way as derived in the Q-car case before.

Numerical values of parameters used and natural frequencies of each system are summarized in Table 3.4 and Table 3.5, respectively.

Similar to Q-car case, typical semi-active damping coefficients are chosen using the relationships of $c_{on1}=c_{on2}=2.2c_s$ and $c_{off1}=c_{off2}=0.2c_s$. Two types of inputs are used in this work. The first type is called heave input signal, where $v_{in1}=v_{in2}=v_{in}$, and the second type is pitch input signal, where $v_{in1}=v_{in}$, $v_{in2}=-v_{in}$. These are illustrated in Fig. 3.10.

Table 3.4: H-car 4-DOF Model Parameters.

Symbol	Description	Units
m_s	Sprung mass	730 kg
I_{yy}	Pitch Moment of Inertia	2460 kg m^2
m_{u1}	Front Unsprung mass	40 kg
m_{u2}	Rear Unsprung mass	35.5 kg
k_{s1}	Front Suspension Stiffness coefficient	19960 N/m
k_{s2}	Rear Suspension Stiffness coefficient	17500 N/m
c_{s1}	Front Suspension Damping coefficient	1290 N s/m
c_{s2}	Rear Suspension Damping coefficient	1620 N s/m
k_{t1}	Front Tire Stiffness coefficient	175500 N/m
k_{t2}	Rear Tire Stiffness coefficient	175500 N/m
l_f	Distance from m_s C.G. to the front axle	1.011 m
l_r	Distance from m_s C.G. to the rear axle	1.803 m

Table 3.5: Natural frequencies of each H-car system and control policy.

System	ω_{n1} (m_s natural frequency), rad/s	ω_{n2} (m_s natural frequency), rad/s	ω_{n3} (m_{us} natural frequency), rad/s	ω_{n4} (m_{us} natural frequency), rad/s
Passive	5.0955	7.1128	69.4906	72.5727
Skyhook	5.1173	6.3917	69.9092	73.7083
Groundhook	5.0482	7.0193	69.9297	73.7622
Hybrid	5.0731	6.9870	69.9247	73.7458

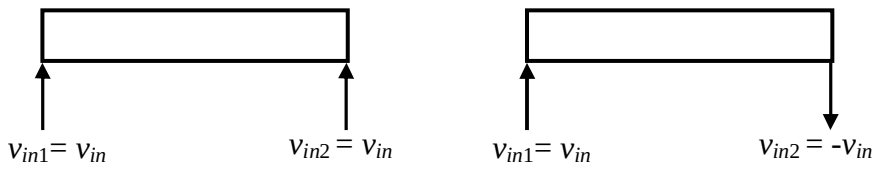

(a) Heave Input (b) Pitch Input

Fig. 3.10: Types of input signals for H-car analysis.

Compared to the Q-car 2-DOF model, H-car model would enable an analysis of either pitching or rolling response of vehicle, besides the heave or bouncing response. This advantage is, of course, comes with a price that the equations of motion become more involved.

3.4.3 Full-car 7-DOF Model

A typical F-car 7-DOF is shown in Fig. 3.11 and its detail derivation is described below. The variables and inputs of the model are summarized in Table 3.6. Similar to the previous models' cases, all passive and semiactive control policies can be obtained from this single model.

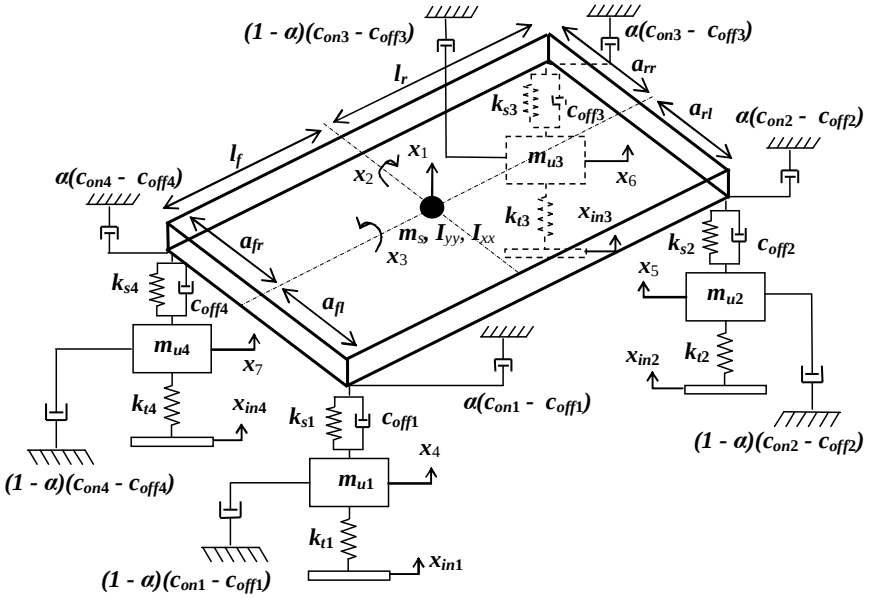

Fig. 3.11: F-car 7-DOF generalized model.

Table 3.6: F-car 7-DOF variables and inputs description.

Symbol	Description	Units
x_1	Sprung mass heave displacement	m
x_2	Sprung mass pitch angular displacement	rad
x_3	Sprung mass roll angular displacement	rad
x_4	Front-Left unsprung mass displacement	m
x_5	Rear-Left unsprung mass displacement	m
x_6	Rear-Right unsprung mass displacement	m
x_7	Front-Right unsprung mass displacement	m
x_{in1}	Front-Left displacement input	m
x_{in2}	Rear-Left displacement input	m
x_{in3}	Rear-Right displacement input	m
x_{in4}	Front-Right displacement input	m

The equations of motion derived from the model are shown below:

$$m_s\ddot{x}_1 + k_{s1}Z_1 + k_{s2}Z_2 + k_{s3}Z_3 + k_{s4}Z_4 + c_{off1}\dot{Z}_1 + c_{off2}\dot{Z}_2 + c_{off3}\dot{Z}_3$$
$$+c_{off4}\dot{Z}_4 + \alpha(c_{on1} - c_{off1})(\dot{Z}_1 + \dot{x}_4) + \alpha(c_{on2} - c_{off2})(\dot{Z}_2 + \dot{x}_5)$$
$$+\alpha(c_{on3} - c_{off3})(\dot{Z}_3 + \dot{x}_6) + \alpha(c_{on4} - c_{off4})(\dot{Z}_4 + \dot{x}_7) = 0 \quad (3.33)$$

$$I_{yy}\ddot{x}_2 + k_{s1}Z_1l_f - k_{s2}Z_2l_r - k_{s3}Z_3l_r + k_{s4}Z_4l_f + c_{off1}\dot{Z}_1l_f - c_{off2}\dot{Z}_2l_r - c_{off3}\dot{Z}_3l_r$$
$$+c_{off4}\dot{Z}_4l_f + \alpha(c_{on1} - c_{off1})(\dot{Z}_1 + \dot{x}_4)l_f - \alpha(c_{on2} - c_{off2})(\dot{Z}_2 + \dot{x}_5)l_r$$
$$-\alpha(c_{on3} - c_{off3})(\dot{Z}_3 + \dot{x}_6)l_r + \alpha(c_{on4} - c_{off4})(\dot{Z}_4 + \dot{x}_7)l_f = 0 \quad (3.34)$$

$$I_{xx}\ddot{x}_3 + k_{s1}Z_1a_{lf} + k_{s2}Z_2a_{lr} - k_{s3}Z_3a_{rr} - k_{s4}Z_4a_{rf} + c_{off1}\dot{Z}_1a_{lf} + c_{off2}\dot{Z}_2a_{lr} - c_{off3}\dot{Z}_3a_{rr}$$
$$-c_{off4}\dot{Z}_4a_{rf} + \alpha(c_{on1} - c_{off1})(\dot{Z}_1 + \dot{x}_4)a_{lf} + \alpha(c_{on2} - c_{off2})(\dot{Z}_2 + \dot{x}_5)a_{lr}$$
$$-\alpha(c_{on3} - c_{off3})(\dot{Z}_3 + \dot{x}_6)a_{rr} - \alpha(c_{on4} - c_{off4})(\dot{Z}_4 + \dot{x}_7)a_{rf} = 0 \quad (3.35)$$

$$m_{u1}\ddot{x}_4 - k_{s1}Z_1 - c_{off1}\dot{Z}_1 + k_{t1}(x_4 - x_{in1}) + (1-\alpha)(c_{on1} - c_{off1})\dot{x}_4 = 0 \quad (3.36)$$

$$m_{u2}\ddot{x}_5 - k_{s2}Z_2 - c_{off2}\dot{Z}_2 + k_{t2}(x_5 - x_{in2}) + (1-\alpha)(c_{on2} - c_{off2})\dot{x}_5 = 0 \quad (3.37)$$

$$m_{u3}\ddot{x}_6 - k_{s3}Z_3 - c_{off3}\dot{Z}_3 + k_{t3}(x_6 - x_{in3}) + (1-\alpha)(c_{on3} - c_{off3})\dot{x}_6 = 0 \quad (3.38)$$

$$m_{u4}\ddot{x}_7 - k_{s4}Z_4 - c_{off4}\dot{Z}_4 + k_{t4}(x_7 - x_{in4}) + (1-\alpha)(c_{on4} - c_{off4})\dot{x}_7 = 0 \quad (3.39)$$

where,

$$Z_1 = x_1 + x_2l_f + x_3a_{lf} - x_4$$

$$Z_2 = x_1 - x_2l_r + x_3a_{lr} - x_5$$

$$Z_3 = x_1 - x_2l_r - x_3a_{rr} - x_6$$

$$Z_4 = x_1 + x_2l_f - x_3a_{rf} - x_7$$

The equations are then transformed to state-space representation. Letting $z_1 = x_1$, $z_2 = x_2$, $z_3 = x_3$, $z_4 = x_4$, $z_5 = x_5$, $z_6 = x_6$, $z_7 = x_7$, $z_8 = \dot{x}_1$, $z_9 = \dot{x}_2$, $z_{10} = \dot{x}_3$, $z_{11} = \dot{x}_4$, $z_{12} = \dot{x}_5$, $z_{13} = \dot{x}_6$, $z_{14} = \dot{x}_7$, and:

$$C_1 = c_{off\,1} + \alpha(c_{on1} - c_{off\,1})$$

$$C_2 = c_{off\,2} + \alpha(c_{on2} - c_{off\,2})$$

$$C_3 = c_{off\,3} + \alpha(c_{on3} - c_{off\,3})$$

$$C_4 = c_{off\,4} + \alpha(c_{on4} - c_{off\,4})$$

the state-space representation of the equations is obtained as:

$$\dot{z}_1 = \dot{x}_1 = z_8 \tag{3.40}$$

$$\dot{z}_2 = \dot{x}_2 = z_9 \tag{3.41}$$

$$\dot{z}_3 = \dot{x}_3 = z_{10} \tag{3.42}$$

$$\dot{z}_4 = \dot{x}_4 = z_{11} \tag{3.43}$$

$$\dot{z}_5 = \dot{x}_5 = z_{12} \tag{3.44}$$

$$\dot{z}_6 = \dot{x}_6 = z_{13} \tag{3.45}$$

$$\dot{z}_7 = \dot{x}_7 = z_{14} \tag{3.46}$$

$$\begin{aligned}\dot{z}_8 = \ddot{x}_1 = &-\frac{\left(k_{s1}+k_{s2}+k_{s3}+k_{s4}\right)}{m_s} z_1 + \frac{\left(-k_{s1}l_f + k_{s2}l_r + k_{s3}l_r - k_{s4}l_f\right)}{m_s} z_2 \\ &+ \frac{\left(-k_{s1}a_{lf} - k_{s2}a_{lr} + k_{s3}a_{rr} + k_{s4}a_{rf}\right)}{m_s} z_3 + \frac{k_{s1}}{m_s} z_4 + \frac{k_{s2}}{m_s} z_5 + \frac{k_{s3}}{m_s} z_6 \\ &+ \frac{k_{s4}}{m_s} z_7 - \frac{\left(C_1+C_2+C_3+C_4\right)}{m_s} z_8 + \frac{\left(-C_1l_f + C_2l_r + C_3l_r - C_4l_f\right)}{m_s} z_9 \\ &+ \frac{\left(-C_1a_{lf} - C_2a_{lr} + C_3a_{rr} + C_4a_{rf}\right)}{m_s} z_{10} \\ &+ \frac{c_{off\,1}}{m_s} z_{11} + \frac{c_{off\,2}}{m_s} z_{12} + \frac{c_{off\,3}}{m_s} z_{13} + \frac{c_{off\,4}}{m_s} z_{14}\end{aligned} \tag{3.47}$$

$$\dot{z}_9 = \ddot{x}_2 = \frac{\left(-k_{s1}l_f + k_{s2}l_r + k_{s3}l_r - k_{s4}l_f\right)}{I_{yy}} z_1 - \frac{\left(k_{s1}{l_f}^2 + k_{s2}{l_r}^2 + k_{s3}{l_r}^2 + k_{s4}{l_f}^2\right)}{I_{yy}} z_2$$

$$+\frac{\left(-k_{s1}l_f a_{lf}+k_{s2}l_r a_{lr}-k_{s3}l_r a_{rr}+k_{s4}l_f a_{rf}\right)}{I_{yy}}z_3+\frac{\left(k_{s1}l_f\right)}{I_{yy}}z_4-\frac{\left(k_{s2}l_r\right)}{I_{yy}}z_5-\frac{\left(k_{s3}l_r\right)}{I_{yy}}z_6$$

$$+\frac{\left(k_{s4}l_f\right)}{I_{yy}}z_7+\frac{\left(-C_1l_f+C_2l_r+C_3l_r-C_4l_f\right)}{I_{yy}}z_8-\frac{\left(C_1{l_f}^2+C_2{l_r}^2+C_3{l_r}^2+C_4{l_f}^2\right)}{I_{yy}}z_9$$

$$+\frac{\left(-C_1l_f a_{lf}+C_2l_r a_{lr}-C_3l_r a_{rr}+C_4l_f a_{rf}\right)}{I_{yy}}z_{10}$$

$$+\frac{\left(c_{off1}l_f\right)}{I_{yy}}z_{11}-\frac{\left(c_{off2}l_r\right)}{I_{yy}}z_{12}-\frac{\left(c_{off3}l_r\right)}{I_{yy}}z_{13}+\frac{\left(c_{off4}l_f\right)}{I_{yy}}z_{14} \tag{3.48}$$

$$\dot{z}_{10}=\ddot{x}_3=\frac{\left(-k_{s1}a_{lf}-k_{s2}a_{lr}+k_{s3}a_{rr}+k_{s4}a_{rf}\right)}{I_{xx}}z_1$$

$$+\frac{\left(-k_{s1}l_f a_{lf}+k_{s2}l_r a_{lr}-k_{s3}l_r a_{rr}+k_{s4}l_f a_{rf}\right)}{I_{xx}}z_2$$

$$+\frac{\left(k_{s1}{a_{lf}}^2+k_{s2}{a_{lr}}^2+k_{s3}{a_{rr}}^2+k_{s4}{a_{rf}}^2\right)}{I_{xx}}z_3+\frac{\left(k_{s1}a_{lf}\right)}{I_{xx}}z_4+\frac{\left(k_{s2}a_{lr}\right)}{I_{xx}}z_5$$

$$-\frac{\left(k_{s3}a_{rr}\right)}{I_{xx}}z_6-\frac{\left(k_{s4}a_{rf}\right)}{I_{xx}}z_7+\frac{\left(-C_1a_{lf}-C_2a_{lr}+C_3a_{rr}+C_4a_{rf}\right)}{I_{xx}}z_8$$

$$+\frac{\left(-C_1l_f a_{lf}+C_2l_r a_{lr}-C_3l_r a_{rr}+C_4l_f a_{rf}\right)}{I_{xx}}z_9$$

$$+\frac{\left(C_1{a_{lf}}^2+C_2{a_{lr}}^2+C_3{a_{rr}}^2+C_4{a_{rf}}^2\right)}{I_{xx}}z_{10}$$

$$+\frac{\left(c_{off1}a_{lf}\right)}{I_{xx}}z_{11}+\frac{\left(c_{off2}a_{lr}\right)}{I_{xx}}z_{12}-\frac{\left(c_{off3}a_{rr}\right)}{I_{xx}}z_{13}-\frac{\left(c_{off4}a_{rf}\right)}{I_{xx}}z_{14} \tag{3.49}$$

$$\dot{z}_{11}=\ddot{x}_4=\frac{k_{s1}}{m_{u1}}z_1+\frac{k_{s1}l_f}{m_{u1}}z_2+\frac{k_{s1}a_{lf}}{m_{u1}}z_3-\frac{\left(k_{s1}+k_{t1}\right)}{m_{u1}}z_4+\frac{c_{off1}}{m_{u1}}z_8$$

$$+\frac{c_{off1}l_f}{m_{u1}}z_9+\frac{c_{off1}a_{lf}}{m_{u1}}z_{10}-\frac{c_{off1}+(1-\alpha)(c_{on1}-c_{off1})}{m_{u1}}z_{11} \tag{3.50}$$

$$\dot{z}_{12}=\ddot{x}_5=\frac{k_{s2}}{m_{u2}}z_1-\frac{k_{s2}l_r}{m_{u2}}z_2+\frac{k_{s2}a_{lr}}{m_{u2}}z_3-\frac{\left(k_{s2}+k_{t2}\right)}{m_{u2}}z_5+\frac{c_{off2}}{m_{u2}}z_8$$

$$-\frac{c_{off\,2}l_r}{m_{u2}}z_9+\frac{c_{off\,2}a_{lr}}{m_{u2}}z_{10}-\frac{c_{off\,2}+(1-\alpha)(c_{on2}-c_{off\,2})}{m_{u2}}z_{12} \tag{3.51}$$

$$\dot{z}_{13}=\ddot{x}_6=\frac{k_{s3}}{m_{u3}}z_1-\frac{k_{s3}l_r}{m_{u3}}z_2-\frac{k_{s3}a_{rr}}{m_{u3}}z_3-\frac{(k_{s3}+k_{t3})}{m_{u3}}z_6+\frac{c_{off\,3}}{m_{u3}}z_8$$

$$-\frac{c_{off\,3}l_r}{m_{u3}}z_9-\frac{c_{off\,3}a_{rr}}{m_{u3}}z_{10}-\frac{c_{off\,3}+(1-\alpha)(c_{on3}-c_{off\,3})}{m_{u3}}z_{13} \tag{3.52}$$

$$\dot{z}_{14}=\ddot{x}_7=\frac{k_{s4}}{m_{u4}}z_1+\frac{k_{s4}l_f}{m_{u4}}z_2-\frac{k_{s4}a_{rf}}{m_{u4}}z_3-\frac{(k_{s4}+k_{t4})}{m_{u4}}z_7+\frac{c_{off\,4}}{m_{u4}}z_8$$

$$+\frac{c_{off\,4}l_f}{m_{u4}}z_9-\frac{c_{off\,4}a_{rf}}{m_{u4}}z_{10}-\frac{c_{off\,4}+(1-\alpha)(c_{on4}-c_{off\,4})}{m_{u4}}z_{14} \tag{3.53}$$

$$[\mathbf{B}]=\begin{bmatrix} 0 & \cdots & & 0 \\ \vdots & & & \vdots \\ \frac{k_{t1}}{m_{u1}} & 0 & & \\ 0 & \frac{k_{t2}}{m_{u2}} & 0 & \\ 0 & 0 & \frac{k_{t3}}{m_{u3}} & 0 \\ 0 & 0 & 0 & \frac{k_{t4}}{m_{u4}} \end{bmatrix}^{14\times 4}$$

where $[\mathbf{B}]$ is a 14 by 4 matrix. The motion variables of interest are sprung mass vertical acceleration ($\ddot{x}_1$), sprung mass pitch angular acceleration ($\ddot{x}_2$), sprung mass roll angular acceleration ($\ddot{x}_3$), Front-Left suspension deflection ($x_1+x_2l_f+x_3a_{lf}-x_4$), Front-Right suspension deflection ($x_1+x_2l_f-x_3a_{rf}-x_7$), Rear-Left suspension deflection ($x_1-x_2l_r+x_3a_{lr}-x_5$), Rear-Right suspension deflection ($x_1-x_2l_r-x_3a_{rr}-x_6$), Front-Left tire deflection (x_4-x_{in1}), Front-Right tire deflection (x_7-x_{in4}), Rear-Left tire deflection (x_5-x_{in2}) and Rear-Right tire deflection (x_6-x_{in3}).

Thus accordingly, output matrices $[\mathbf{Y}]$, $[\mathbf{C}]$ and $[\mathbf{D}]$ can be derived based on the motion variables of interest the same way as described in the Q-car case before.

Using this type of model, obtaining vehicle responses in bounce, pitch and roll as well as the possibility of interaction between these responses would become possible. However, complication in the mathematical representation which then would significantly increases computational requirement has hindered many researchers to employ this approach.

Numerical values used in this analysis which are typical for passenger vehicle are summarized in Table 3.7. Typical semi-active damping coefficients are chosen using the relationships of $c_{on1} = c_{on2} = c_{on3} = c_{on4} = 2.2c_s$ and $c_{off1} = c_{off2} = c_{off3} = c_{off4} = 0.2c_s$. Using built-in MATLAB command, natural frequencies of each system are obtained as shown in Table 3.8.

Three types of inputs are possible for this F-car model and used in this work. The first type is called heave input signal, where $x_{in1} = x_{in2} = x_{in3} = x_{in4} = x_{in}$, the second type is pitch input signal, where $x_{in1} = x_{in4} = x_{in}$, $x_{in2} = x_{in3} = -x_{in}$, and the third type is roll input signal, where $x_{in1} = x_{in2} = x_{in}$, $x_{in3} = x_{in4} = -x_{in}$. These inputs are illustrated in Fig. 3.12.

Table 3.7: F-car 7-DOF Model Parameters.

Symbol	Description	Units
m_s	Sprung mass	1460 kg
I_{yy}	Pitch Moment of Inertia	2460 kg m^2
I_{xx}	Roll Moment of Inertia	460 kg m^2
m_{u1}	Front-Left unsprung mass	40 kg
m_{u2}	Rear-Left unsprung mass	35.5 kg
m_{u3}	Rear-Right unsprung mass	35.5 kg
m_{u4}	Front-Right unsprung mass	40 kg
k_{s1}	Front-Left Suspension Stiffness coefficient	19960 N/m
k_{s2}	Rear-Left Suspension Stiffness coefficient	17500 N/m
k_{s3}	Rear-Right Suspension Stiffness coefficient	17500 N/m
k_{s4}	Front-Right Suspension Stiffness coefficient	19960 N/m
c_{s1}	Front-Left Suspension Damping coefficient	1290 N s/m
c_{s2}	Rear-Left Suspension Damping coefficient	1620 N s/m
c_{s3}	Rear-Right Suspension Damping coefficient	1620 N s/m
c_{s4}	Front-Right Suspension Damping coefficient	1290 N s/m
k_{t1}	Front-Left Tire Stiffness coefficient	175500 N/m
k_{t2}	Rear-Left Tire Stiffness coefficient	175500 N/m
k_{t3}	Rear-Right Tire Stiffness coefficient	175500 N/m
k_{t4}	Front-Right Tire Stiffness coefficient	175500 N/m
l_f	Side distance from m_s C.G. to the front axle	1.011 m
l_r	Side distance from m_s C.G. to the rear axle	1.803 m
a_{lf}	Frontal distance from m_s C.G. to the Front-Left axle	0.761 m
a_{lr}	Frontal distance from m_s C.G. to the Rear-Left axle	0.755 m
a_{rr}	Frontal distance from m_s C.G. to the Rear-Right axle	0.755 m
a_{rf}	Frontal distance from m_s C.G. to the Front-Right axle	0.761 m

Table 3.8: Natural frequencies of each F-car system and control policy.

System	ω_{n1}	ω_{n2}	ω_{n3}	ω_{n4}	ω_{n5}	ω_{n6}	ω_{n7}
Passive	6.3164	8.1954	9.4216	69.3515	69.3869	71.9656	72.5396
Skyhook	6.2705	8.0018	9.1994	69.9042	69.9101	73.7042	73.6903
Groundhook	6.2959	7.9954	9.1877	69.9358	69.9407	73.7602	73.7764
Hybrid	6.2677	7.9967	9.1911	69.9296	69.931	73.7431	73.7497

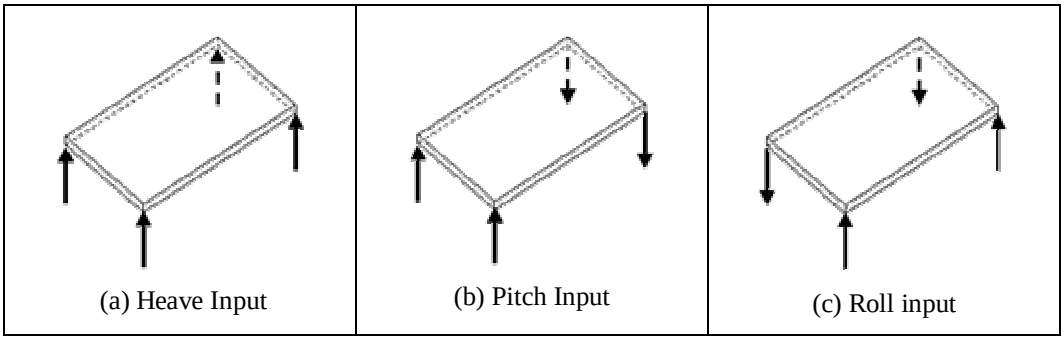

Fig. 3.12: Types of input signals for F-car analysis.

3.5 PERFORMANCE CRITERIA

In the next three chapters, responses of passive system and semiactive control policies of Q-car, H-car and F-car models are compared and analyzed. Three different analyses were conducted, that include frequency-domain response, time-domain transient state response and time-domain steady state response. From these complete analyses, performance comparison between various semiactive control policies and passive system is obtained.

Sprung mass acceleration is observed for ride quality indication. Even though there are several other criteria suggested for this purpose, such as jerk (third derivative of displacement or the slope of acceleration) it is generally accepted by researchers in this area that acceleration provide good indication for vehicle ride. For H-car model, pitch angular accelerations are also looked at and additionally, roll angular acceleration for F-car model.

Other states are also observed to identify any compromise in the other aspects of vehicle dynamics. This includes suspension deflection for rattle space requirement (suspension design limitation) and tire deflection for road holding requirement (vehicle handling). Performance criteria for each analysis are described here.

3.5.1 Frequency-domain Analysis

In frequency-domain analysis, transfer functions of the states of interest are plotted over a frequency span. Transfer function of a linear, time invariant differential equations is generally defined as the ratio of the Laplace transform of the output or response function, to the Laplace transform of the input or driving function with all initial conditions are set to zero (Ogata, 1997). This can be simplified as:

$$\text{Transfer function, TF} = \left.\frac{L[output]}{L[input]}\right|_{\substack{\text{zero initial}\\ \text{conditions}}}$$

Using this analysis, general response of each model and control policies throughout the frequency span can be obtained. Usually one is interested in peak responses or resonances, which occur at the natural frequencies of the system. Response trend at low frequencies – below the natural frequencies, and high frequencies beyond the natural frequencies are also noted and compared. Low responses are preferred in all cases.

There are several ways to obtain this frequency response plot. The one that is used here is by obtaining the steady state peak values of the system response to sinusoidal input, with which the input frequencies are varied throughout the intended frequency span. The frequency response is basically just the maximum response at steady state for each input frequency. To ensure that the approach and code used is correct, initial trial was conducted to compare the simple Q-car 2-DOF model response to another alternative approach.

In this alternative approach, transfer function of any state of the system is obtained by either using MATHEMATICA or using built-in function available in MATLAB. This transfer function, which is in s-domain is then transformed to frequency-domain using MATHEMATICA and the result is transferred back to

MATLAB for plotting. Identical results are obtained in all states of interest except that in some cases the former approach gives different response at low frequency. This is later resolved by setting the steady state time to be higher, since low frequency input would take longer time to reach steady state.

The results for Q-car 2-DOF and F-car 7-DOF were also compared to the work done by Blanchard (2003) with velocity input and identical results are obtained in all Q-car cases while match satisfactorily in the sprung mass response in the F-car model. The unsprung mass, suspensions and tires responses are not identical since the model and method of evaluation used are slightly different. A sample code for Q-car 2-DOF frequency response is attached in Appendix A for reference.

3.5.2 Time-domain Transient State Analysis

In transient state response analysis, the performance criteria of a system usually are specified in terms of the response to a unit step input since this input function can easily be generated and is sufficiently drastic (Ogata, 1997).

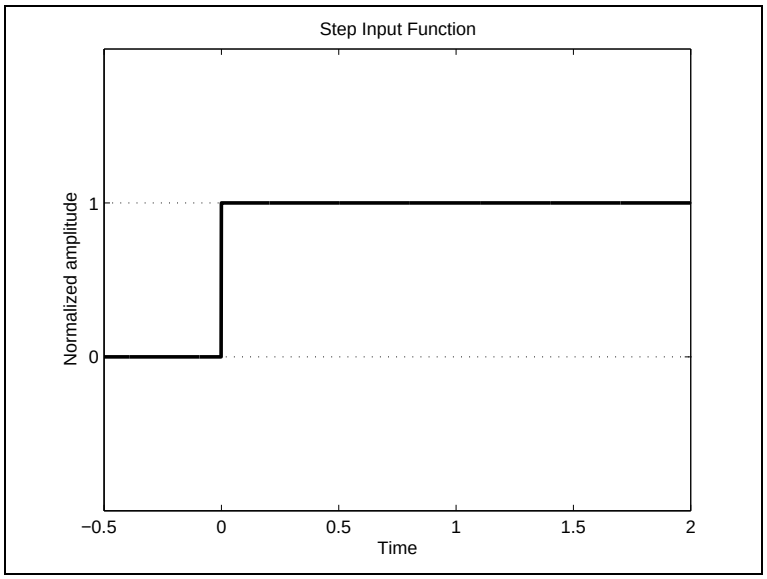

Fig. 3.13: Step input function for transient state response analysis.

The step input function with normalized amplitude is shown in Fig. 3.13. Amplitude of 0.05 m is used throughout this work. This amplitude value has been used by several researchers in their analysis such as Barak *et al.* (2004) and Sun *et al.* (2002), thus is simply taken here for consistency. For this step input signal, the system is set to be at rest (no disturbance) at time, $t < 0$. At time $t = 0$, suddenly the step input of amplitude equal to 0.05 m is applied.

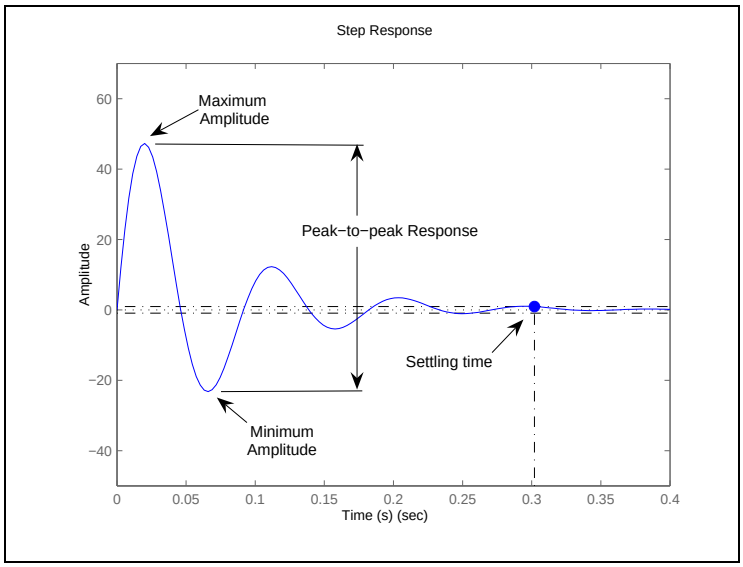

Fig. 3.14: Typical transient state response curve for step input function.

There are several standard performance criteria in control system theory. However for the purpose of this work, only three of them are used that are:

1. Peak-to-peak (PTP) displacement or acceleration.
2. Settling time, t_s.
3. Steady state value.

PTP values are calculated as:

$$\text{PTP} = \max\left(x(t)\right) - \min\left(x(t)\right)$$

where $x(t)$ is either displacement or acceleration, depending on the response of interest. The minimums and maximums are defined as the maximums and minimums of the overshoot. This is shown in Fig. 3.14. This criterion indicate the maximum fluctuation occur in each system and control policies at transient state. Naturally, small fluctuation or PTP value is preferred.

Settling time, t_s is defined as the time required for the system in order for the response to reach and stay within 2% range of steady state value. This is also shown in Fig. 3.14. This criterion indicate how fast the system response to the desired change. Faster response and thus smaller t_s value is desired.

Steady state value is simply the final value of the response as it settles down. Since the input function is only a step function, the steady state value is expected to be zero for sprung mass and unsprung mass accelerations, tire and suspension deflections, while for the sprung mass deflection should converge to 0.05 m if the steady state error is zero in the system.

To ensure that the code used in this analysis is valid, several results obtained in the Q-car 2-DOF using velocity input are compared to the one obtained by Blanchard (2003) and identical results were obtained. A sample code for F-car 7-DOF transient state response is attached in Appendix A for reference.

3.5.3 Time-domain Steady State Analysis

Only a single criterion is used to analyze steady state response that is the Peak-to-peak (PTP) value. Similar to the transient state analysis, PTP can be defined as:

$$\text{PTP} = \max\left(x(t)\right) - \min\left(x(t)\right)$$

However, these maximums and minimums values are taken as the system reaches steady state condition. Sinusoidal function with amplitude of 0.05 m is used as

the input to the system and to obtain the worst case scenario, frequency of the input function is set equal to the natural frequency of the system. The function used is:

Input, $u = 0.05\sin(\omega t)$

where ω is the input frequency and equivalent to the natural frequency of the system. To get a complete observation on all possible worst case scenario, all natural frequencies of the system are analyzed, that is two input frequencies for Q-car, four for H-car and seven for F-car, even though similar responses are expected in some of them due to identical conditions and parameters.

Again the code is compared against the results by Blanchard (2003) for Q-car 2-DOF with velocity input for verification purpose. A sample code for H-car 4-DOF steady state response is attached in Appendix A for reference.

CHAPTER FOUR

FREQUENCY RESPONSE COMPARISON

4.1 INTRODUCTION

In this chapter, the frequency response for each model is presented and comparisons are made between the various models, input types and states. At first, states that are common for all models are compared - m_s vertical acceleration, suspension deflection and tire deflection. Then the response of m_s pitch angular acceleration from the H-car and F-car models are compared. This response is not available and cannot be predicted by the Q-car model.

4.2 ALL MODEL COMPARISON

4.2.1 Sprung Mass Vertical Acceleration

Figs. 4.1 – 4.3 show the frequency response plot of the m_s vertical acceleration response for Q-car, H-car and F-car, respectively. Generally all plots show very similar trends of response. At low frequencies - frequencies below the m_s natural frequencies, all system give identical responses.

As frequency reaches m_s natural frequencies, response in groundhook control become worse than passive while skyhook and hybrid controls become better with skyhook giving the best response. As frequency move further to m_{us} natural frequencies, groundhook control response gives the best response while skyhook and hybrid still have better responses than passive system. Beyond the natural frequencies of the system, all semiactive control policies converge toward the same point, which is

significantly lower passive system. It is noted that hybrid control gives better response than passive throughout the frequency span.

Comparing between heave and pitch input shows quite similar pattern, except in the region between m_s and m_{us} natural frequencies, in which all responses are lower in pitch input.

Comparison between models show that all models give almost identical responses. All responses, regardless of input type have identical convergence of responses towards low and high frequencies. In between the peaks at the natural frequencies, heave input response in H-car and F-car models give very similar responses except that two peaks are observed at the sprung mass natural frequency region – each for pitch and vertical natural frequencies of the sprung mass, instead of only one in the Q-car model. Responses in pitch input however show more significant variations and are generally lower in magnitude.

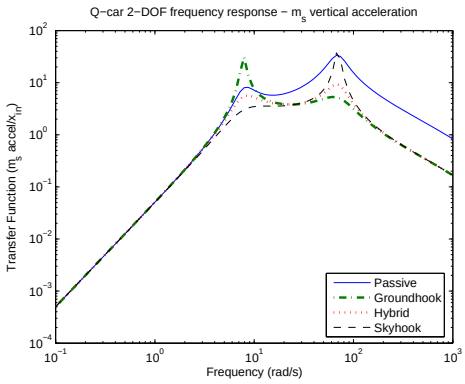

Fig. 4.1: Q-car frequency-domain response - m_s vertical acceleration.

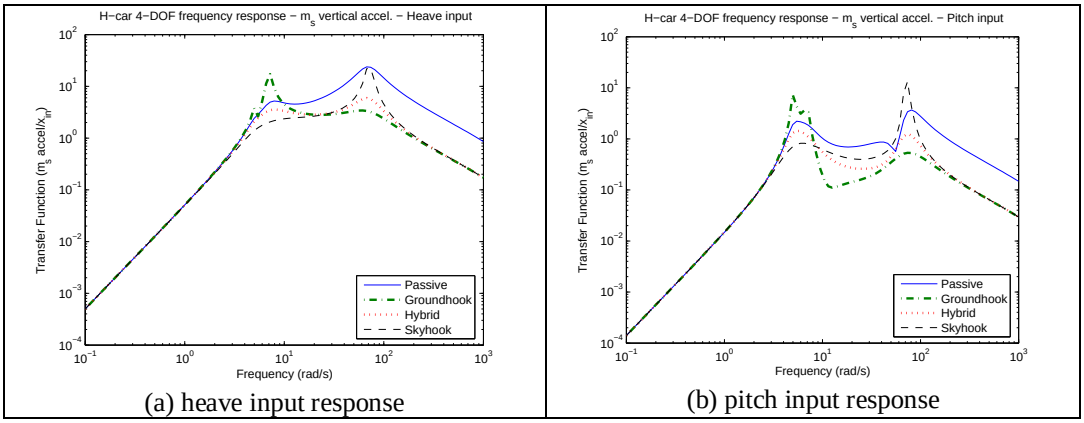

(a) heave input response (b) pitch input response

Fig. 4.2: H-car frequency-domain response - m_s vertical acceleration.

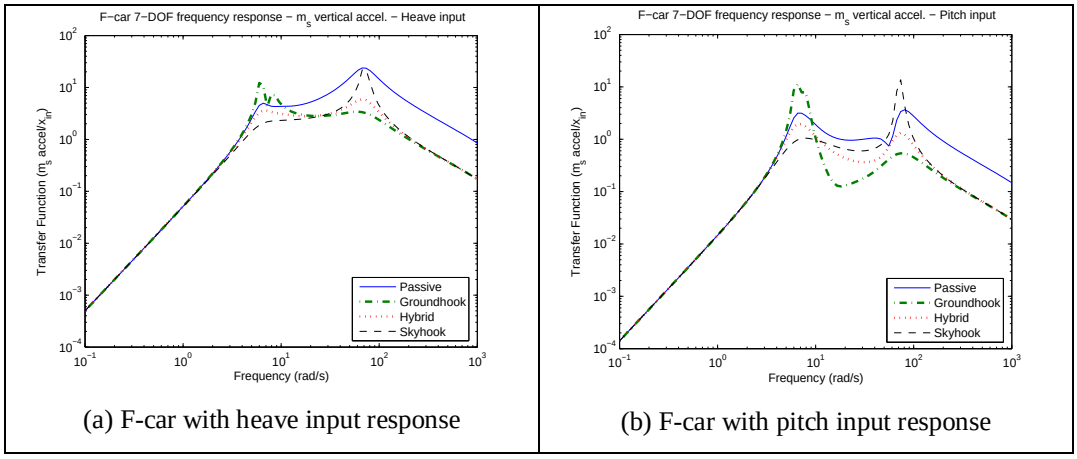

(a) F-car with heave input response (b) F-car with pitch input response

Fig. 4.3: F-car frequency-domain response - m_s vertical acceleration.

4.2.2 Suspension Deflection

Figs. 4.4 – 4.6 show the frequency response plot of the suspension deflection response for Q-car, H-car and F-car, respectively. All suspension response plots show that at low frequencies, groundhook control gives almost exactly the same response as passive. However skyhook and hybrid control policies give significantly higher responses with skyhook being the worst of all, which is up to nearly two orders of magnitude.

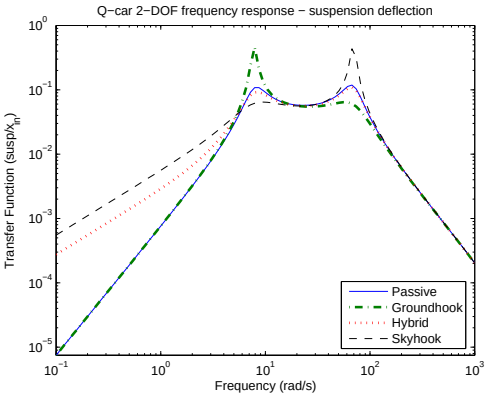

Fig. 4.4: Q-car frequency-domain response - suspension deflection.

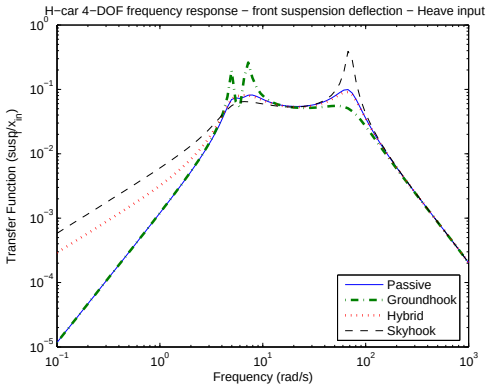

(a) H-car with heave input response - front

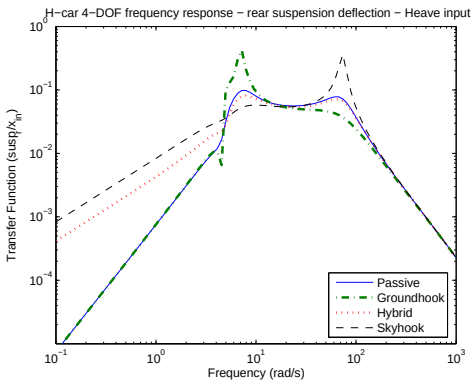

(b) H-car with heave input response - rear

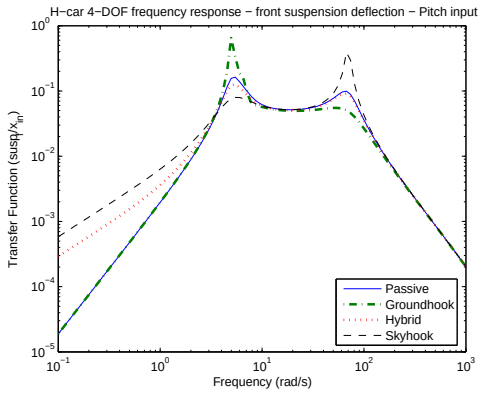

(c) H-car with pitch input response - front

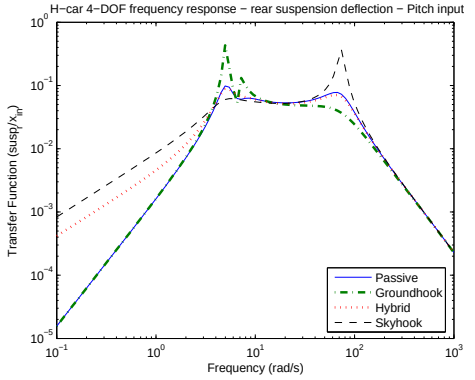

(d) H-car with pitch input response - rear

Fig. 4.5: H-car frequency-domain response - suspension deflection.

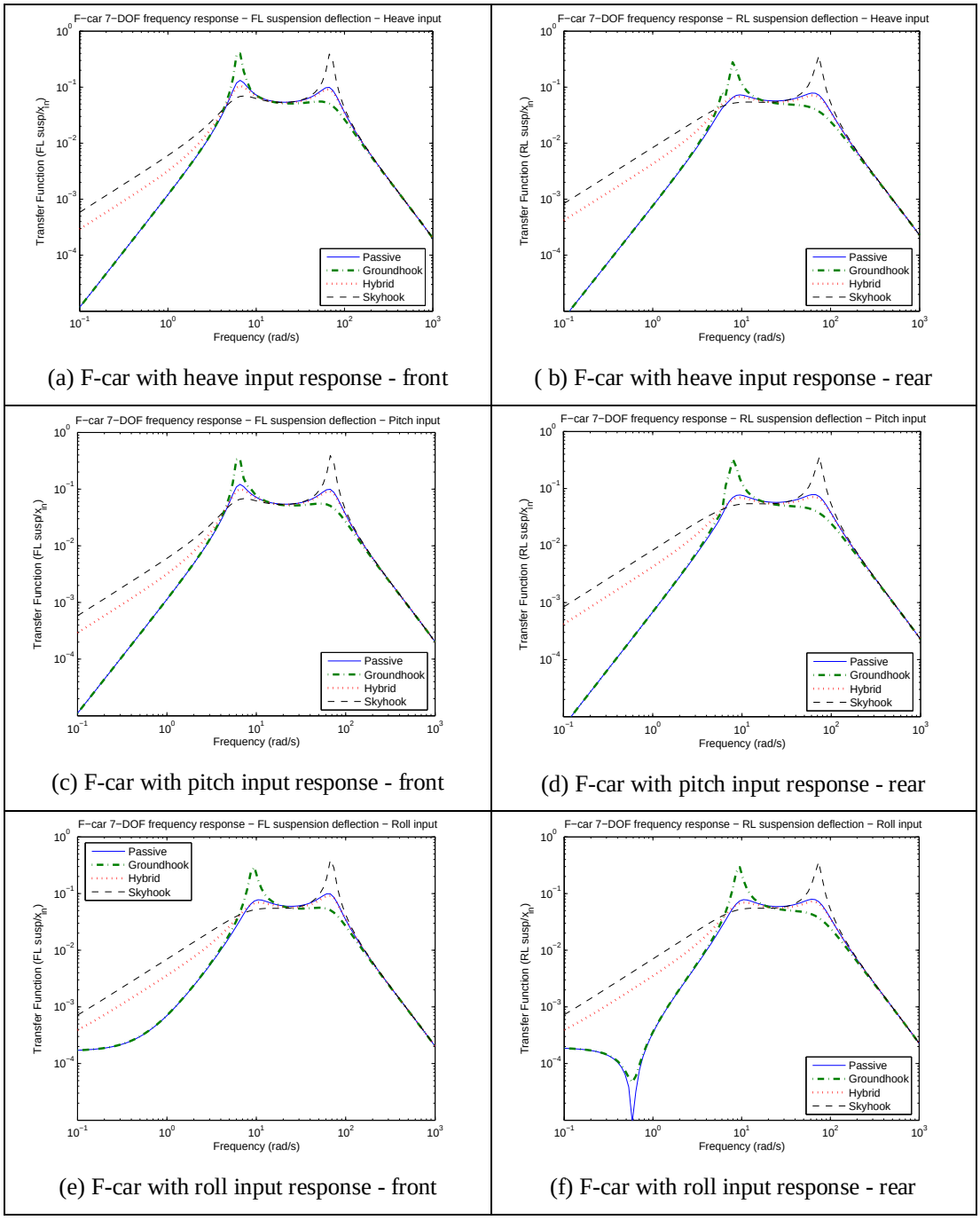

(a) F-car with heave input response - front

(b) F-car with heave input response - rear

(c) F-car with pitch input response - front

(d) F-car with pitch input response - rear

(e) F-car with roll input response - front

(f) F-car with roll input response - rear

Fig. 4.6: F-car frequency-domain response - suspension deflection.

As frequency reaches m_s natural frequencies, response in groundhook control become worse while skyhook and hybrid controls become better than passive. Between the m_s and m_{us} natural frequencies, all systems have almost similar responses. As frequency reaches m_{us} natural frequencies, groundhook control response

give the best response, hybrid control give quite similar response to passive while skyhook control give the worst. Beyond the natural frequencies of the system, all systems converge toward the same value. No significant different in the trends between the front and rear responses. All responses at m_s and m_{us} natural frequencies are at the same order of magnitude.

Comparing between different input types shows very similar trends in all responses with no significant variation other than a sudden drop for passive system and groundhook control policy in roll input at low frequency.

Comparison between models show that while identical convergence is observed at high frequencies, low frequencies responses converge to different values. This phenomenon occurs in all passive and semiactive control policies. Responses in frequency region between the natural frequencies are almost identical except in H-car model where two peaks at m_s natural frequencies are observed. Responses in the fronts are also differs to the rears for both H-car and F-car models. Low frequencies responses of F-car model with roll input show significant variations than the others. This may be due to the computational errors where higher iterations are required for more accurate responses.

4.2.3 Tire Deflection

Figs. 4.7 – 4.9 show the frequency response plot of the tire deflection response for Q-car, H-car and F-car, respectively. At low frequencies, all semiactive control policies give very similar response but significantly higher than passive. As frequency reaches m_s natural frequencies, response in groundhook control become worse while skyhook control become better than passive. Hybrid control gives higher response at the first natural frequency before getting better as the frequency move further.

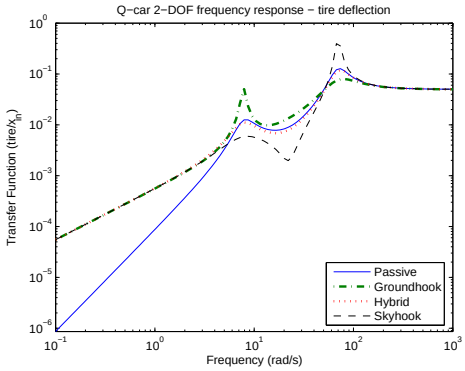

Fig. 4.7: Q-car frequency-domain response - tire deflection.

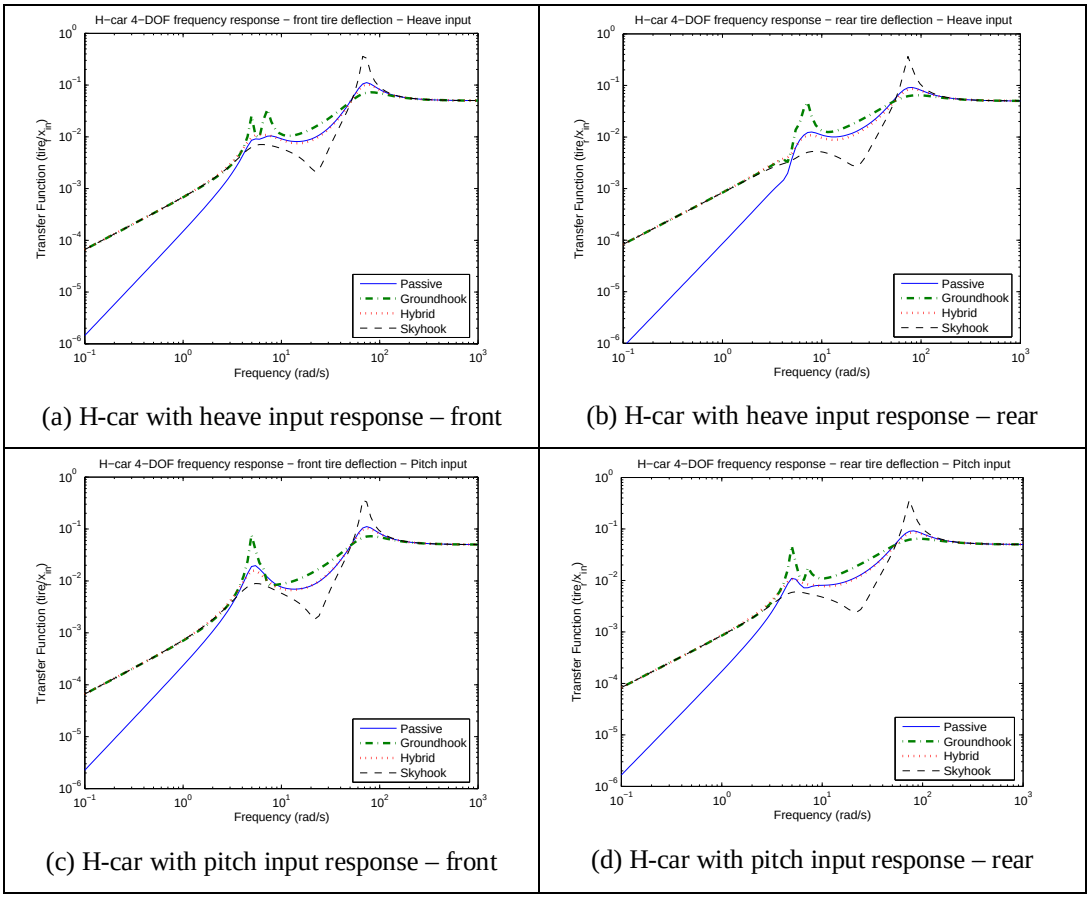

(a) H-car with heave input response – front

(b) H-car with heave input response – rear

(c) H-car with pitch input response – front

(d) H-car with pitch input response – rear

Fig. 4.8: H-car frequency-domain response - tire deflection.

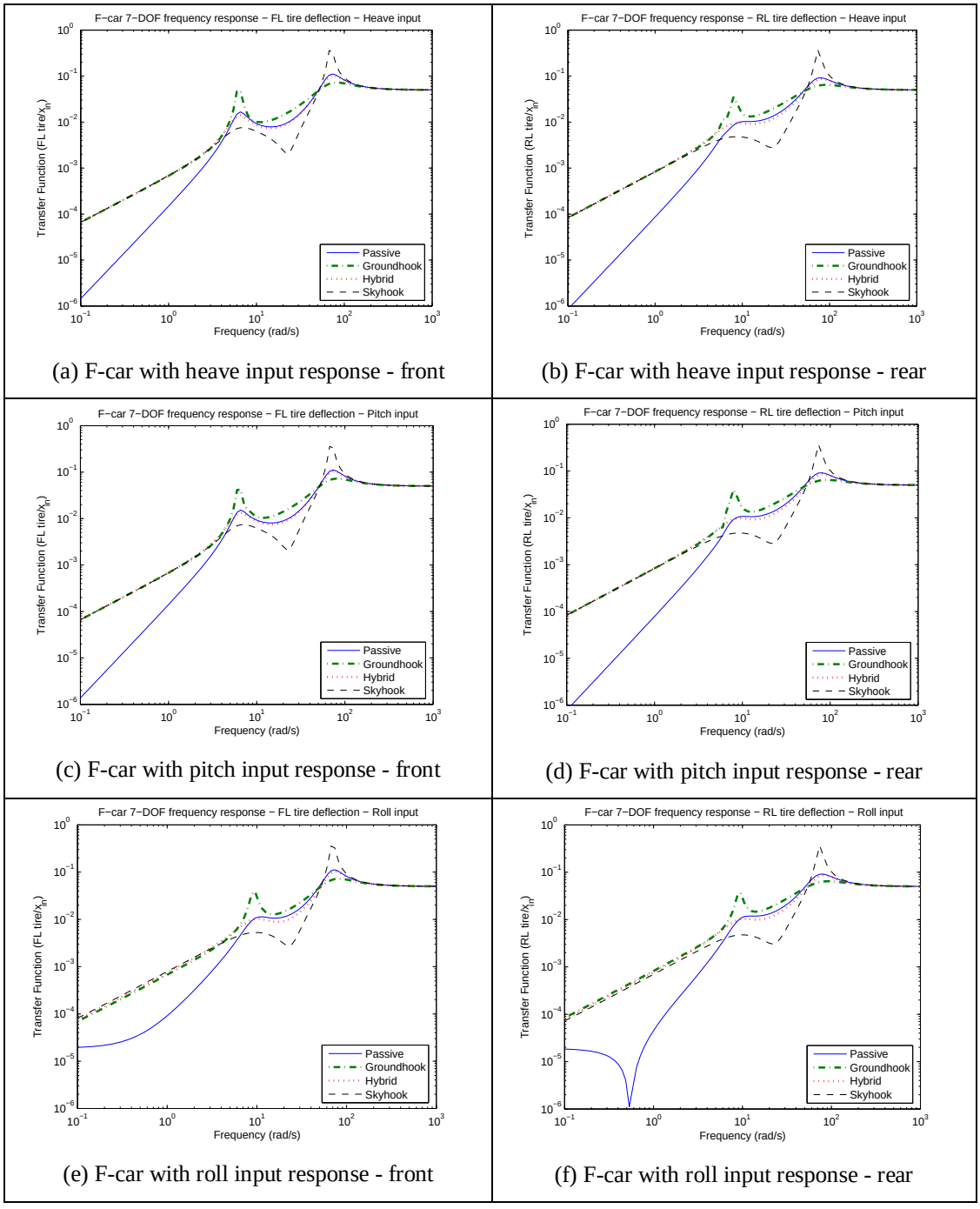

(a) F-car with heave input response - front

(b) F-car with heave input response - rear

(c) F-car with pitch input response - front

(d) F-car with pitch input response - rear

(e) F-car with roll input response - front

(f) F-car with roll input response - rear

Fig. 4.9: F-car frequency-domain response - tire deflection.

Towards the m_{us} natural frequencies, groundhook control response gives the best response, hybrid control gives relatively better response while skyhook gives the worst. Beyond the natural frequencies of the system, all systems converge toward the

same value. It is also noted that the peak at m_{us} natural frequencies are about an order of magnitude higher than that at m_s natural frequencies.

No significant difference in the trends between the fronts and the rears responses other than a sudden drop for passive system and groundhook control policy in roll input at low frequency. Their responses at lower frequencies are also higher than in the heave and pitch input cases.

Comparison between models shows almost similar response as in suspension deflection case. While identical convergence is observed at high frequencies, low frequencies responses converge to different values for all passive and semiactive control policies. Responses in frequency region between the natural frequencies are almost identical except in H-car model where two peaks at m_s natural frequencies are observed. Apparent difference in response between front and rear tires is also present.

4.3 H-CAR AND F-CAR COMPARISON OF PITCH RESPONSE

Almost similar observations as on the m_s vertical acceleration can be made to pitch angular acceleration, except for several differences. At low frequencies, semiactive control policies give significantly higher responses than passive with skyhook being the worst of all. These increases are as high as nearly an order of magnitude. Another different characteristic is skyhook response at m_{us} natural frequencies, where it gives higher response than passive.

Comparing between heave and pitch input shows that at low frequency responses for pitch angular acceleration of semiactive control policies in the pitch input are all similar to passive, while they are higher in heave input.

Comparison between the H-car and F-car models shows that very identical responses are obtained in both models for both input types particularly in low and high

frequency ranges. In the range between the natural frequencies, apparent but not so significant differences are present except that the peak at m_s natural frequencies in F-car model is higher in heave input, but lower in pitch input.

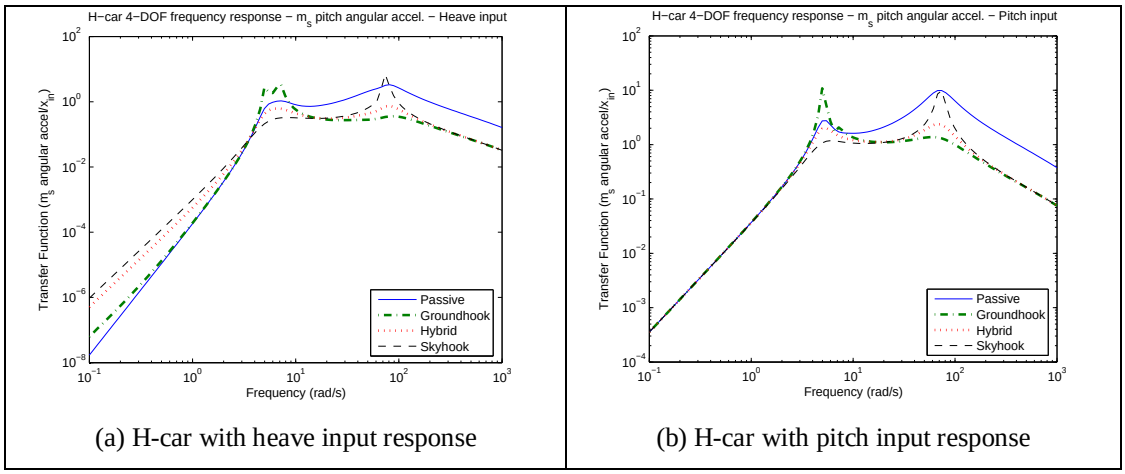

(a) H-car with heave input response (b) H-car with pitch input response

Fig. 4.10: H-car frequency-domain response - m_s pitch angular acceleration.

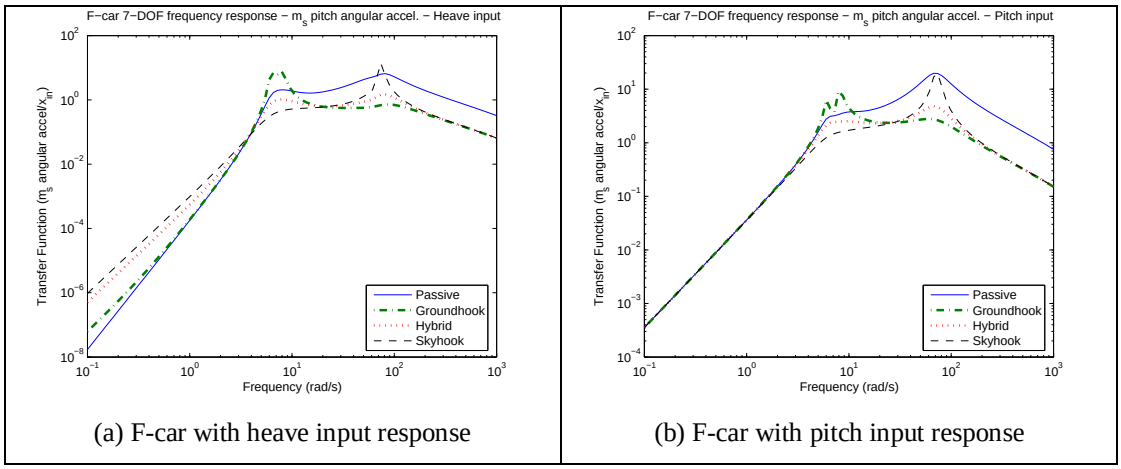

(a) F-car with heave input response (b) F-car with pitch input response

Fig. 4.11: F-car frequency-domain response - m_s pitch angular acceleration.

4.4 CONCLUDING REMARK

With all frequency-domain response observations, it can be said that generally skyhook control policy significantly improves performance of all responses – m_s

accelerations, suspension and tire deflections when input frequency is equivalent to m_s natural frequencies, $\omega_{input} = \omega_{ms}$, while groundhook control policy significantly improves the responses when input frequency is equivalent to m_{us} natural frequencies, $\omega_{input} = \omega_{mus}$. However, their improvements are at the expense of the other responses. Responses in skyhook control policy significantly increase relative to passive system when $\omega_{input} = \omega_{mus}$. Similar case happen in groundhook control policy at $\omega_{input} = \omega_{ms}$. Hybrid system can be considered as a compromise between the two semi-active systems, and generally performs better than the passive system except in some cases particularly at low frequencies.

At frequencies below the natural frequencies of the system, all semiactive control policies do not improve the response but may instead increase. At frequencies beyond the natural frequencies, semiactive control policies either do not change or improve responses. Peak responses at $\omega_{input} = \omega_{mus}$ are generally at least an order of magnitude higher than at $\omega_{input} = \omega_{mus}$ for tire deflection responses.

Comparing between the different input types, generally vertical and pitch accelerations responses are prominent in heave and pitch inputs cases while only roll acceleration response is prominent in roll input. The suspensions and tires responses are generally having similar trends for frequencies toward m_s natural frequencies and beyond. At lower frequencies, suspension and tire responses for roll input of passive system and groundhook are higher.

CHAPTER FIVE

TRANSIENT STATE RESPONSE COMPARISON

5.1 INTRODUCTION

In this chapter, the transient state response for each model is presented and comparisons are made between the various models, input types and states. As discussed at length in Chapter 3, three criteria are observed in the analysis – steady state value, Peak-to-Peak value (*PTP*) and settling time, t_s. At first, states that are common for all models are compared - m_s vertical acceleration, suspension deflection and tire deflection. Then the response of m_s pitch angular acceleration from the H-car and F-car models are compared. This response is not available and cannot be predicted by the Q-car model.

5.2 ALL MODEL COMPARISON

5.2.1 Sprung Mass Vertical Acceleration

Figs. 5.1 – 5.3 show the summary of m_s vertical acceleration response in transient state response plot for Q-car, H-car and F-car, respectively and Table 5.1 summarizes for all models. The results generally show that skyhook control gives better response than passive in *PTP* in the heave input, while passive response are better than all semiactive control policies in the pitch input. In the settling time, t_s skyhook turns out to give the best response overall. Groundhook control gives better *PTP* response but with significantly the largest t_s. Hybrid control gives the best *PTP* value but come with a slight increase in t_s. All responses converge to zero at steady state.

Comparisons between models show that both settling time and *PTP* values vary in all model, location and input type. While there is no particular trend in settling time, *PTP* values in Q-car model are generally higher than H-car and F-car models. Pitch input for both H-car and F-car models generally give higher settling time value, but smaller in *PTP* relative to heave input.

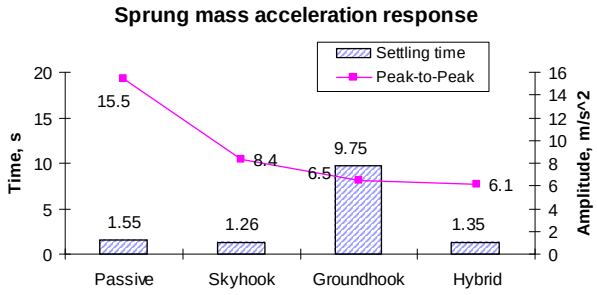

Fig. 5.1: Q-car transient state response - m_s vertical acceleration.

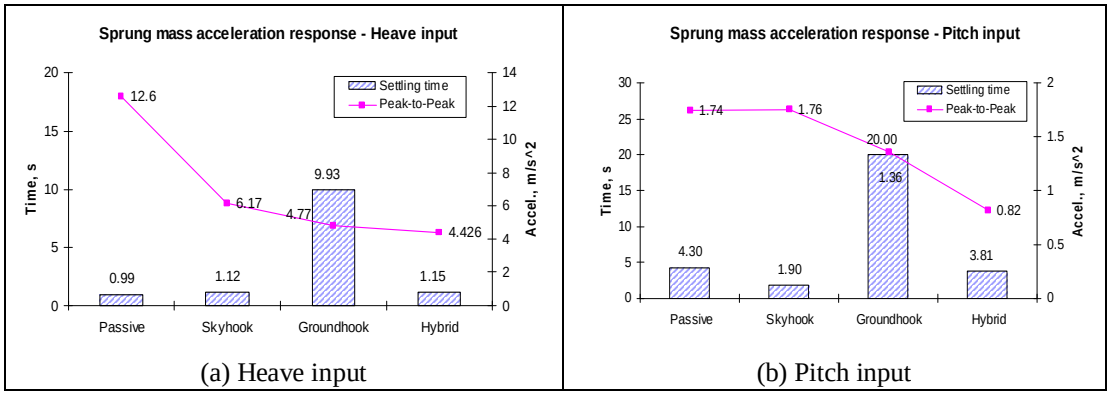

(a) Heave input (b) Pitch input

Fig. 5.2: H-car transient state response - m_s vertical acceleration.

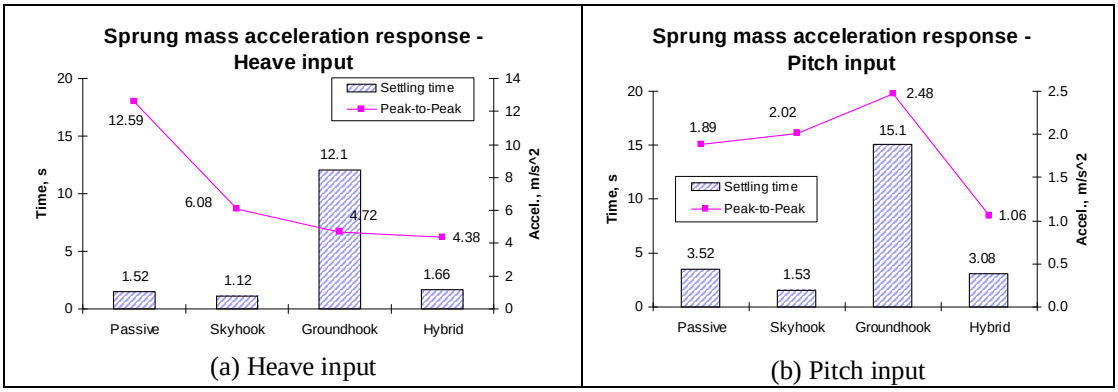

Fig. 5.3: F-car transient state response - m_s vertical acceleration.

Table 5.1: All models time domain transient state response – m_s vertical acceleration.

Model	Input type	Settling time (s)				Peak-to-Peak (m/s^2)			
		Passive	Skyhook	Grndhook	Hybrid	Passive	Skyhook	Grndhook	Hybrid
Q-car		1.55	1.26	9.75	1.35	15.45	8.38	6.49	6.09
H-car	Heave	0.99	1.12	9.93	1.15	12.6	6.17	4.77	4.43
H-car	Pitch	4.3	1.9	20	3.81	1.74	1.76	1.36	0.82
F-car	Heave	1.52	1.12	12.1	1.66	12.59	6.08	4.72	4.38
F-car	Pitch	3.52	1.53	15.1	3.08	1.89	2.02	2.48	1.06

5.2.2 Suspension Deflection

Figs. 5.4 – 5.6 show the summary of suspension deflection responses in transient state response plot for Q-car, H-car and F-car, respectively and Table 5.2 summarizes for all models. All figures show that skyhook control gives the worst response in *PTP* but the best response in t_s. Groundhook control gives better *PTP* response than passive in the front suspension but worse in the rear. Its response however is significantly the largest in t_s. Lastly, hybrid control gives the best *PTP* value and better than passive in t_s. All responses converge to zero at steady state. Responses in the front suspension are higher than in the rear.

Comparison between models show that settling time in all models, locations and input types varies from one to another. Thus F-car response can not be predicted

accurately by Q-car and H-car models. The trend of responses according to the system and control policies however remains consistent, that is skyhook and groundhook control policies giving the best and the worst responses, respectively. *PTP* values are almost similar in all models even though in general F-car values are slightly lower than the others.

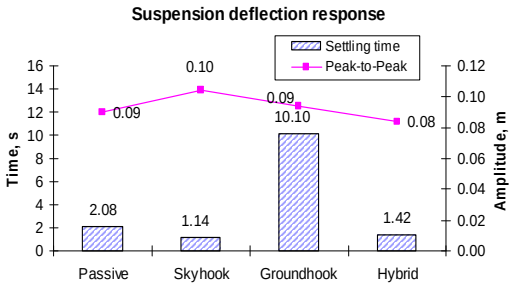

Fig. 5.4: Q-car transient state response - suspension deflection.

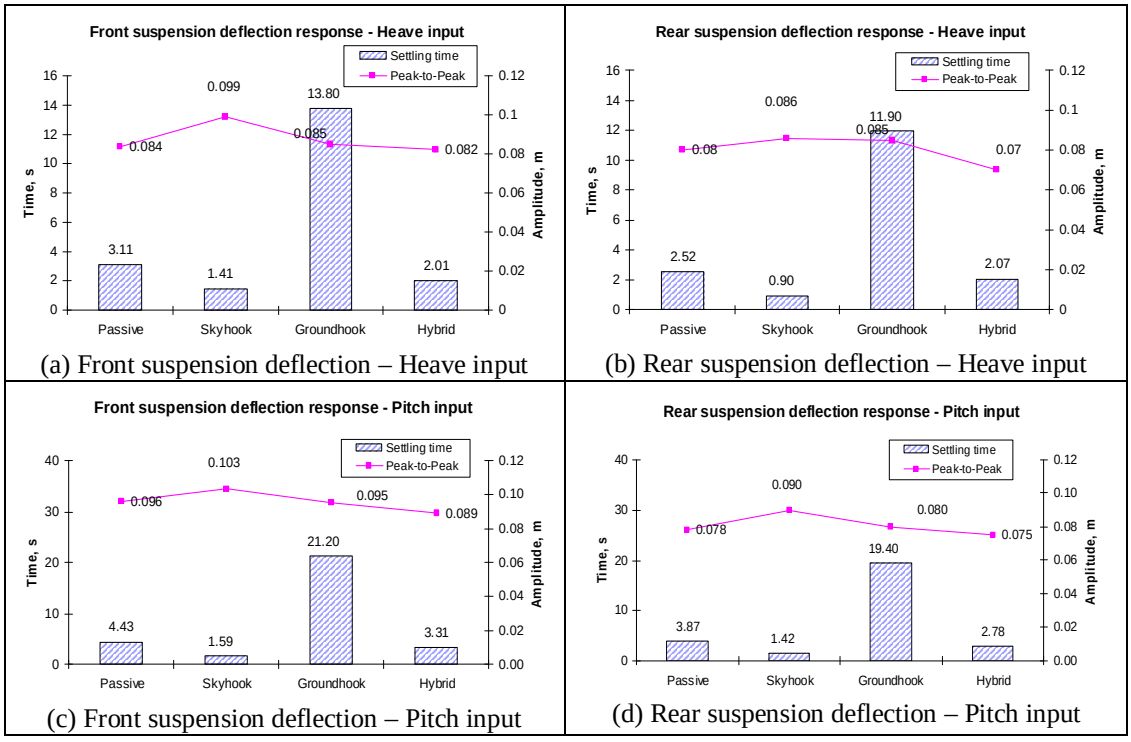

(a) Front suspension deflection – Heave input

(b) Rear suspension deflection – Heave input

(c) Front suspension deflection – Pitch input

(d) Rear suspension deflection – Pitch input

Fig. 5.5: H-car transient state response - suspension deflection.

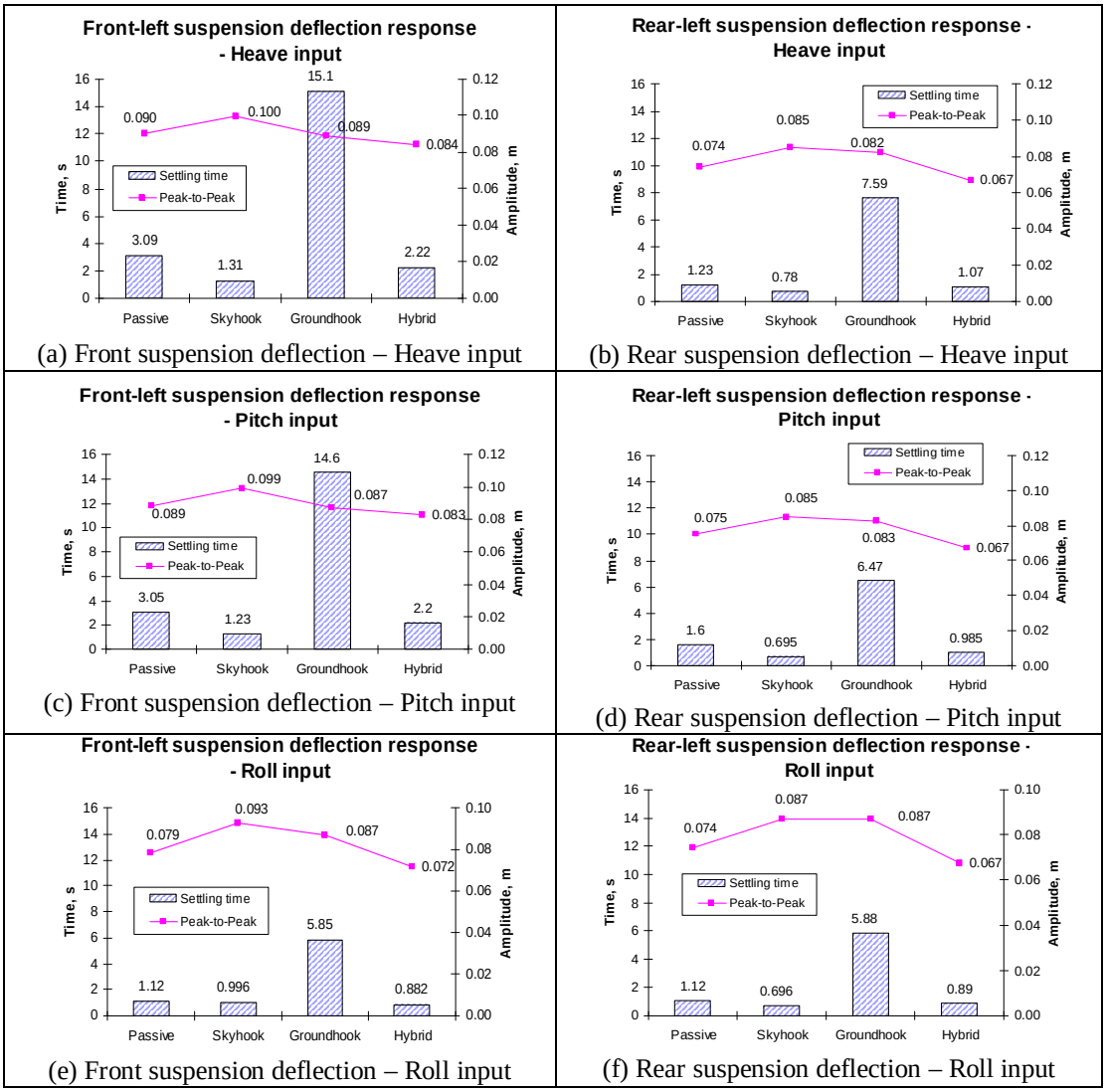

(a) Front suspension deflection – Heave input

(b) Rear suspension deflection – Heave input

(c) Front suspension deflection – Pitch input

(d) Rear suspension deflection – Pitch input

(e) Front suspension deflection – Roll input

(f) Rear suspension deflection – Roll input

Fig. 5.6: F-car transient state response - suspension deflection.

Table 5.2: All models time domain transient state response – suspension deflection.

	Input type	Location	Settling time (s)				Peak-to-Peak (m)			
Model			Passive	Skyhook	Grndhook	Hybrid	Passive	Skyhook	Grndhook	Hybrid
Q-car			2.08	1.14	10.1	1.42	0.09	0.1	0.09	0.08
H-car	Heave	Front	3.11	1.41	13.8	2.01	0.084	0.099	0.085	0.082
H-car	Heave	Rear	2.52	0.9	11.9	2.07	0.08	0.086	0.085	0.07
H-car	Pitch	Front	4.43	1.59	21.2	3.31	0.096	0.103	0.095	0.089
H-car	Pitch	Rear	1.91	1.27	9.4	1.44	0.078	0.09	0.08	0.075
F-car	Heave	Front	3.09	1.31	15.1	2.22	0.09	0.1	0.089	0.084
F-car	Heave	Rear	1.23	0.78	7.59	1.07	0.074	0.085	0.082	0.067
F-car	Pitch	Front	3.05	1.23	14.6	2.2	0.089	0.099	0.087	0.083
F-car	Pitch	Rear	1.6	0.695	6.47	0.985	0.075	0.085	0.083	0.067
F-car	Roll	Front	1.12	0.996	5.85	0.882	0.079	0.093	0.087	0.072
F-car	Roll	Rear	1.12	0.696	5.88	0.89	0.074	0.087	0.087	0.067

5.2.3 Tire Deflection

Figs. 5.7 – 5.9 show the summary of suspension deflection responses in transient state response plot for Q-car, H-car and F-car, respectively and Table 5.3 summarizes for all models. All figures show that skyhook control gives the worst response in *PTP*. The responses in t_s are lower than passive for the front tires but higher in the rear. Groundhook control gives the best *PTP* response but the worst in t_s. Lastly, hybrid control gives better than passive in all responses except for the rear t_s. All responses converge to zero at steady state.

Comparing between the rears and fronts responses shows that in all cases the front responses are higher than the rear. Comparing between all input types, the values are almost the same for *PTP* in all cases and t_s for the rears in roll input. t_s for the front tires in roll input is noticeably lower than the others.

Comparison between models show that settling time in all models, locations and input types varies from one to another. Thus F-car response can not be predicted accurately by Q-car and H-car models. The trend of responses according to the system and control policies also varies – while either skyhook or hybrid give the best response in H-car and Q-car, passive system gives the best in most of F-car model. Groundhook control however remains consistently the worst response. *PTP* values are almost similar in all models even though in general Q-car values are slightly higher than the others.

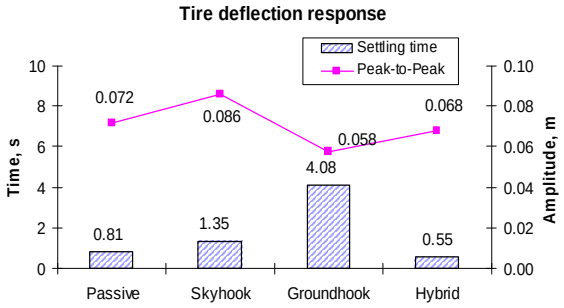

Fig. 5.7: Q-car transient state response - tire deflection.

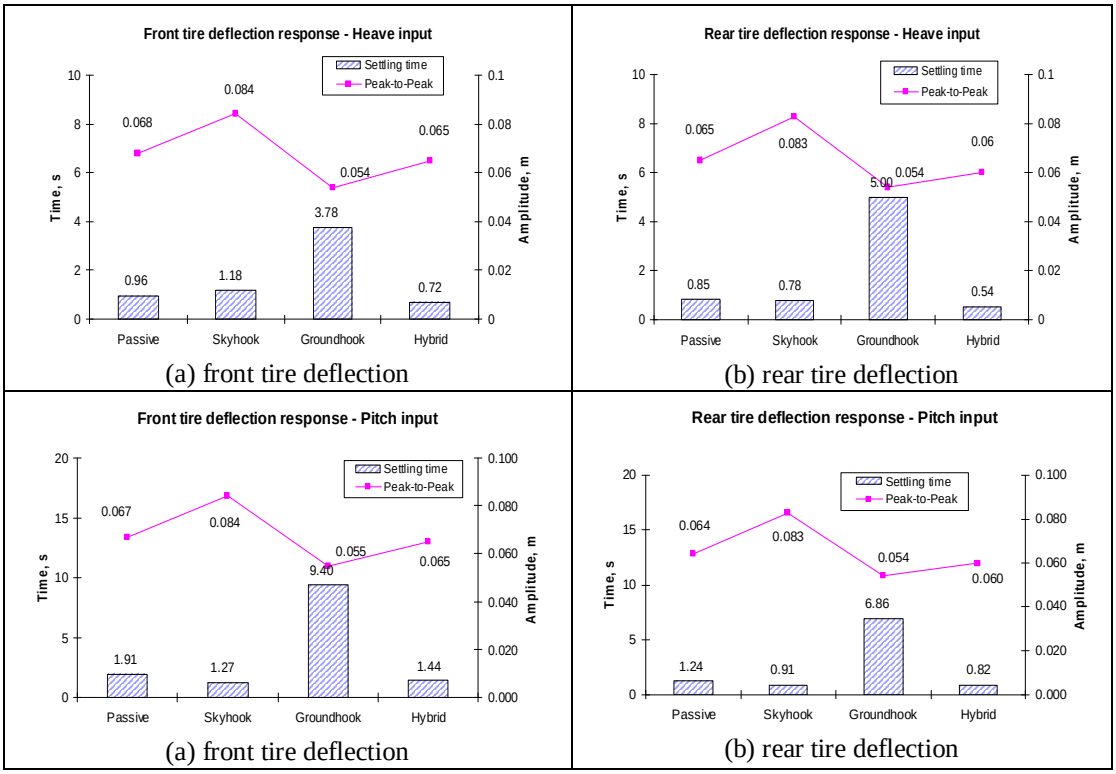

Fig. 5.8: H-car transient state response - tire deflection.

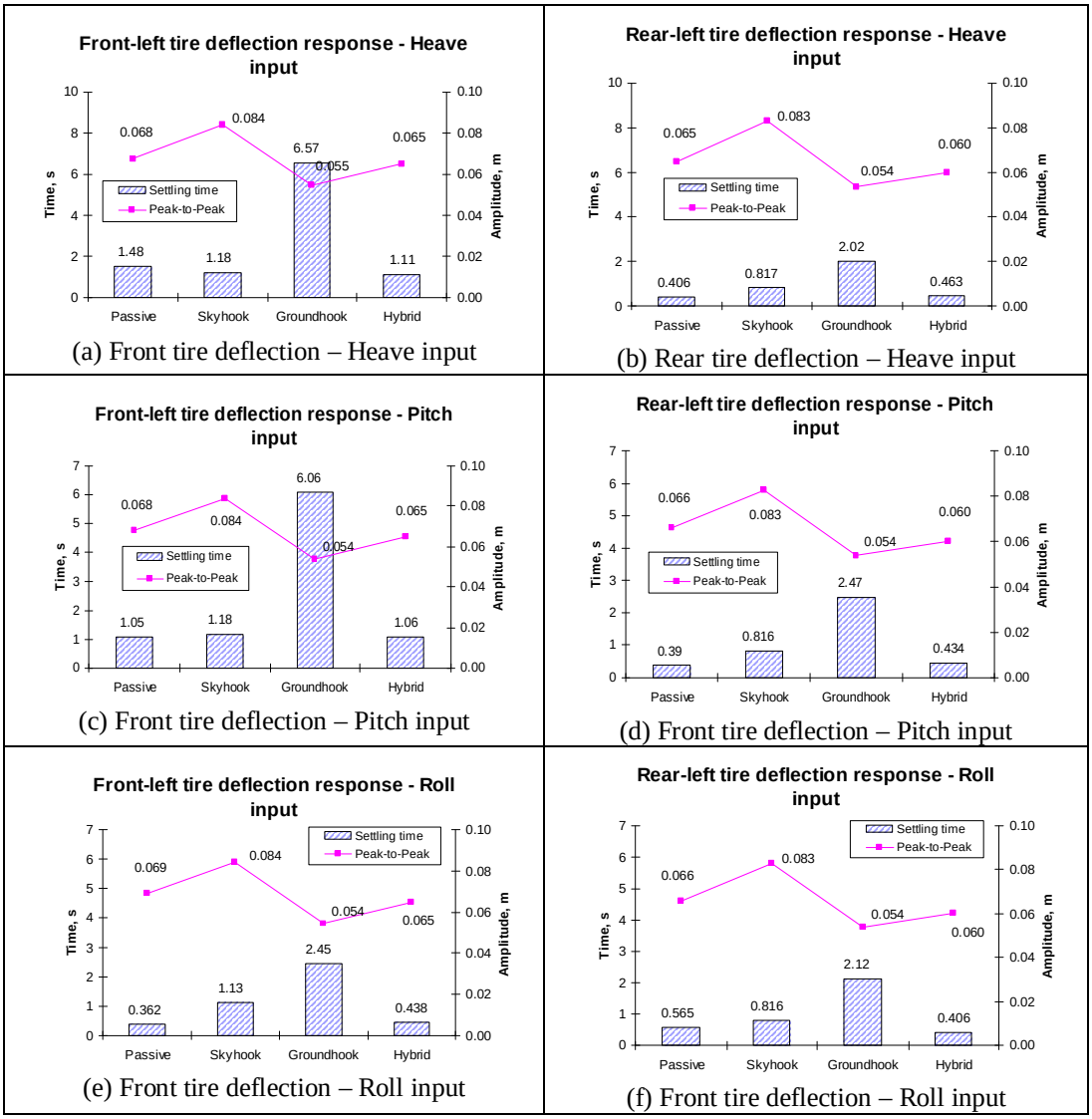

Fig. 5.9: F-car transient state response - tire deflection.

Table 5.3: All models time domain transient state response – Tire deflection.

Model	Input type	Location	Settling time (s)				Peak-to-Peak (m)			
			Passive	Skyhook	Grndhook	Hybrid	Passive	Skyhook	Grndhook	Hybrid
Q-car			0.81	1.35	4.08	0.55	0.072	0.086	0.058	0.068
H-car	Heave	Front	0.96	1.18	3.78	0.72	0.068	0.084	0.054	0.065
H-car	Heave	Rear	0.85	0.78	5	0.54	0.065	0.083	0.054	0.06
H-car	Pitch	Front	1.91	1.27	9.4	1.44	0.067	0.084	0.055	0.065
H-car	Pitch	Rear	1.24	0.91	6.86	0.82	0.064	0.083	0.054	0.06
F-car	Heave	Front	1.48	1.18	6.57	1.11	0.068	0.084	0.055	0.065
F-car	Heave	Rear	0.406	0.817	2.02	0.463	0.065	0.083	0.054	0.06
F-car	Pitch	Front	1.05	1.18	6.06	1.06	0.068	0.084	0.054	0.065
F-car	Pitch	Rear	0.39	0.816	2.47	0.434	0.066	0.083	0.054	0.06
F-car	Roll	Front	0.362	1.13	2.45	0.438	0.069	0.084	0.054	0.065
F-car	Roll	Rear	0.565	0.816	2.12	0.406	0.066	0.083	0.054	0.06

5.3 H-CAR AND F-CAR COMPARISON OF PITCH RESPONSE

The m_s pitch angular acceleration response, as shown in Figs. 5.10 and 5.11, and Table 5.4, shows similar observation as in the vertical acceleration response. Comparing between vertical acceleration and pitch acceleration responses shows that generally vertical acceleration gives higher response in *PTP*, while t_s value is higher in pitch acceleration.

Comparison between models shows that settling time in transient state responses are different in all models and input types. It is also noted that the value in H-car model is generally higher than F-car model in the respective input type. *PTP* values are also different in all models and input types, but it appears that the values in F-car are about twice the values of H-car in the respective input type.

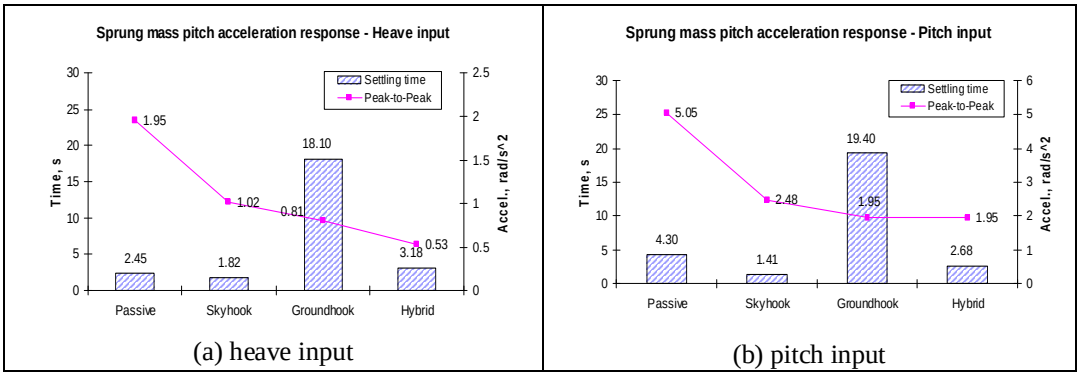

(a) heave input (b) pitch input

Fig. 5.10: H-car transient state response – m_s pitch angular acceleration.

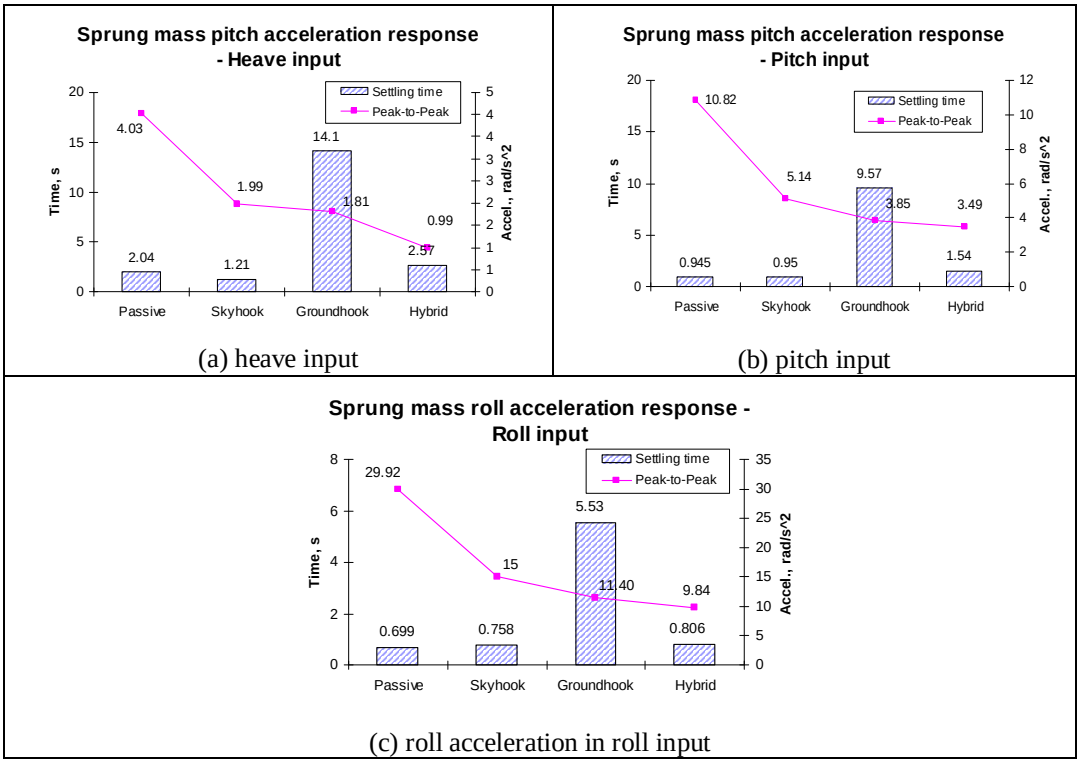

Fig. 5.11: F-car transient state response – m_s pitch angular acceleration.

Table 5.4: H-car and F-car models time domain transient state response – m_s pitch angular acceleration.

Model	Input type	Settling time (s)				Peak-to-Peak (rad/s^2)			
		Passive	Skyhook	Grndhook	Hybrid	Passive	Skyhook	Grndhook	Hybrid
H-car	Heave	2.45	1.82	18.1	3.18	1.95	1.02	0.81	0.53
H-car	Pitch	4.3	1.41	19.4	2.68	5.05	2.48	1.95	1.95
F-car	Heave	2.04	1.21	14.1	2.57	4.03	1.99	1.81	0.99
F-car	Pitch	0.95	0.95	9.57	1.54	10.82	5.14	3.85	3.49

5.4 CONCLUDING REMARK

With all transient state time-domain response observations, it can be said that generally, for peak-to-peak response, hybrid control policy turns out to give the best response in m_s (vertical, pitch and roll acceleration) and suspension deflection responses for all input types. On the other hand, groundhook control gives the best responses for tire deflection responses. For the settling time, t_s skyhook control gives

the best response to m_s and suspension responses in heave and pitch inputs. Other than that, there is no particular control that is advantageous than the others.

It is also noted that responses in groundhook system generally takes significantly longer time to settle. Even though in some cases, passive system gives the best response, it can be said that hybrid control provides the best compromise of response overall.

Generally the front system gives higher responses than the rear system in all input types. Also vertical response is higher than pitch response in heave input case, while pitch response is higher in pitch input. The tire and suspension responses do not vary significantly in heave and pitch input. The settling times in roll input are generally lower than in other input types.

CHAPTER SIX

STEADY STATE RESPONSE COMPARISON

6.1 INTRODUCTION

In this chapter, the steady state response for each model is presented and comparisons are made between the various models, input types and states. As discussed in Chapter 3, to obtain the worst case scenario, frequency of the input function is set equal to the natural frequency of the system. Thus, in the case of Q-car model, two input frequencies are analyzed, while four and seven input frequencies are used in the H-car and F-car, respectively. For the purpose of comparison, the input frequencies are categorized into two, namely the m_s natural frequencies ($\omega_{input} = \omega_{ms}$) and m_{us} natural frequencies ($\omega_{input} = \omega_{ms}$). Only the highest response values (i.e. the worst response) in each category are presented here.

At first, states that are common for all models are compared - m_s vertical acceleration, suspension deflection and tire deflection. Then the response of m_s pitch angular acceleration from the H-car and F-car models are compared.

6.2 ALL MODEL COMPARISON

6.2.1 Sprung Mass Vertical Acceleration

Figs. 6.1 – 6.3 show the summary of m_s vertical acceleration and pitch angular acceleration responses (*PTP* values) in steady state for Q-car, H-car and F-car, respectively and Table 6.1 summarizes for all models. For vertical acceleration response, comparing to passive system as reference, skyhook control policy gives better response for cases when $\omega_{input} = \omega_{ms}$, but worse when $\omega_{input} = \omega_{mus}$. On the other

hand, response of groundhook control policy is the worse overall for cases when $\omega_{input} = \omega_{mus}$, but worse when $\omega_{input} = \omega_{ms}$. Hybrid control policy provides significantly better response than passive in all input frequencies. Generally heave and pitch input types give almost similar response trends.

Comparisons between models show that, steady state response values vary in all cases, which means that the values depends on model, location and input type. While the values in Q-car model responses are generally high in both m_s and m_{us} natural frequencies, the values in H-car and F-car models are generally almost similar.

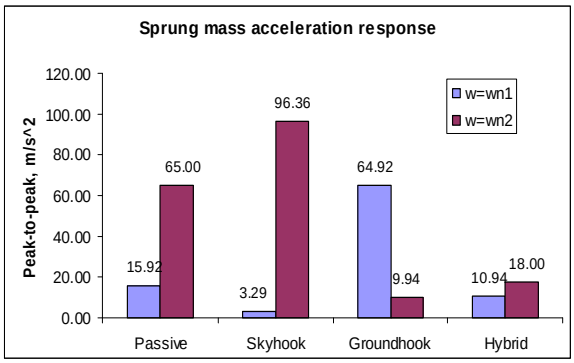

Fig. 6.1: Q-car steady state response - m_s vertical acceleration.

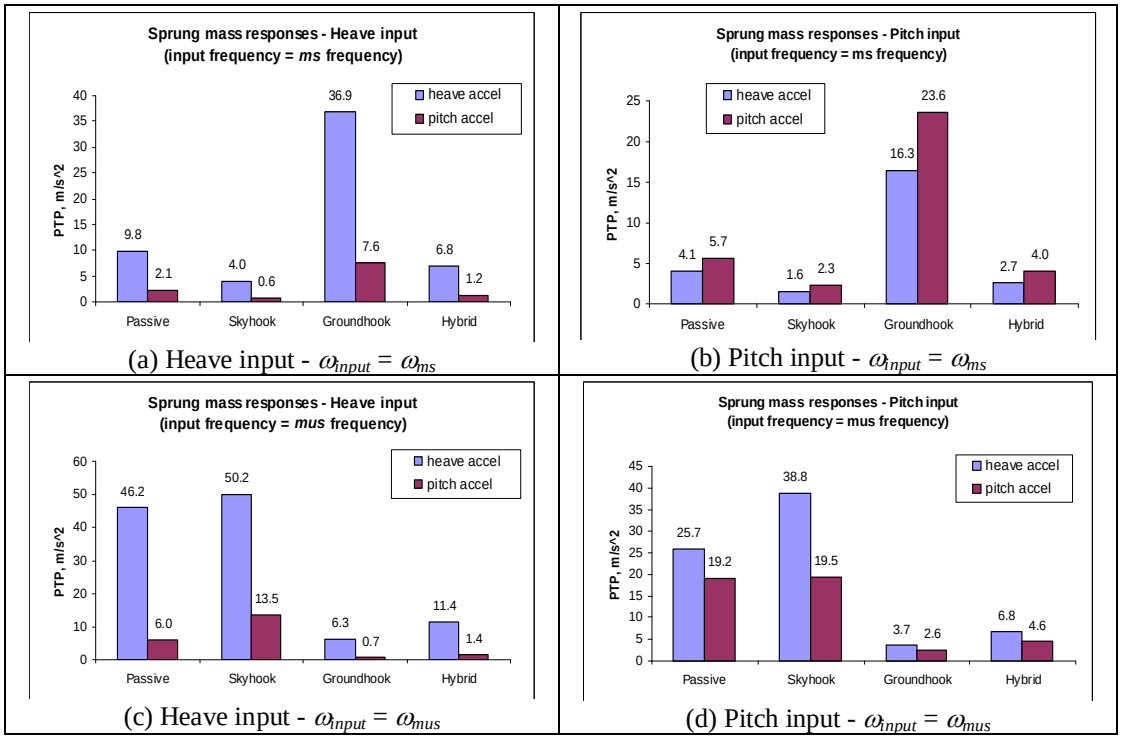

(a) Heave input - $\omega_{input} = \omega_{ms}$ (b) Pitch input - $\omega_{input} = \omega_{ms}$

(c) Heave input - $\omega_{input} = \omega_{mus}$ (d) Pitch input - $\omega_{input} = \omega_{mus}$

Fig. 6.2: H-car steady state response – m_s vertical acceleration.

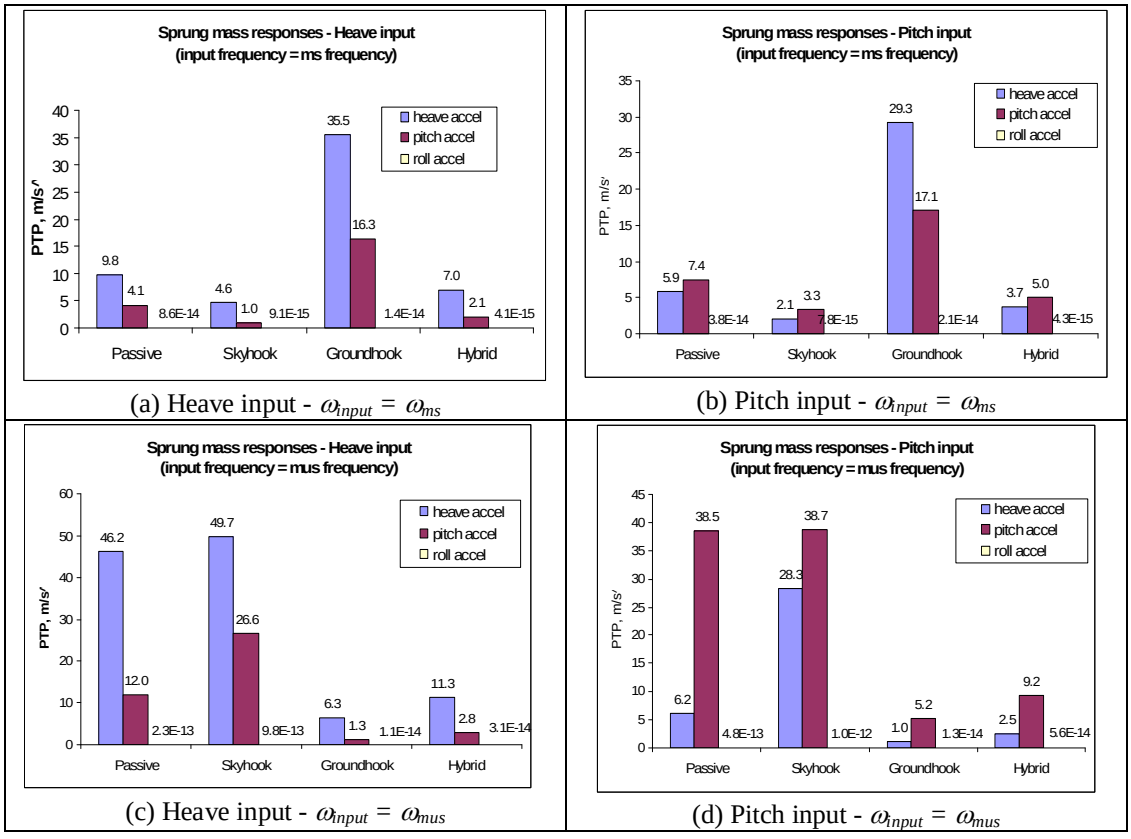

(a) Heave input - $\omega_{input} = \omega_{ms}$ (b) Pitch input - $\omega_{input} = \omega_{ms}$

(c) Heave input - $\omega_{input} = \omega_{mus}$ (d) Pitch input - $\omega_{input} = \omega_{mus}$

Fig. 6.3: F-car steady state response – m_s vertical acceleration.

Table 6.1: All models time domain steady state response – m_s vertical acceleration.

	Model	Input type	Peak-to-Peak (m/s^2)			
			Passive	Skyhook	Grndhook	Hybrid
m_s peak	Q-car		15.92	3.29	64.92	10.94
	H-car	Heave	9.78	4.02	36.88	6.8
	H-car	Pitch	4.07	1.46	16.34	2.7
	F-car	Heave	9.84	4.63	35.48	7
	F-car	Pitch	5.92	2.028	29.29	3.75
m_{us} peak	Q-car		65	96.36	9.94	18
	H-car	Heave	46.16	50.2	6.34	11.36
	H-car	Pitch	25.75	38.78	3.68	6.83
	F-car	Heave	46.2	49.68	6.34	11.33
	F-car	Pitch	6.18	28.31	1.04	2.53

6.2.2 Suspension Deflection

Figs. 6.4 – 6.6 show the summary of suspension deflection response in steady state for Q-car, H-car and F-car, respectively and Table 6.2 summarizes for all models. Generally, skyhook control policy gives better response at $\omega_{input} = \omega_{ms}$ but the worse at $\omega_{input} = \omega_{mus}$. On the other hand, groundhook control policy is the worst at $\omega_{input} = \omega_{ms}$, but the best at $\omega_{input} = \omega_{mus}$. Hybrid control policy provides better response than passive in all input frequencies. Comparing between the front and the rear suspensions shows no significant difference.

Comparisons between models show that *PTP* values in m_s natural frequencies vary in all models, locations and input types. The values in m_{us} natural frequencies are very similar for H-car and F-car models, while Q-car values are relatively higher.

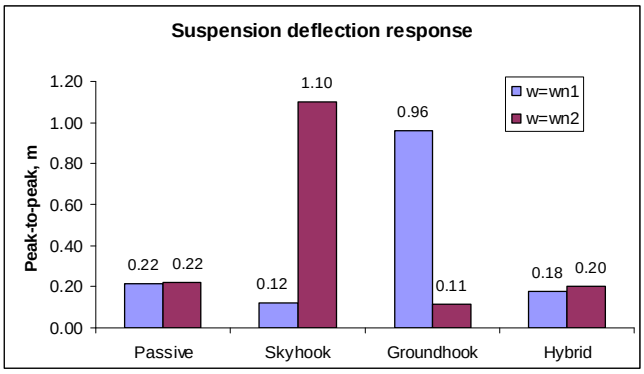

Fig. 6.4: Q-car steady state response – suspension deflection.

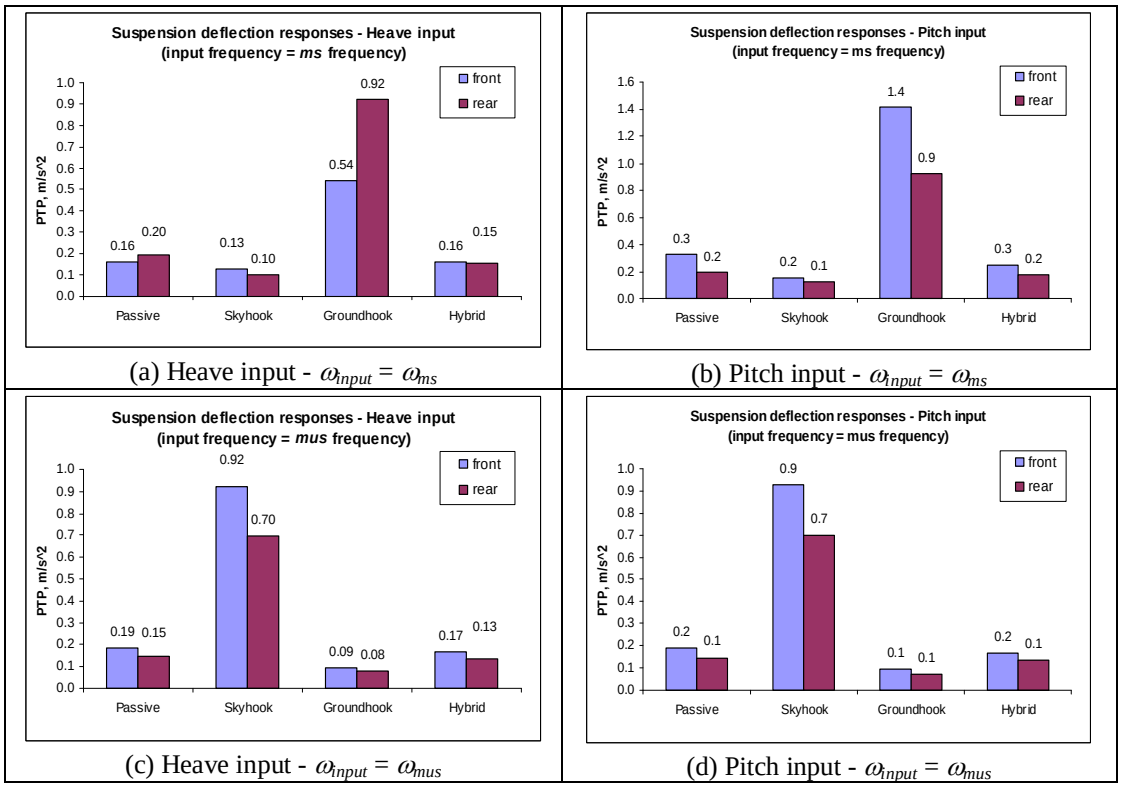

(a) Heave input - $\omega_{input} = \omega_{ms}$

(b) Pitch input - $\omega_{input} = \omega_{ms}$

(c) Heave input - $\omega_{input} = \omega_{mus}$

(d) Pitch input - $\omega_{input} = \omega_{mus}$

Fig. 6.5: H-car steady state response – suspension deflection.

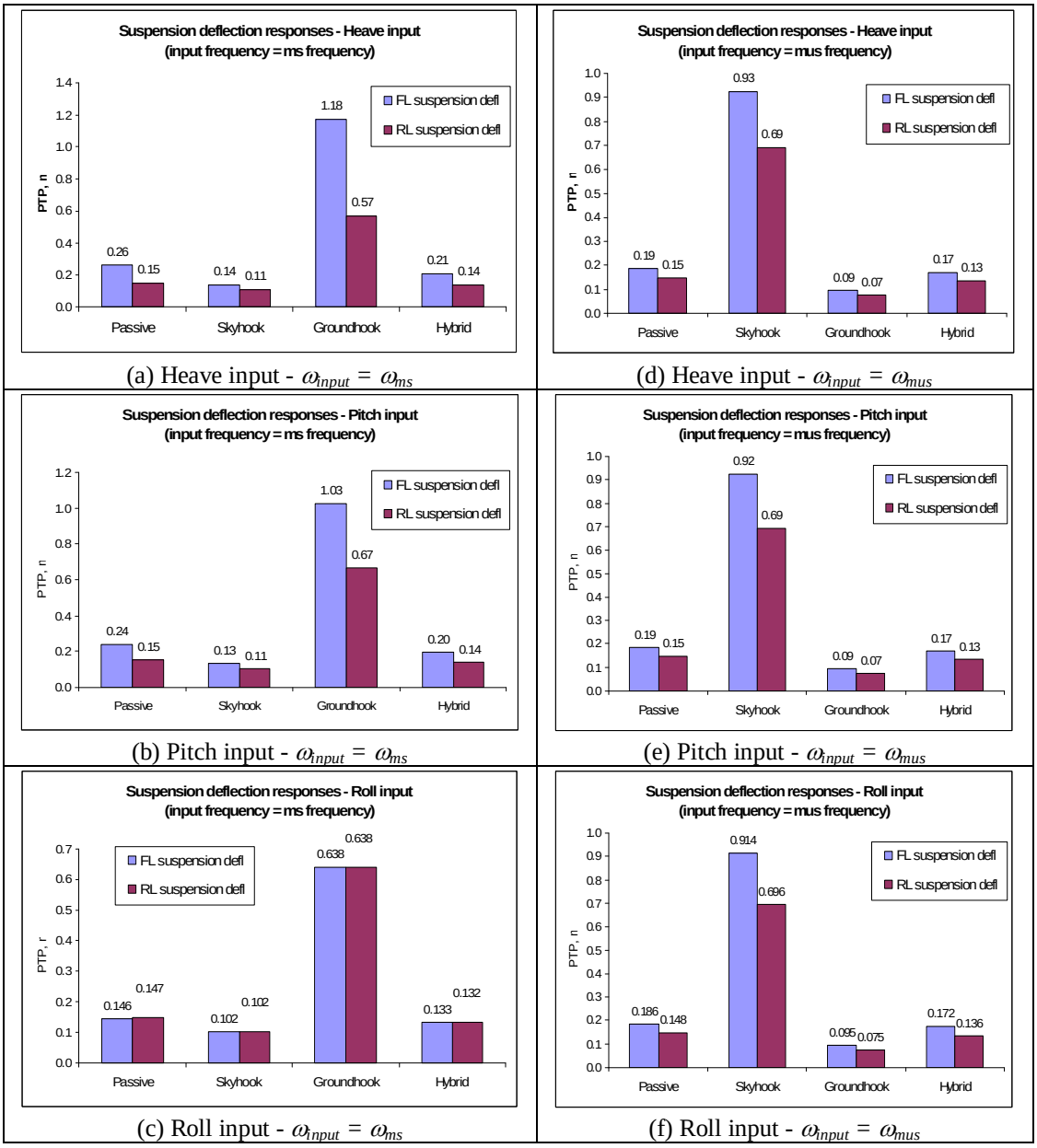

Fig. 6.6: F-car steady state response – m_s acceleration.

Table 6.2: All models time domain steady state response – suspension deflection.

	Model	Input type	Location	Peak-to-Peak (m)			
				Passive	Skyhook	Grndhook	Hybrid
m_s peak	Q-car			0.22	0.12	0.96	0.18
	H-car	Heave	Front	0.162	0.13	0.544	0.162
	H-car	Heave	Rear	0.196	0.102	0.92	0.154
	H-car	Pitch	Front	0.326	0.154	1.411	0.25
	H-car	Pitch	Rear	0.2	0.122	0.928	0.176
	F-car	Heave	Front	0.262	0.137	1.176	0.208
	F-car	Heave	Rear	0.146	0.106	0.57	0.136
	F-car	Pitch	Front	0.24	0.134	1.025	0.196
	F-car	Pitch	Rear	0.154	0.106	0.667	0.138
	F-car	Roll	Front	0.146	0.102	0.638	0.133
	F-car	Roll	Rear	0.147	0.102	0.638	0.132
m_{us} peak	Q-car			0.22	1.1	0.11	0.2
	H-car	Heave	Front	0.186	0.924	0.094	0.17
	H-car	Heave	Rear	0.148	0.696	0.076	0.134
	H-car	Pitch	Front	0.188	0.93	0.094	0.17
	H-car	Pitch	Rear	0.148	0.696	0.074	0.134
	F-car	Heave	Front	0.187	0.926	0.094	0.171
	F-car	Heave	Rear	0.148	0.693	0.075	0.135
	F-car	Pitch	Front	0.187	0.925	0.094	0.171
	F-car	Pitch	Rear	0.148	0.693	0.075	0.135
	F-car	Roll	Front	0.186	0.914	0.094	0.172
	F-car	Roll	Rear	0.148	0.696	0.075	0.136

6.2.3 Tire Deflection

Figs. 6.4 – 6.6 show the summary of tire deflection response in steady state for Q-car, H-car and F-car, respectively and Table 6.2 summarizes for all models. Generally, skyhook control policy gives better response at $\omega_{input} = \omega_{ms}$ but the worse at $\omega_{input} = \omega_{mus}$. On the other hand, groundhook control policy is the worst at $\omega_{input} = \omega_{ms}$, but the best at $\omega_{input} = \omega_{mus}$. Hybrid control policy provides better response than passive in all input frequencies. Comparing between the front and rear tires, and between different input type shows no significant difference.

Comparisons between models show that *PTP* values in m_s natural frequencies vary in all models, locations and input types. The values in m_{us} natural frequencies are very similar for H-car and F-car models, while Q-car values are relatively higher.

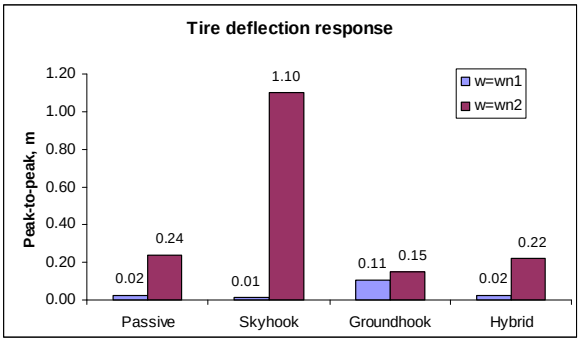

Fig. 6.7: Q-car steady state response – suspension deflection.

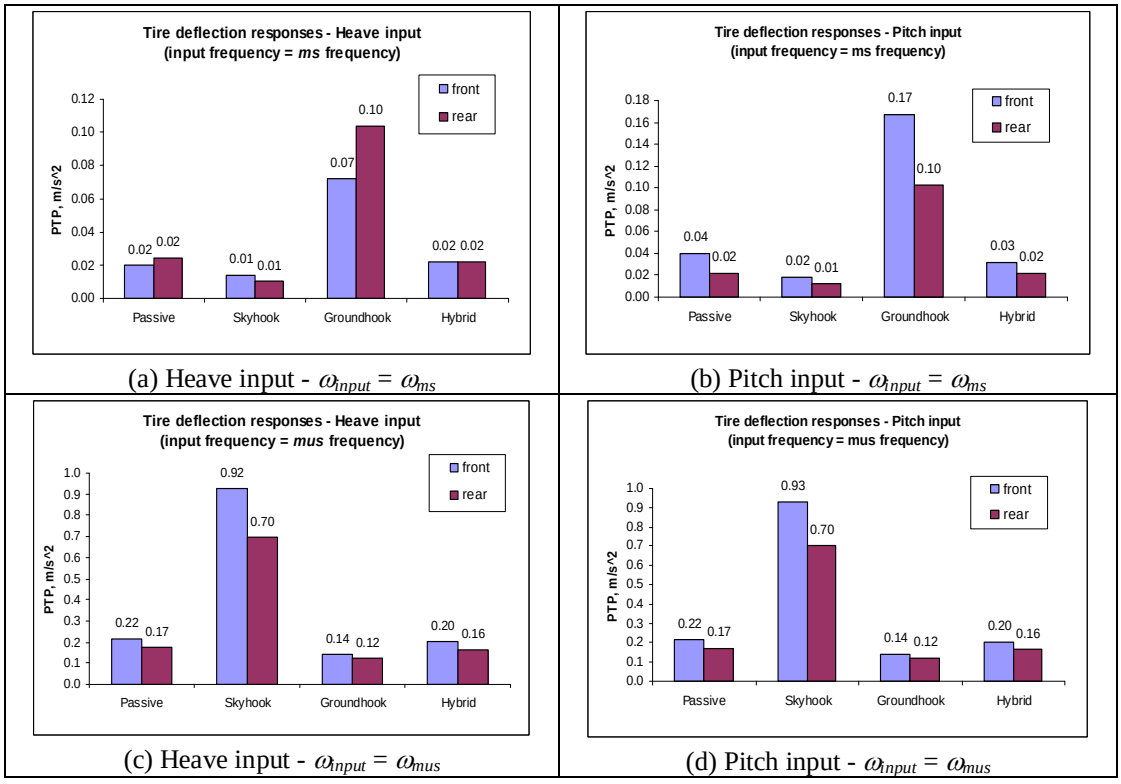

(a) Heave input - $\omega_{input} = \omega_{ms}$

(b) Pitch input - $\omega_{input} = \omega_{ms}$

(c) Heave input - $\omega_{input} = \omega_{mus}$

(d) Pitch input - $\omega_{input} = \omega_{mus}$

Fig. 6.8: H-car steady state response – tire deflection.

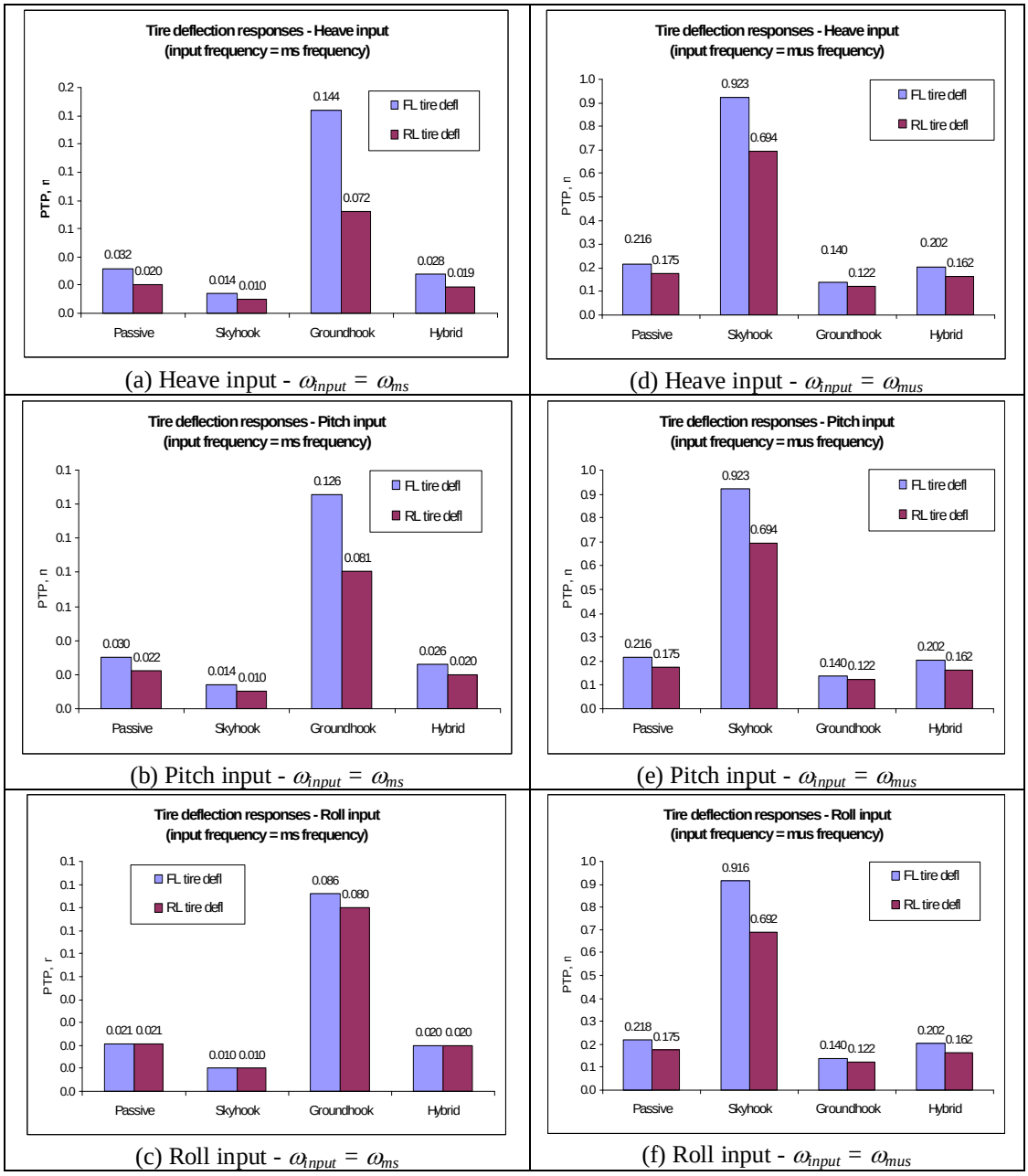

(a) Heave input - $\omega_{input} = \omega_{ms}$

(d) Heave input - $\omega_{input} = \omega_{mus}$

(b) Pitch input - $\omega_{input} = \omega_{ms}$

(e) Pitch input - $\omega_{input} = \omega_{mus}$

(c) Roll input - $\omega_{input} = \omega_{ms}$

(f) Roll input - $\omega_{input} = \omega_{mus}$

Fig. 6.9: F-car steady state response – tire deflection.

Table 6.3: All models time domain steady state response – tire deflection.

	Model	Input type	Location	Peak-to-Peak (m)			
				Passive	Skyhook	Grndhook	Hybrid
m_s peak	Q-car			0.02	0.01	0.11	0.02
	H-car	Heave	Front	0.02	0.014	0.072	0.022
	H-car	Heave	Rear	0.024	0.01	0.104	0.022
	H-car	Pitch	Front	0.04	0.018	0.168	0.032
	H-car	Pitch	Rear	0.022	0.012	0.102	0.022
	F-car	Heave	Front	0.032	0.014	0.144	0.028
	F-car	Heave	Rear	0.02	0.01	0.072	0.019
	F-car	Pitch	Front	0.03	0.014	0.126	0.026
	F-car	Pitch	Rear	0.022	0.01	0.081	0.02
	F-car	Roll	Front	0.021	0.01	0.086	0.02
	F-car	Roll	Rear	0.021	0.01	0.08	0.02
m_{us} peak	Q-car			0.24	1.1	0.15	0.22
	H-car	Heave	Front	0.216	0.924	0.14	0.202
	H-car	Heave	Rear	0.174	0.696	0.122	0.162
	H-car	Pitch	Front	0.216	0.928	0.14	0.202
	H-car	Pitch	Rear	0.174	0.7	0.122	0.162
	F-car	Heave	Front	0.216	0.923	0.14	0.202
	F-car	Heave	Rear	0.175	0.694	0.122	0.162
	F-car	Pitch	Front	0.216	0.923	0.14	0.202
	F-car	Pitch	Rear	0.175	0.694	0.122	0.162
	F-car	Roll	Front	0.218	0.916	0.14	0.202
	F-car	Roll	Rear	0.175	0.691	0.122	0.162

6.3 H-CAR AND F-CAR COMPARISON OF PITCH RESPONSE

The summary of results for m_s pitch angular acceleration responses is already shown in Figs. 6.1 – 6.3 and Table 6.4 summarizes for all models. Very similar response trend as in vertical acceleration response is observed, that is comparing to passive system as reference, skyhook control policy gives better response for cases when $\omega_{input} = \omega_{ms}$, but worse when $\omega_{input} = \omega_{mus}$. On the other hand, response of groundhook control policy is the worse overall for for cases when $\omega_{input} = \omega_{mus}$, but worse when $\omega_{input} = \omega_{ms}$. Hybrid control policy provides significantly better response than passive in all input frequencies. Generally heave and pitch input types give almost similar response trends.

Comparisons between models show that at both m_s and m_{us} natural frequencies, values in H-car model are generally lower than in F-car. Closer look at the values indicate that at m_s natural frequencies, F-car values are about twice the values of H-car model in heave input, while in pitch input the difference is slightly lower. At m_{us} natural frequencies, F-car values are twice the values of H-car in both input types.

Table 6.4: H-car and F-car models time domain steady state response – m_s pitch angular acceleration.

	Model	Input type	Peak-to-Peak (m/s^2)			
			Passive	Skyhook	Grndhook	Hybrid
m_s peak	H-car	Heave	2.14	0.64	7.62	1.24
	H-car	Pitch	5.66	2.32	23.55	4
	F-car	Heave	4.14	1.01	16.31	2.08
	F-car	Pitch	7.43	3.33	17.12	5.03
m_{us} peak	H-car	Heave	6.02	13.46	0.66	1.38
	H-car	Pitch	19.24	19.54	2.58	4.62
	F-car	Heave	11.97	26.62	1.31	2.77
	F-car	Pitch	38.48	38.72	5.18	9.23

6.4 CONCLUDING REMARK

With all steady state time-domain response observations, it can be said that, generally skyhook control policy significantly improves performance of all responses – m_s vertical accelerations, and suspension and tire deflections when input frequency is equivalent to m_s natural frequencies, while groundhook control policy significantly improves responses when input frequency is equivalent to m_{us} natural frequencies. However, their improvements are at the expense of the other responses. Responses in skyhook control policy significantly increase relative to passive system when $\omega_{input} = \omega_{mus}$ while similar case happened in groundhook control policy at $\omega_{input} = \omega_{ms}$. Hybrid system can be considered as a compromise between the two semi-active systems, and generally performs better than passive system.

Comparing between front and rear system responses (suspension and tire deflection), generally shows no significant difference. Comparing between different input types, generally vertical response is higher than pitch response in heave input case, while pitch response is higher in pitch input. Roll response is not significant at heave and pitch inputs, while vertical and pitch responses are not significant at roll input. Suspensions and tires responses in heave and pitch inputs are generally similar in all input frequencies.

CHAPTER SEVEN

RMS ANALYSIS OF H-CAR 2-DOF MODEL

7.1 INTRODUCTION

The work shown here is based on a H-car 2-DOF model. This is to some extent an extension of the work done by Chalasani (1986a) for Q-car passive and active suspensions system, and Blanchard (2003) for Q-car semiactive suspensions using the skyhook, groundhook, and hybrid configurations.

The objective of this work is to study the root mean square responses (RMS) to velocity and acceleration input for four state variables: the m_s vertical acceleration, the m_s pitch angular acceleration and the deflection of the suspensions. The RMS values for the first two variables can be used as a measure of vibration isolations for m_s vertical and pitch motion, and the third and fourth as a measure of the rattle space requirement. After deriving the expressions of interest, the relationship between vibration isolations and suspension deflections are studied and discussed.

7.2 MODEL FORMULATION

The model of passive system is shown in Fig. 7.1 and semiactive system in Fig. 7.2. The model of the semiactive system used in this analysis is actually uses the actual passive representation of the semiactive suspension. This is discussed in detail by Goncalves (2001) for the skyhook, groundhook, and hybrid configurations. The model that is in use here is skyhook semiactive configuration.

Comparing the two models, it is apparent that the passive system model can be thought as a simplification of the semiactive system model, obtained by

letting $c_{off1} = c_{s1}$, $c_{off2} = c_{s2}$, $c_{on1} = c_{off1}$ and $c_{on2} = c_{off2}$. The model consists of a single m_s free to move in the vertical direction and rotate around its center of gravity, connected to the input by suspension system both in the front and the rear of the sprung mass. The suspension system is modeled as a linear spring of stiffness k_{s1} and k_{s2}, and a linear damper with a damping coefficient of c_{off1} and c_{off2}. A linear damper with a damping rate of (c_{on1} - c_{off1}) and (c_{on2} - c_{off2}) connect the m_s at each ends to some inertial reference in the sky. This configuration is typically called as a skyhook semiactive system.

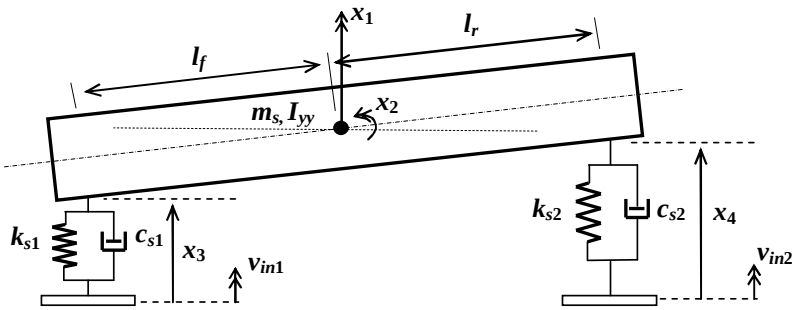

Fig. 7.1: H-car 2-DOF passive model.

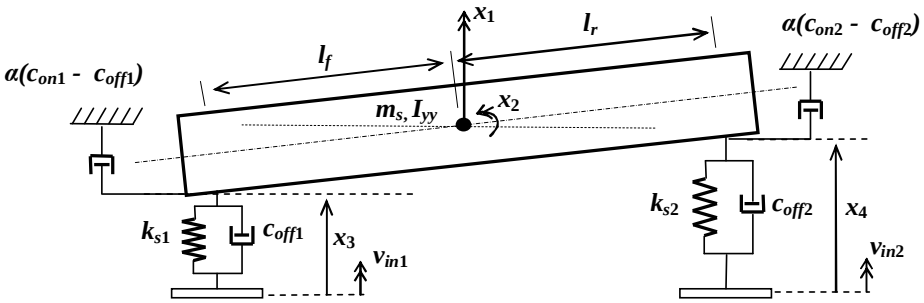

Fig. 7.2: H-car 2-DOF semiactive model.

One apparent missing part in this model is the m_{us} which typically representing tires in the actual vehicle. This is intentionally removed so as to have a H-car 2-DOF model and as a result, making this analysis plausible. Initial studies on H-car 4-DOF

indicates that the order of the equation, in using the Residue integration formula which will be discussed later, is up to the power of 10 in the numerator and 16 in the denominator. An alternative solution to take into account the unsprung masses is to have the tire dynamics study be conducted separately and its output is then feed into the model presently analyzed.

The variables and inputs of the model are summarized in Table 7.1. The input signal is modeled as a white noise input. This assumption is reasonable since studies on road irregularities have shown that the vertical displacement of road surfaces can be reasonably well approximated by an integrated white-noise input, except at very low frequencies (Chalasani, 1986a). Furthermore, it can also be thought that the input signals in this model are the results of a transfer function for the separate tire dynamics analysis.

Table 7.1: H-car 2-DOF variables and inputs description.

Symbol	Description	Units
x_1	m_s velocity	m/s
x_2	Pitch angular velocity	rad/s
x_3	Front suspension deflection	m
x_4	Rear suspension deflection	m
v_{in1}	Front velocity input	m/s
v_{in2}	Rear velocity input	m/s

7.3 MEAN SQUARE RESPONSES OF INTEREST

In ride quality study, the total response of the vertical and pitch angular motion of m_s over all frequency range are particularly of interest. Thus, mean square values can provide useful information. Mean square response can be obtained by using the following relationship:

$$E\left[y^2\right] = S_0 \int_{-\infty}^{\infty} \left|H_y(\omega)\right|^2 d\omega \tag{7.1}$$

where S_0 is the spectral density of the white-noise input, and $H_y(\omega)$ is the transfer function relating the response variable y to the white-noise input (Chalasani, 1986a).

The motion variables of interest in this analysis are: the m_s vertical acceleration $\dot{x}_1$, the m_s pitch angular acceleration $\dot{x}_2$, and the front and rear deflection of the suspension x_3 and x_4, respectively.

The equations of motion derived from the semiactive model are shown below:

$$m_s\dot{x}_1 + k_{s1}x_3 + k_{s2}x_4 + c_{off1}\dot{x}_3 + c_{off2}\dot{x}_4 + \alpha(c_{on1} - c_{off1})(\dot{x}_3 + v_{in1}) +$$

$$\alpha(c_{on2} - c_{off2})(\dot{x}_4 + v_{in2}) = 0 \tag{7.2}$$

$$I_{yy}\dot{x}_2 - k_{s1}x_3 l_f + k_{r1}x_4 l_r - c_{off1}\dot{x}_3 l_f + c_{off2}\dot{x}_4 l_r -$$

$$\alpha(c_{on1} - c_{off1})(\dot{x}_3 + v_{in1})l_f + \alpha(c_{on2} - c_{off2})(\dot{x}_4 + v_{in2})l_r = 0 \tag{7.3}$$

where the state relation can further be related as:

$$\dot{x}_3 = x_1 - l_f x_2 - v_{in1} \tag{7.4}$$

$$\dot{x}_4 = x_1 + l_r x_2 - v_{in2} \tag{7.5}$$

The equations of motion for passive system can be easily obtained from the same figure by letting $c_{off1} \to c_{s1}$, $c_{off2} \to c_{s2}$, and $\alpha = 0$. With these assumptions, the following equations of motion are obtained:

$$m_s\dot{x}_1 + k_{s1}x_3 + k_{s2}x_4 + c_{s1}\dot{x}_3 + c_{s2}\dot{x}_4 = 0 \tag{7.6}$$

$$I_{yy}\dot{x}_2 - k_{s1}x_3 l_f + k_{r1}x_4 l_r - c_{s1}\dot{x}_3 l_f + c_{s2}\dot{x}_4 l_r = 0 \tag{7.7}$$

where the state relation remain the same as Eqs. 7.4 and 7.5. Transforming these equations of motion into the s domain using Laplace transform and rearrange the

variables, transfer functions of interest can then be obtained. The transfer functions of interest are $H_{\dot{x}_1}(s) = \frac{\dot{x}_1}{\dot{v}_{in}}(s)$, $H_{\dot{x}_2}(s) = \frac{\dot{x}_2}{\dot{v}_{in}}(s)$, $H_{x_3}(s) = \frac{x_3}{\dot{v}_{in}}(s)$, and $H_{x_4}(s) = \frac{x_4}{\dot{v}_{in}}(s)$.

Two types of input velocity are used in this work. The first type is called heave input signal, where $v_{in1} = v_{in2} = v_{in}$, and the second type is pitch input signal, where $v_{in1} = v_{in}$, $v_{in2} = -v_{in}$. The input is illustrated in Fig. 7.3.

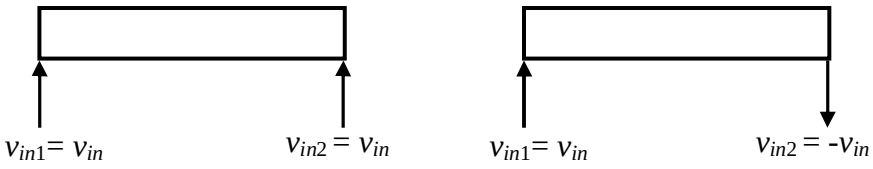

(a) Heave Input (b) Pitch Input

Fig. 7.3: Types of input signals used.

MATHEMATICA symbolic computation package is used to derive the transfer functions and the results are summarized in the Appendix C. Note that these transfer function is against the input acceleration, i.e. $\dot{v}_{in}$ and are represented in the s-domain. Replacing *s* by j·ω in the equations yield the transfer functions in the frequency domain.

Solution for Eq. 7.1 can be obtained by using the residue integration formula. In order to use this formula, $\left|H_y(\omega)\right|^2$ which is the square of the transfer function must be arranged in the following form, letting $T(\omega)$ as $\left|H_y(\omega)\right|^2$:

$$\left|H_y(\omega)\right|^2 = T(\omega) = \frac{a_1\omega^6 + a_2\omega^4 + a_3\omega^2 + a_4}{\left(\omega^4 - b_2\omega^2 + b_4\right)^2 + \left(b_1\omega^3 + b_3\omega\right)^2} \tag{7.8}$$

It should be noted that $\int_{-\infty}^{\infty} T(\omega)\, d\omega$ is always defined when $T(\omega)$ has the form shown in Eq. 7.8 and $b_4 \neq 0$. The expression in Eq. 7.8 can be expanded and expressed as a function of its 4 pairs of complex conjugate poles (± j ω_1, ± j ω_2, ± j ω_3, and ± j ω_4),

$$T(\omega) = \frac{a_1\omega^6 + a_2\omega^4 + a_3\omega^2 + a_4}{\left(\omega^4 + jb_1\omega^3 - b_2\omega^2 - jb_3\omega + b_4\right) + \left(\omega^4 - jb_1\omega^3 - b_2\omega^2 + jb_3\omega + b_4\right)} \tag{7.9}$$

The coefficients b_1, b_2, b_3 and b_4 can be expressed as a function of the poles, ω_1, ω_2, ω_3, and ω_4. This is shown below,

$$b_1 = \omega_1 + \omega_2 + \omega_3 + \omega_4 \tag{7.10}$$

$$b_2 = \omega_1\omega_2 + \omega_1\omega_3 + \omega_1\omega_4 + \omega_2\omega_3 + \omega_2\omega_4 + \omega_3\omega_4 \tag{7.11}$$

$$b_3 = \omega_1\omega_2\omega_3 + \omega_1\omega_2\omega_4 + \omega_1\omega_3\omega_4 + \omega_2\omega_3\omega_4 \tag{7.12}$$

$$b_4 = \omega_1\omega_2\omega_3\omega_4 \tag{7.13}$$

Substituting these relationships to Eq. 7.9 yields,

$$T(\omega) = \frac{a_1\omega^6 + a_2\omega^4 + a_3\omega^2 + a_4}{(\omega + j\omega_1)(\omega - j\omega_1)(\omega + j\omega_2)(\omega - j\omega_2)(\omega + j\omega_3)(\omega - j\omega_3)(\omega + j\omega_4)(\omega - j\omega_4)} \tag{7.14}$$

Now, the integral $\int_{-\infty}^{\infty} T(\omega)\, d\omega$ can be expressed as a function of ω_1, ω_2, ω_3, and ω_4 by using the Residue integration formula.

$$\int_{-\infty}^{\infty} T(\omega)\, d\omega = 2\pi j \sum \mathrm{Res}\left[T(\omega)\right] \tag{7.15}$$

where $\mathrm{Res}\left[T(\omega)\right]$ denotes a residue of $T(\omega)$ corresponding to a pole of $T(\omega)$ located in the upper-half of the complex plane (Asami and Nishihara, 2002). Also, ω_1, ω_2, ω_3,

and ω_4 are positive numbers because the coefficients b_1, b_2, b_3 and b_4 that are obtained when deriving Eq. 7.8 are always positive.

$$\int_{-\infty}^{\infty} T(\omega)\, d\omega = 2\pi j \sum_{k=1}^{n} \lim \left(\omega - i\omega_k\right) T(\omega) \tag{7.16}$$

Applying the formula to Eq. 7.14 and rearranging the term using MATHEMATICA package, the mean square response of the system can be given as the following relationship.

$$\int_{-\infty}^{\infty} T(\omega)\, d\omega = \pi \frac{a_1 b_4 \left(-b_1 b_4 + b_2 b_3\right) + a_2 \left(b_3 b_4\right) + a_3 \left(b_1 b_4\right) + a_4 \left(b_1 b_2 - b_3\right)}{b_4 \left(b_1 b_2 b_3 - b_3^2 - b_1^2 b_4\right)} \tag{7.17}$$

where the coefficients a_1, a_2, a_3 and a_4 are the numerators of the square of the transfer function as defined in Eq. 7.8, and b_1, b_2, b_3 and b_4 are defined in Eqs. 7.10 to 7.13. Further substituting these coefficients with corresponding algebraic expression yields:

$$\int_{-\infty}^{\infty} T(\omega)\, d\omega = f\left(m_s, I_{yy}, k_{s1}, k_{s2}, c_{on1}, c_{on2}, c_{off1}, c_{off2}, l_f, l_r\right) \tag{7.18}$$

for semiactive system and for passive system,

$$\int_{-\infty}^{\infty} T(\omega)\, d\omega = f\left(m_s, I_{yy}, k_{s1}, k_{s2}, c_{s1}, c_{s2}, l_f, l_r\right) \tag{7.19}$$

These mean square responses for each transfer function of both passive and semiactive systems are shown in Appendix D.

7.4 RELATIONSHIP BETWEEN THE VARIOUS STATE VARIABLES

Two different analyses are presented here, namely the transfer function and RMS analyses. Frequency response plots of the transfer functions would provide a good way to understand the characteristics of any particular system. This curve shows how the state variable of interest responses to input signal over frequency span. In this

work, frequency responses on both acceleration and velocity heave and pitch input signals are studied and discussed.

Each figure is presented with three damping coefficient to show the effect of the coefficient to the response. The damping coefficient values are shown in Table 7.2. Semiactive damping coefficients are chosen using the relationships of $c_{on} = 2.2c_s$ and $c_{off} = 0.2c_s$ (Chalasani, 1986b). These relationships yield to $\left(c_{on} - c_{off}\right) = 2c_s$. The same model parameters are used for every configuration. Their numerical values are summarized in Table 7.3.

Table 7.2: Damping coefficient values relationships.

Damping case	**Passive** $\left(\mathrm{N \cdot s/m}\right)$	**Semiactive** $\left(\mathrm{N \cdot s/m}\right)$
Lightly damped suspension	$c_{s1} = c_{s2} = 196$	$c_{on1} = c_{on2} = 431.2$ $c_{off1} = c_{off2} = 39.2$
Typical passenger car damping value	$c_{s1} = c_{s2} = 980$	$c_{on1} = c_{on2} = 2156$ $c_{off1} = c_{off2} = 196$
Heavily damped suspension	$c_{s1} = c_{s2} = 3920$	$c_{on1} = c_{on2} = 8624$ $c_{off1} = c_{off2} = 784$

Table 7.3: H-car 2-DOF Model Parameters.

Symbol	**Description**	**Units**
m_s	Sprung mass	730 Kg
I_{yy}	Pitch Moment of Inertia	2460 Kg m^2
k_{s1}	Front Stiffness coefficient	17500 N/m
k_{s2}	Rear Stiffness coefficient	17500 N/m
l_f	Longitudinal distance from m_s C.G. to the front axle	1.011 m
l_r	Longitudinal distance from m_s C.G. to the rear axle	1.803 m

Another approach worth in analyzing responses is to look at the total response over the frequency span. In this RMS analysis, four different comparisons are made between the RMS pitch angular velocity, RMS vertical velocity, RMS rear suspension deflection, and RMS front suspension deflection.

For each plot, the influence of the damping coefficient and the suspension's stiffness is displayed. The vehicle is assumed to travel at a constant speed on a random road surface. The same model parameters were used as in Table 7.3, except the spring stiffness, which was varied. For the purpose of representing it as a spring ratio, r_k, the 'tire' stiffness was taken as 175000 N/m. This r_k values was varied from 5 representing soft spring to 20 representing stiff spring. For each value of r_k, various damping ratio, ζ_s were used, varies from 0.05 as a lightly damped to 1 as a heavily damped system. For the case of semiactive system, c_{on} and c_{off} are related to c_s in the passive system by $c_{on} = 2.2\ c_s$, and $c_{off} = 0.2\ c_s$. Thus, $c_{on} - c_{off} = 2\ c_s$. The same values of c_s were then used.

7.4.1 Transfer Function Analysis

Since RMS front and rear suspension deflections for semiactive system is unable to be obtained in the acceleration heave and pitch input, an alternative option is to have the two systems be compared at the velocity heave and pitch input. This would be able to solve the non-converging values of the suspension deflections responses at low frequencies, but at the same time will cause the values of the vertical acceleration and pitch angular acceleration responses to become unbounded or non-converging. This is simply because, having the input as velocity, the transfer function equations will have both numerator and denominator having the same highest root. Thus as the frequency

is approaching infinity, the transfer function value will remain as a constant value of the highest root.

To overcome this problem, vertical velocity and pitch angular velocity responses are used for this velocity input analysis. Velocity output however, is not commonly used or preferred in the study of vibration. This is due to the difficulty to directly contemplate the results as oppose to the deflection output, which is nothing but direct motion of an object and acceleration output, which can easily related to ride comfort due to well establish works referring to this type of output. Therefore, it is very much generally acceptable that most work and papers published in this area are using deflection or acceleration output. However, due to the constraint faced in this analysis, velocity output could not be avoided.

Figs. 7.4 to 7.7 show in frequency domain, the effects of varying damping coefficients on the m_s velocity response, the pitch angular velocity, the front suspension deflection and the rear suspension deflection respectively. For each figure, response to heave velocity input and pitch velocity input signals are compared for both passive and semiactive system

Fig. 7.4 shows that for all four cases (passive and semiactive systems, heave and pitch inputs), increasing the damping coefficient reduces the value of the vertical acceleration at the m_s natural frequencies ω_{n1} (pitch natural frequency) and ω_{n2} (heave natural frequency). The value at ω_{n1} appears to be the peak value for the pitch input cases. Similarly, the value at ω_{n2} is the peak value for the heave input cases. As the frequency goes beyond the natural frequencies, the responses increase with the increase of the damping coefficient. Thus, the area under the curves does not necessarily decrease with the decrease of the peak values. Therefore, the measure of the vibration level $\mathrm{E}\left[x_1^{\,2}\right]$ cannot be simply deduced by the peak value of the curve.

Comparing between the passive and semiactive systems, the peak values for both heave and pitch inputs appears to be lower in the semiactive cases. The area under the curves is also expected to be lower than the passive cases since relatively smaller increase in responses at higher frequencies.

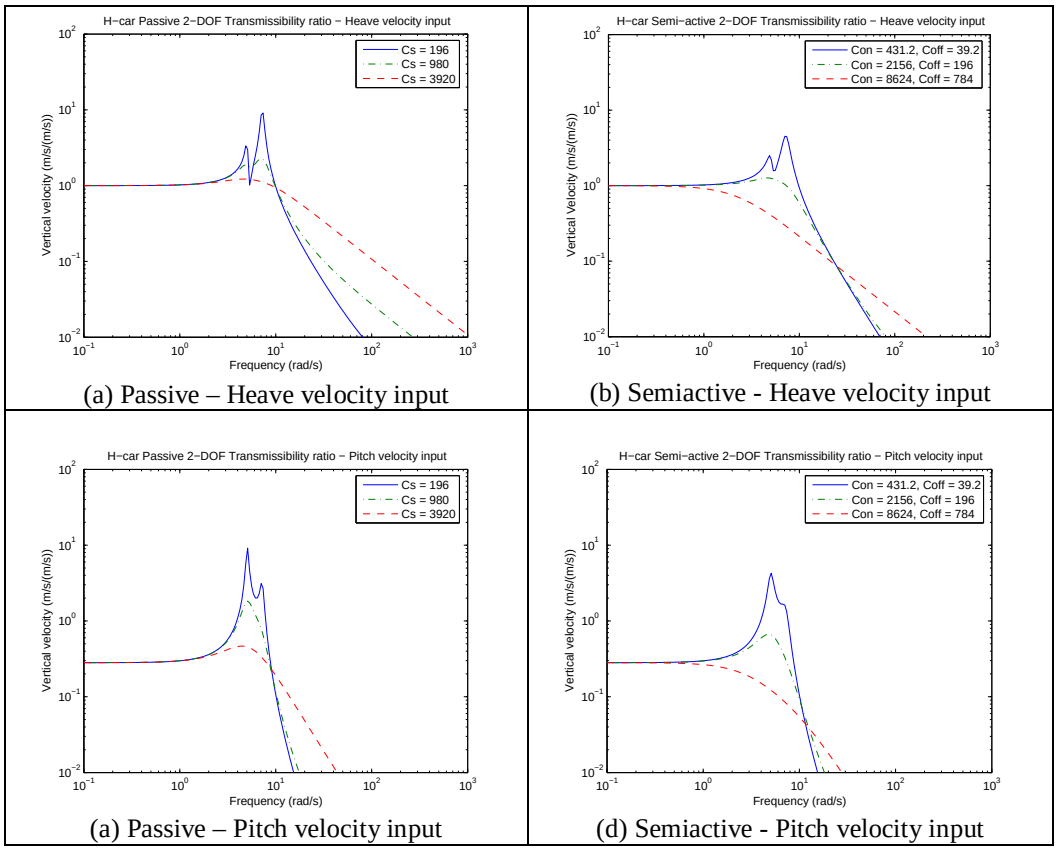

(a) Passive – Heave velocity input

(b) Semiactive - Heave velocity input

(a) Passive – Pitch velocity input

(d) Semiactive - Pitch velocity input

Fig. 7.4: Transfer function of m_s vertical velocity for various damping coefficients.

Fig. 7.5 shows that for all four cases (passive and semiactive systems, heave and pitch inputs), increasing the damping coefficient reduces the value of the pitch angular acceleration at the m_s natural frequencies ω_{n1} (pitch natural frequency) and ω_{n2} (heave natural frequency). The value at ω_{n1} appears to be the peak value for both the pitch input cases and the heave input cases.

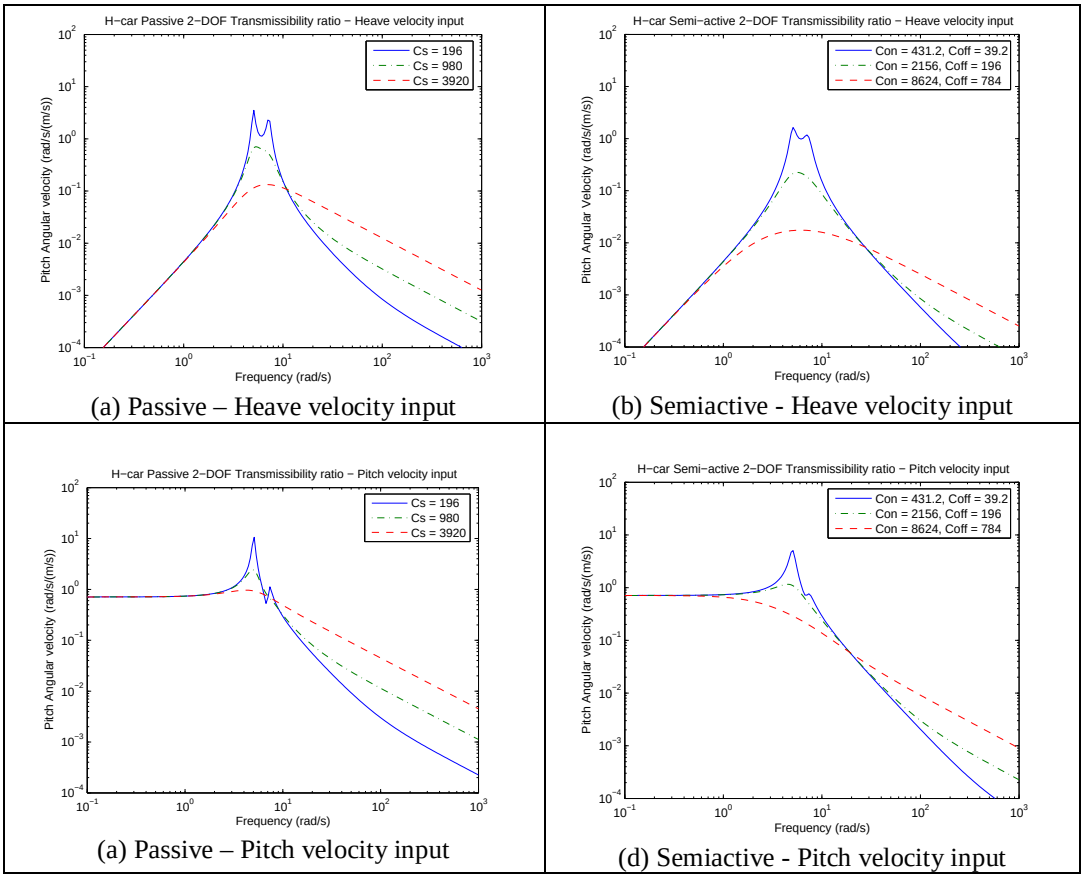

Fig. 7.5: Transfer function of m_s pitch angular velocity for various damping coefficients.

As the frequency goes beyond the natural frequencies, the responses increase with the increase of the damping coefficient. Thus, the area under the curves does not necessarily decrease with the decrease of the peak values. Therefore, the measure of the pitch angular acceleration level $\mathrm{E}\left[x_2^{\,2}\right]$ cannot be simply deduced by the peak value of the curve.

Comparing between the passive and semiactive systems, the peak values for both heave and pitch inputs appears to be lower in the semiactive cases. The area under the curves is also expected to be lower than the passive cases since relatively smaller increase in responses at higher frequencies.

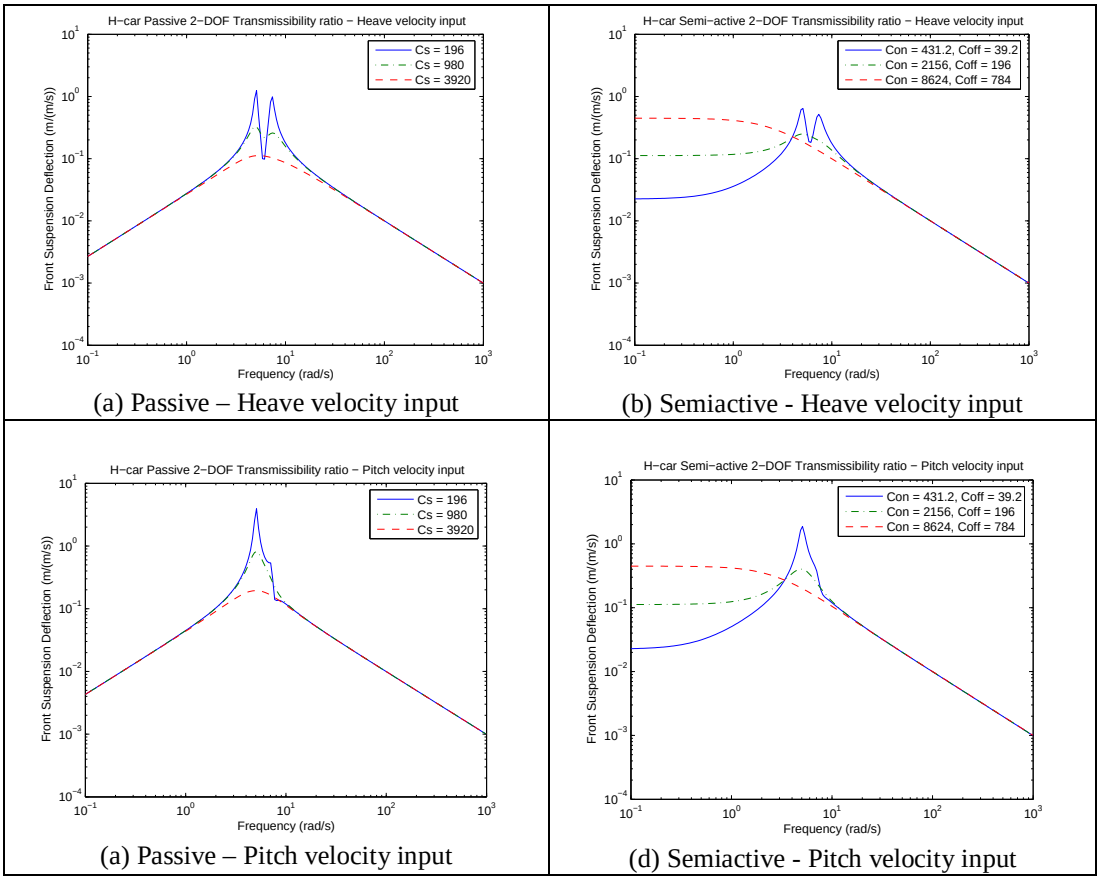

Fig. 7.6: Transfer function of front suspension deflection for various damping coefficients.

Fig. 7.6 shows that for all four cases (passive and semiactive systems, heave and pitch inputs), increasing the damping reduces the value of the front suspension deflection at the m_s natural frequencies ω_{n1} (pitch natural frequency) and ω_{n2} (heave natural frequency). The value at ω_{n1} appears to be the peak value for all cases. For the semiactive system, the value seems to approach a constant value as the frequency reduces. This constant tends to increase as the coefficient increase and could exceed the peak value at the natural frequencies. As the frequency increases beyond the natural frequencies, the responses seem to converge towards the same point for all damping coefficient for all passive and semiactive cases. Therefore, the measure of

the front suspension deflections $\mathrm{E}\left[x_3^{\,2}\right]$ may be deduced by the peak value of the curve in the case of passive system but not in the case of semiactive system.

Comparing between the passive and semiactive systems, the peak values for both heave and pitch inputs appears to be slightly lower in the semiactive cases. However, the area under the curves apparently decreases with the decrease of the peak values in the passive system case but increases in the case of semiactive due to the higher curve at low frequencies. So, it is expected that area under the curve of the passive system would decrease as the coefficient increased, but semiactive would increase.

Fig. 7.7 shows that for all four cases (passive and semiactive systems, heave and pitch inputs), increasing the damping reduces the value of the rear suspension at the m_s natural frequencies ω_{n1} (pitch natural frequency) and ω_{n2} (heave natural frequency). The value at ω_{n2} appears to be the peak value for both passive and semiactive systems with heave input – Figs. 7(a) and 7(b), and ω_{n1} appears to be the peak value for both passive and semiactive systems with pitch input – Figs. 7(c) and 7(d). For the semiactive system, the value seems to approach a constant as the frequency reduces. This constant tends to increase as the coefficient increase and could exceed the peak value at the natural frequencies. As the frequency increases beyond the natural frequencies, the responses seem to converge towards the same point for all damping coefficient for all passive and semiactive cases. Therefore, the measure of the front suspension deflections $\mathrm{E}\left[x_4^{\,2}\right]$ may be deduced by the peak value of the curve in the case of passive system but not in the case of semiactive system.

Comparing between the passive and semiactive systems, the peak values for both heave and pitch inputs appears to be slightly lower in the semiactive cases.

However, the area under the curves apparently decreases with the decrease of the peak values in the passive system case but increases in the case of semiactive due to the higher curve at low frequencies. So, it is expected that area under the curve of the passive system would decrease as the coefficient increased, but semiactive would increase.

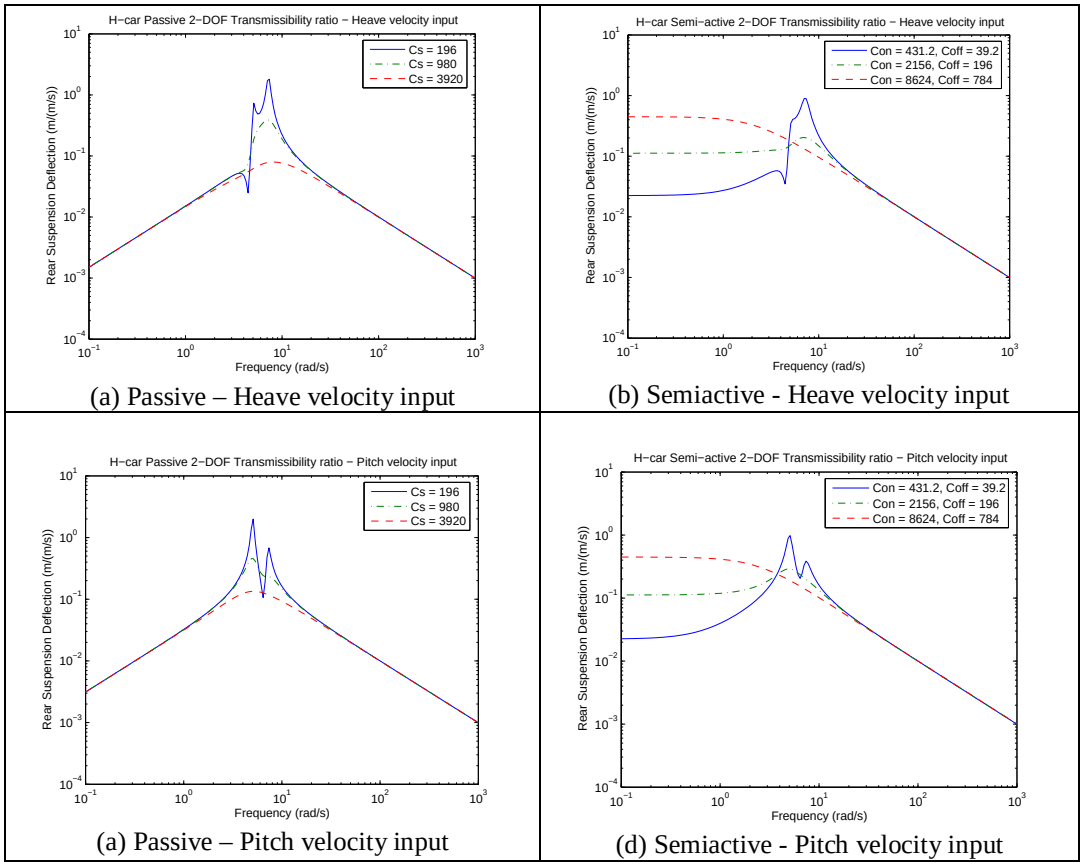

(a) Passive – Heave velocity input

(b) Semiactive - Heave velocity input

(a) Passive – Pitch velocity input

(d) Semiactive - Pitch velocity input

Fig. 7.7: Transfer function of rear suspension deflection for various damping coefficients.

7.4.2 RMS analysis

The next analysis is to study the relationship of root mean square (RMS) of the state variables. Similar approach with to the one in the earlier case was employed, except that this time the input is in velocity signals.

Fig. 7.8 shows the relationship between RMS pitch angular velocity and RMS vertical velocity for both passive and semiactive systems with the two types of input signals.

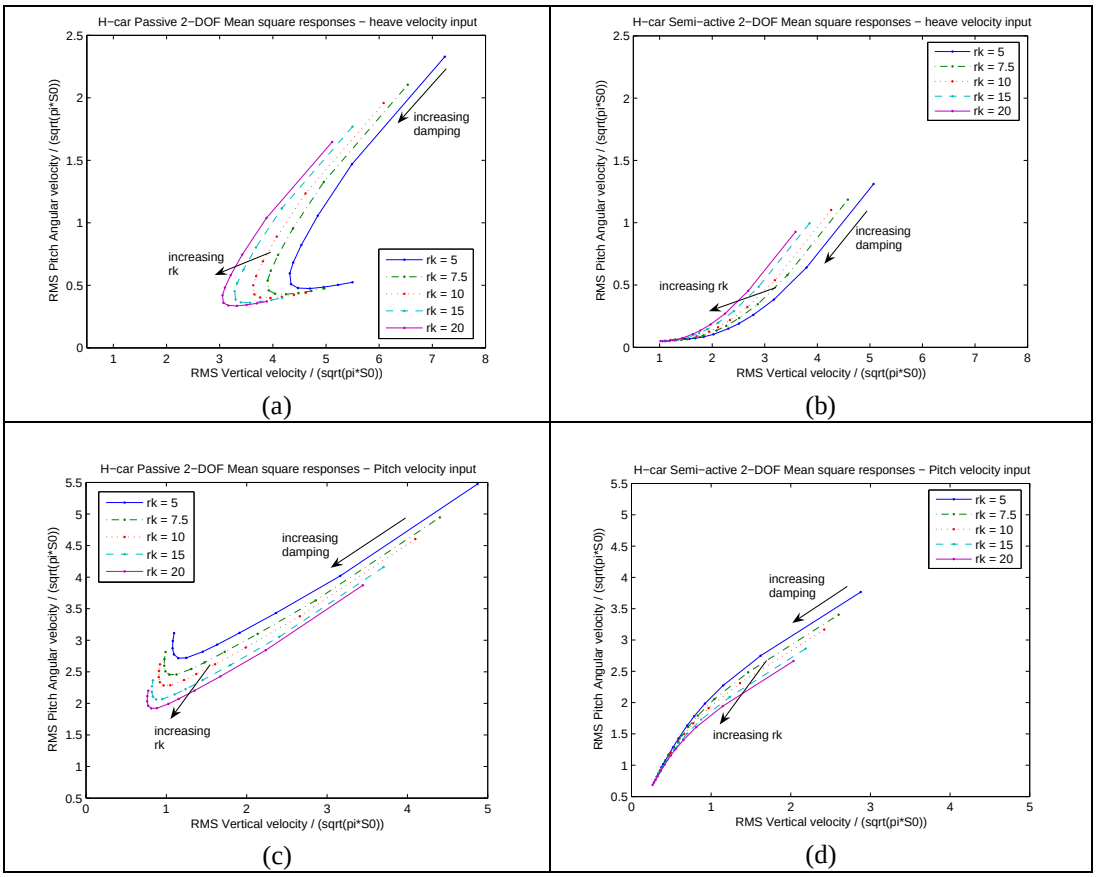

Fig. 7.8: Relationship between RMS pitch angular velocity to RMS vertical velocity.

Figs. 7.8(a) and 7.8(c) shows that for the passive suspension system with heave velocity input and pitch velocity input, increasing the damping coefficient from a low value to a midrange value causes to lower the RMS pitch angular velocity and RMS vertical velocity. Increasing the damping further results in a slight increase in RMS pitch angular velocity, but more significantly higher RMS vertical velocity in the heave velocity input case. The opposite trend is observed in the pitch velocity

input, whereby more significant increase occurs in RMS pitch angular velocity and only slight increase in RMS vertical velocity.

This influence of damping coefficient in the RMS value can be understood by referring back to the frequency domain responses discussed earlier. For the passive systems, Fig. 7.4(a) and Fig. 7.4(c), increasing the damping coefficient reduces the peak values of vertical velocity at the natural frequencies, but at the same time increases the values at higher frequencies. Increasing the damping coefficient therefore, could initially reduce the RMS value of the vertical velocity, as the reduction in the peak values at the natural frequencies is more significant than the increase values at higher frequencies. However, further increase in the coefficient would increase the RMS values as the increasing values at higher frequencies become relatively more significant. Similar argument is also applicable for the case of pitch angular velocity curves in Figs. 7.5(a) and 7.5(c).

Also, comparing the heave velocity input and pitch velocity input responses of the vertical velocity shown in Figs. 7.4(a) and 7.4(c), it is apparent that the increase of values at high frequencies is more in the case of heave input than the pitch input. However, the case for pitch angular velocity, Figs. 7.5(a) and 7.5(c) is not very obvious to deduce directly from the curves.

For the semiactive system with heave velocity input, Fig. 7.8(b) and Fig. 7.8(d), increasing the damping coefficient decreases RMS pitch angular velocity as well as RMS vertical velocity. As the coefficient is further increased, the RMS values are further decrease, with less rapidly for the pitch angular velocity and more rapidly for the vertical velocity in the case of heave input. The opposite trend is observed in the pitch input case – decrease more rapidly for the pitch angular velocity and less rapidly for the vertical velocity.

Similar observations can be deduced from the frequency domain responses, Figs. 7.4(b) and 7.4(d) and Figs. 7.5(b) and 7.5(d), as in the passive system case discussed above. Comparing the RMS values between the passive and semiactive responses, it is apparent that semiactive control scheme significantly reduces the RMS values for all values of damping coefficient.

Finally, observing the curves, it can be concluded that for all cases, increasing the spring ratio reduces the values of both RMS pitch angular velocity and RMS vertical velocity. This is true for passive system as well as semi-active.

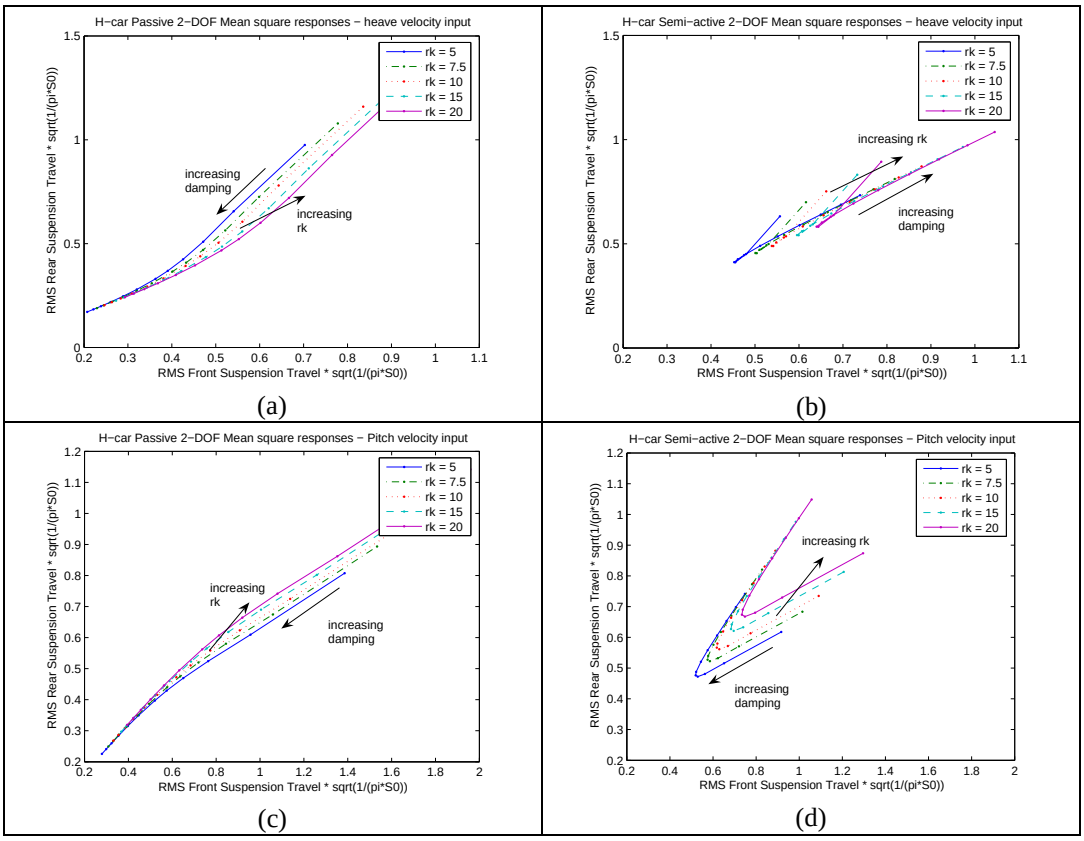

Fig. 7.9: Relationship between RMS rear suspension deflection to RMS front suspension deflection.

Fig. 7.9 shows the relationship between RMS rear suspension deflection and RMS front suspension deflection for both passive and semiactive systems with the two

types of input signals. Figs. 7.9(a) and 7.9(c) show that for the passive suspension system, both heave velocity input and pitch velocity input, increasing the damping coefficient value lowers the RMS rear suspension deflection as well as the front suspension deflection. This is also similar to the one obtained in the acceleration input case. This influence of damping coefficient in the RMS value can be understood by referring back to the frequency domain responses in Figs. 7.6 and 7.7. In Fig. 7.6(a) and Fig. 7.6(c), increasing the damping coefficient reduces the peak values of front suspension deflection at the natural frequencies, while the values at lower and higher frequencies remain almost similar regardless of the coefficient values. Increasing the damping coefficient therefore, would obviously reduce the RMS front suspension deflection value. Similar argument is also applicable for the case of rear suspension deflection curves in Figs. 7.7(a) and 7.7(c).

Figs. 7.9(b) and 7.9(d) show that for the semiactive system, increasing the damping coefficient from a low value to a midrange value significantly decreases both RMS front suspension deflection and RMS rear suspension deflection. As the coefficient is further increased, significant increase occur in both cases as well. This is consistent with the observations discussed earlier in the frequency domain responses, Figs. 7.6(b) and 7.6(d) and Figs. 7.7(b) and 7.7(d).

Comparing the RMS values between the passive and semiactive responses, semiactive control scheme significantly reduces the RMS values for a low value to a midrange value of the damping coefficient. However, as the coefficient is further increase, passive system performs better as the RMS values are further reduced while the RMS for the semiactive system increased.

The increase in stiffness ratio, r_k, increases both RMS rear suspension deflection and RMS front suspension deflection in the passive and semiactive systems.

Fig. 7.10 shows the relationship between RMS vertical velocity and RMS front suspension deflection for passive system with the two types of input signals.

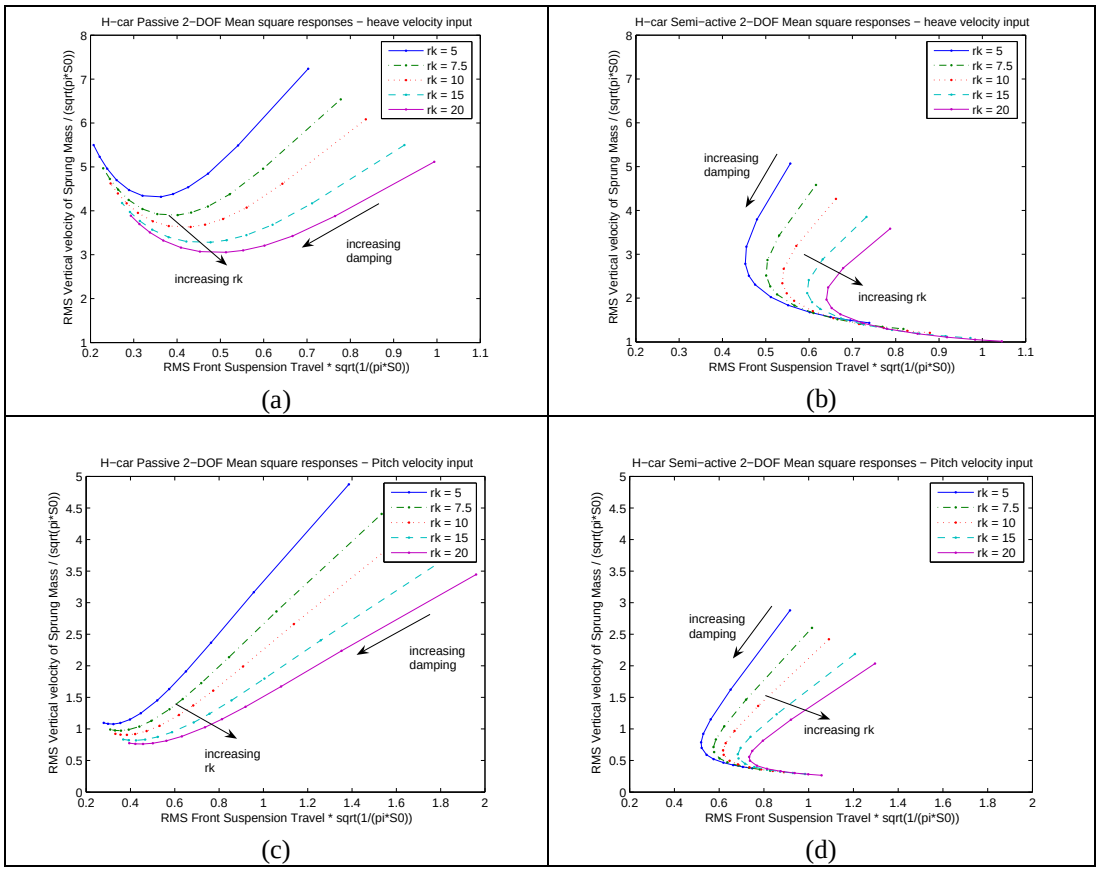

Fig. 7.10: Relationship between RMS vertical velocity to RMS front suspension deflection.

Fig. 7.10(a) shows that for the passive suspension system with heave velocity input, increasing the damping coefficient from a low value to a midrange value reduces the RMS vertical velocity and the RMS front suspension deflection. However, while increasing the damping further results in an increase in the RMS vertical velocity, the RMS front suspension deflection further reduces. In Fig. 7.10(b), the pitch velocity input causes a slight increase in the RMS vertical velocity while the RMS front suspension deflection further reduces. This is in agreement with the

corresponding frequency domain responses for each state variable as previously discussed.

For the semiactive system, increasing the damping coefficient from a low value to a midrange value reduces the RMS vertical velocity and the RMS front suspension deflection. However, while increasing the damping further results in a significant increase in the RMS front suspension deflection, the RMS vertical velocity further decreases. Less significant decrease of the RMS vertical velocity is observed in the pitch velocity input than the heave velocity input.

Comparing the RMS values between the passive and semiactive responses, semiactive control scheme significantly reduces the RMS values for a low value to a midrange value of the damping coefficient. However, as the coefficient is further increase, passive system performs better as the RMS values are further reduced while the RMS for the semiactive system increased.

The increase in stiffness ratio, r_k decreases RMS vertical acceleration while increases RMS front suspension deflection in all cases.

Fig. 7.11 shows the relationship between RMS pitch angular velocity and RMS front suspension deflection for passive systems with the two types of input signals. Fig. 7.11(a) shows that for the passive suspension system with heave velocity input, increasing the damping coefficient from a low value to a midrange significantly reduces the RMS pitch angular velocity, and slightly reduces the RMS front suspension deflection. However, increasing the coefficient further results in a slight increase in the RMS pitch angular velocity, while the RMS front suspension deflection further reduces. Almost a similar scenario is observed inn the pitch velocity input in Fig. 7.11(b), but with a relatively more significant increase in the RMS pitch

angular velocity. This is in agreement with the frequency domain responses for each state variable as previously discussed.

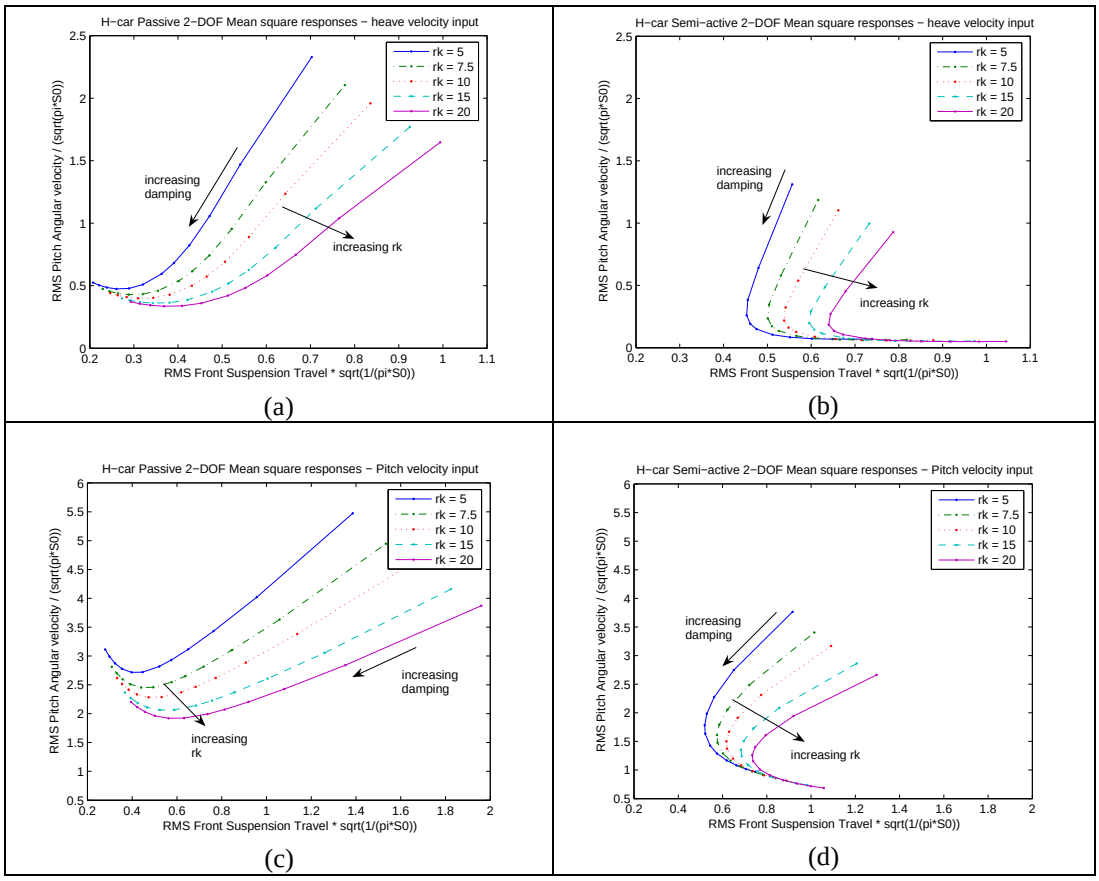

Fig. 7.11: Relationship between RMS pitch angular velocity to RMS front suspension deflection for passive system.

For the semiactive system, increasing the damping coefficient from a low value to a midrange value reduces the RMS pitch angular velocity and the RMS front suspension deflection. However, while increasing the damping further results in a significant increase in the RMS front suspension deflection, the RMS pitch angular velocity further decreases. Less significant decrease of the RMS pitch angular velocity is observed in the heave velocity input than the pitch velocity input.

Comparing the RMS values between the passive and semiactive responses, semiactive control scheme significantly reduces the RMS values for a low value to a midrange value of the damping coefficient. However, as the coefficient is further increase, passive system performs better as the RMS values are further reduced while the RMS for the semiactive system increased.

The increase in stiffness ratio, r_k decreases RMS pitch angular acceleration while increases RMS front suspension deflection in all cases.

7.5 CONCLUDING REMARK

H-car 2-DOF models were presented and the equations of motion were derived. Residue integration formula for computing RMS value of the transfer functions of the states variables was discussed. Using the Residue formula, the root mean square of the transfer functions were obtained and discussed. Even though the result can not be directly compared against the work that was done for a Q-car 2-DOF by Blanchard (2003), general trends in the RMS curves show some similarities.

Comparison between the RMS values of the passive and semiactive systems, it can be concluded that semiactive system significantly improves the m_s responses – both vertical velocity and pitch angular velocity for both heave and pitch input. However, this improvement comes with a price to the suspension deflections for high values of damping coefficient. This problem is actually expected since the model used closely resembles a skyhook semiactive system.

A potential work as a continuation of this is to separately look at and analyze the tire dynamics model, and later combine the system to the present work by feeding the output of the tire dynamics as an input to it.

CHAPTER EIGHT

CONCLUSION AND RECOMMENDATION

8.1 HIGHLIGHTS AND CONTRIBUTIONS OF THE STUDY

This work attempts to investigate and analyze semiactive characteristics particularly involving ride quality analysis. Some of the major highlights and contributions of this study to this area of research are:

1. Full-car 7-DOF model study on semiactive control policies to verify the commonly used quarter-car and half-car models.
2. Comprehensive analysis involving all frequency-domain and both transient and steady state, time-domain analyses for both passive system and semiactive control policies. Most of the previous work concentrated only on either frequency response or steady state response analysis. Only recently researchers started looking at the transient response, such as Barak *et al* (2004) on F-car 7-DOF passive system.
3. Extensive comparison on Q-car, H-car and F-car models of passive and semiactive. So far to the author's knowledge, there has been no attempt in comparing responses of the different models particularly on the semiactive system.
4. Analyzes the H-car 2-DOF model of semiactive system for RMS study. This is a new extension to the one conducted before on the Q-car 2-DOF model.

8.2 CONCLUSIONS

Several conclusions can be derived from the work conducted here:

1. From all analyses presented in Chapters 4-6, skyhook and groundhook control policies are advantageous at improving a particular aspect in vehicle response (m_s and m_{us}, respectively) while compromising on the other. Hybrid semiactive control policy, which is basically a combination effect of both skyhook and groundhook controls, on the other hand shows significant advantages to passive system in improving the ride quality of passenger vehicle without compromising the road holding ability.
2. There is no direct correlation in terms of response magnitude value in all cases between Q-car, H-car and F-car model that can be derived. Thus simply analyzing the Q-car model would not lead to an accurate conclusion to ride quality study. The response trends in comparing between the passive system and the semiactive control policies however are almost similar in all models.
3. Furthermore simpler model lacks the ability to provide comprehensive analysis. Q-car model for example would not be able to give the effect of pitch and roll angular acceleration responses as well as the effect of pitch and roll input signals to the system. H-car model would enable either the pitch or roll effect at a time, depending on the parameters defined. Thus, F-car model analysis should be preferred as it would give a complete view of the effect to real vehicle responses. Again, no direct correlation that can be obtained in order to derive the pitch and/or roll effect from the simpler models.

4. For F-car model, the response for the left and right side of vehicle fronts and rears system (m_{us} acceleration, suspension deflection and tire deflection) are identical, regardless of the input type. It is noted that typical passenger vehicle would have the fronts system parameters slightly different than the rears. Thus analysis on only one of the sides is necessary in the future. 5.
5. In the H-car 2-DOF analysis, presented in Chapter 8, it can be concluded that semiactive system significantly improves the ms responses – both vertical acceleration and pitch angular acceleration for both heave and pitch input. However, this improvement comes with a price to the suspension deflections for high values of damping coefficient. This problem is expected since the model used closely resembles a skyhook semiactive system.

8.3 RECOMMENDATIONS FOR FUTURE STUDIES

Several potential studies can be conducted further as continuation of this work:

1. Since this study focuses only on the effect on a typical passenger car, the parameters used were all consistent through out the study. In the future, it is possible to study the effect of changing these vehicle parameters to ride quality and vehicle dynamics, and possibly come out with optimized parametric relationship.
2. An immediate extension of this work is to study on possibility of estimating F-car or H-car responses using Q-car results. Since there is no direct correlation between the results, in terms of magnitude, one may want to attempt finding ways for correlation. Should this attempt proved

fruitful, it would tremendously simplify any future vehicle dynamic analysis since the complexity in higher order models is increase by several orders of magnitude.

3. Another interesting extension from this work is to find the effect in incorporate engine vibration input to the model. This is particularly important when RMS analysis is conducted since generally vibration generated from engine is in the range of 25Hz, which is considered beyond the crucial range of ride quality (0 – 25 Hz) (Barak *et al*, 2004). Other source of disturbance to vehicle could also be incorporated in the future analysis. Even though individually, they may not posses significant effect, collectively there could be some prominent effect to ride quality of the vehicle.
4. Since the RMS study in Chapter 8 only modeled vehicle as a single mass system, a natural extension of the work is to integrate the unsprung mass, thus to have a 4-DOF model and subsequently to analyze for F-car model. However, major obstacle in terms of the limitation of the formulation used must first be overcome.

BIBLIOGRAPHY

Ahmadian, M. (1997a). A Hybrid Semiactive Control for Secondary Suspension Applications. Proceedings of 6th ASME Symposium of Advanced Automotive Technologies, Dallas, TX.

Ahmadian, M. (1997b). Semiactive Control of Multiple Degree of Freedom Systems. Proceedings of the 1997 ASME Design Engineering Technical Conference, Sacramento, CA. Paper No. DETC97/VIB-4123.

Ahmadian, M. (1999). On the Isolation Properties of Semiactive Dampers. *Journal of Vibrations and Control*, vol. 5, pp. 217-232,.

Ahmadian, M., Reichert, B.A. and Song, X. (1997). Harmonic Analysis of Semiactive Suspensions. Proceedings of 1997 ASME Design Engineering Technical Conferences, Sacramento, CA. Paper No. DETC97/VIB-4122.

Allen, R.E. (1975). Limits of Ride Quality through cab isolation. SAE Paper No 750165.

Asami, T. and Nishihara, O. (2002). H2 Optimization to Semiactive of the Three-Element Type Dynamic Vibration Absorbers. *Journal of Vibration and Acoustics*, vol. 124, No. 4, pp. 583-592.

Barak, P. (1989). Design and Evaluation of An Adjustable Automobile Suspension. SAE Paper No. 890089.

Barak, P. (1991). Magic Numbers in Design of Suspensions for Passenger Cars. SAE Paper No. 911921.

Barak, P. (1992). Passive versus Active and Semi-active suspension from theory to application in North American Industry. SAE paper 922140.

Barak, P., Panakanti, N. and Desai, T. (2004). Effect of Chassis Design Factor (CDF) on the Ride Quality Using a Seven Degree of Freedom Vehicle Model. SAE Technical Paper Series No. 2004-01-1555.

Blanchard, E.D. (2003). On the Control Aspects of Semiactive Suspensions for Automobile Applications. Masters Thesis, Virginia Tech.

Boileau, P.E., Pakheja, S. and Liu, P.J. (1997). A Combined Suspension Seat-Vehicle Driver Model for Estimation the Exposure to Whole-body Vehicular Vibration and Shock. *Heavy Vehicle Systems, Special Series, Int. J. of Vehicle Design,* Vol. 4. No. 2-4. pp. 244-265.

Brüel and Kjael Instruments. *Mechanical Vibrations and Shock Measurement*. Cleveland, Ohio.

Butkunas, A.A. (1966). Power Spectral Density and ride evaluation. SAE Paper No. 660138, pp. 681-687.

Carlson, J.D., Catanzarite, D.M. and St. Clair, K.A. (1995). Commercial Magnetorheological Fluid Devices. *International Journal of Modern Physics B*, Vol. 10, No. 23-24, pp. 2857-2865.

Chalasani, R.M. (1986a). Ride Performance Potential of Active Suspension Systems - Part I: Simplified Analysis Based on a Quarter-Car Model. ASME Symposium on Simulation and Control of Ground Vehicles and Transportation Systems, AMD-vol. 80, DSC-vol. 2, pp. 187-204.

Chalasani, R.M. (1986b). Ride Performance Potential of Active Suspension Systems - Part II: Comprehensive Analysis Based on a Full-car Model. Proceedings of 1986 ASME Winter Annual Meeting, Los Angeles, CA.

Corbridge, C. and Griffin, M.J. (1986). Vibration and comfort: vertical and lateral motion in the range 0.5 to 5.0 Hz. *Ergonomics*, Vol. 29, Nos 2, pp. 249-272.

Corbridge, C. and Griffin, M.J. (1991). Effect on vibration on passenger activities: writing and drinking. *Ergonomics*, Vol. 34, No. 10, pp. 1313-1332.

Demic, M., Lukic, J. and Milic, Z. (2002). Some aspect of the investigation of random vibration influence on ride comfort. *J. of Sound and Vibration*, Vol. 253, No. 1, pp. 109-129.

Dempsey, T.K., Leatherwood, J.D. and Clevenson, S.A. (1979). Development of noise and vibration ride comfort criteria. *J. of Acoustical Society of America*, Vol. 65, No. 1, pp. 124-132.

Donati, P., Grosjean, A., Mistrot, P. and Roure, L. (1983). The subjective equivalence of sinusoidal and random whole-body vibration in the sitting position (an experimental study using the 'floating reference vibration' method). *Ergonomics*, Vol. 26, No. 3, pp. 251-273.

Dorft, R.C. and Bishop, R.H. (1995). *Modern Control Systems*. Addison-Wesley, pp. 118-120.

ElMadany, M.M. and El-Tamimi, A. (1990). On a Subclass of Nonlinear Passive and Semiactive Damping for Vibration Isolation. *Computers and Structures*, Vol. 36, No. 5, pp. 921-931.

ElMadany, M.M., Dokainish, M.A. and Allan, A.B. (1979). Ride dynamics of articulated vehicles – A literature survey. *Vehicle System Dynamics*, Vol. 8, pp. 287-316.

Fairley, T.E. and Griffin, M.J. (1988). Predicting the discomfort caused by simultaneous vertical and fore-and-aft whole-body vibration. *Journal of Sound and Vibration*, Vol. 124, No. 1, pp. 141-156.

Gillespie, T.D. (1992). *Fundamentals of Vehicle Dynamics*. SAE.

Gillespie, T.D. and Karamihas, S.M. (2000). Simplified models for truck dynamic response to road input. Heavy Vehicle Systems, *Int. J. of Vehicle Design*, Vol. 7, No. 1, pp. 52-63.

Goldman, D.E. (1948). A review of subjective responses to vibratory motion of the human body in the frequency range 1 to 70 cycles per second. Naval Medical Research Institute Report No. 1.

Goncalves, F.D. (2001). Dynamic Analysis of Semi-Active Control Techniques for Vehicle Applications. Masters Thesis, Virginia Tech.

Greenberg, M.D. (1998). *Advanced Engineering Mathematics*. 2nd Edition, Prentice Hall, pp. 1240-1255.

Guignard, J.C. and Irving, A. (1979). Measurement of the eye movement during low frequency vibration. *Aerospace Medicine*, Vol. 33, pp. 1230-1238.

Guignard, J.C. and McCauley, M.E. (1982). Motion sickness incidence induced by complex periodic wave forms. *Aviation, Space and Environmental Medicine*, Vol. 53, pp. 554-563.

Hong, K.S., Sohn, H.C. and Hedrick, J.K. (2002). Modified Skyhook Control of Semiactive Suspensions: A New Model, Gain Scheduling, and Hardware-in-the-loop Tuning. Transactions of the ASME, Vol. 124, pp. 158-167.

ISO 2631 (1997), *Mechanical Vibration and Shock – Evaluation of Human Exposure to Whole-body Vibration – Part 1: General Requirements.*

ISO 5805 (1997), *Mechanical Vibration and Shock – Human Exposure – Vocabulary.*

Ivers, D.E. and Miller, L.R. (1989). Experimental Comparison of Passive, Semiactive on/off, and Semiactive Continuous Suspensions. SAE Paper No. 892484.

Janeway, R.N. (1948). Vehicle vibration limits to fit the passenger. Presented at SAE National Passenger Car and Production Meeting, Detroit.

Jiang, Z., Streit, D.A. and El-Gindy, M. (2001). Heavy vehicle ride comfort: Literature survey", *Heavy Vehicle System, A Series of the Int. J. of Vehicle Design*, Vol. 8, No ¾, pp. 258-284.

Jones, A.J. and Saunders, D. (1972). A scale of human reaction whole body vertical, sinusoidal vibration. *Journal of Sound and Vibration*, Vol. 23, pp. 1-14.

Koo, J.H. and Ahmadian, M. (2001). Dynamic Analysis of Semiactive Tuned Vibration Absorbers Using Closed-form Equivalent Models. ASME 2001 Int. Mechanical Engineering Congress and Exposition, New York.

Lee, R.A. and Pradko, F. (1968). Analytical Analysis of Human vibration. SAE Paper No. 680091.

Miller, L.R. (1988). Tuning Passive, Semiactive, and Fully Active Suspension Systems. Proceedings of the 27th Conference on Decision and Control, Austin, TX, pp. 2047-2053.

Ogata, K. (1997). *Modern Control Engineering*. Prentice Hall.

Olley, M. (1934). Independent wheel suspension – its why and wherefores. SAE Journal, pp.73.

Papalukopulos, C., Giagopulos, D. and Natsiavas, S. (2005). Dynamics Of Large Scale Vehicle Models Coupled With Driver Biodynamic Models. 5th GRACM International Congress on Computational Mechanics, Limassol.

Pradko, F. (1965). Human Response to random vibration. The Shock and Vibration Buletin, US Naval Research Institute, WA, Vol. 34, No. 4.

Pradko, F. and Lee, R.A. (1966). Vibration Comfort criteria. SAE paper 660139.

Pradko, F., Lee, R.A. and Kaluza, V. (1966). Theory of Human Vibration Response. ASME Paper No. 66WA/BHF-15.

Rakheja, S. and Boileau, P.E. (1993). Contributed chapter, *Automotive Engineering and Ligitation*. John Wiley and Sons, Vol. 5, pp. 247-442.

Riley, R.Q. Automobile Ride, Handling, and Suspension Design: With Implications for Low-Mass Vehicles. Retrieved October 15, 2005. http://www.rqriley.com/suspensn.html.

SAE J6a. (1965). *Ride and Vibration Data Manual.*

Sharp, R.S. and Hassan, S.A. (1986). The Relative Performance Capabilities of Passive, Active and Semiactive Car Suspension Systems. Proceedings of IMechE, Vol. 200, No. D3, pp. 219-227.

Soliman, A.M.A., Abd Allah, S.A., El-Beter, A.A. and Hamid, M.S. (2001). Effect of suspension spring stiffness on vehicle dynamics. *Heavy Vehicle System, A Series of the Int. J. of Vehicle Design*, Vol. 8, No 3/4, pp. 316-334.

Stone, M.R. and Demetriou, M.A. (2000). Modeling and simulation of vehicle ride and handling performance. Proceedings of the 15th IEEE International Symposium on Intelligent Control, Rio, Patras, Greece.

Sun, T., Zhang, Y. and Barak P. (2002). 4-DOF Vehicle Ride Model. SAE Paper No. 2002-01-1580.

Tao, J.J. and Bishop, T.A. (2000). System Modeling of A Damper Module. SAE Technical Papers Series, No. 2000-01-0727, Detroit, MI.

Tong, R.T. (2001). Ride control – a two-state design for heavy vehicle suspension. Ph. D. Thesis, University of Illinois, Chicago.

van Deusen, B.D. (1968). Human Response to vehicle vibration. SAE Paper No. 680090.

von Eldik Thieme, H.C. (1961). Passenger Riding Comfort Criteria and Methods of Analysing Ride and Vibration Data. SAE Paper No. 610173.

Wong, J.Y. (2003). *TheTheory of Ground Vehicle*. John Wiley and Sons Inc.

Yao, G.Z., Yap, F.F., Chen, G., Li, W.H. and Yeo, S.H. (2002). MR Damper and Its Application for Semiactive Control of Vehicle Suspension System. Technical Note, Mechatronics, Vol. 12, pp. 963-973.

APPENDIX A

SAMPLES OF MATLAB CODES

A.1 Q-CAR 2-DOF FREQUENCY RESPONSE CODE

```
% FILENAME: Q2DOF_TF_convway.m
% This program is to get the frequency domain response of the model
% This program will plot all systems in one single plot for various
% variable.

% Note: The program is based on model derived for the following state % space
representation:
% x1 = sprung mass vertical deflection
% x2 = unsprung mass deflection
% x3 = sprung mass vertical velocity
% x4 = unsprung mass velocity

clear all
figplot = 1;    % 0 if do not want to plot the result, 1 if otherwise

% Our parameter values
cs = 980;
ms = 240;
ks = 16000;
mu = 36;
kt = 160000;
D = 0; % Will be used when we write 'sys1  = ss(A,L,C,D)'

for system=1:4;
if (system == 1)% this is for the passive case
    cof = cs; con = cs;
    alp = 1;
end
if (system == 2)% this is for the groundhook semi active case
    cof = 0.2*cs; con = 2*cs;
    alp = 0;
end
if (system == 3)% this is for the hybrid semi active case
    cof = 0.2*cs; con = 2*cs;
    alp = 0.5;
end
if (system == 4)% this is for the skyhook semi active casee
    cof = 0.2*cs; con = 2*cs;
    alp = 1;
end

% My A matrices
A = [0 0 1 0; 0 0 0 1; -ks/ms ks/ms -(cof+alp*(con-cof))/ms cof/ms;...
    ks/mu -(ks+kt)/mu cof/mu -(cof+(1-alp)*(con-cof))/mu];

% My B matrix
B = [0; 0; 0; kt/mu];

w = logspace(-1, log10(1000), 100);   % w is in rad/s
ymax = zeros(length(w),4);

for k=1:length(w)
tstep = 0.001;
tmax = 100;
```

```
tss = 50;   % time after which we say it's steady state

t = 0:tstep:tmax;

xin = 0.05*sin(w(k)*t); % amplitude is 0.05m
input = [xin];

%%%%%%%%%%%%%%%%%%%%%%%%%%%%%%%%
% For sprung mass responses
    C1 = [-ks/ms ks/ms -(cof+alp*(con-cof))/ms cof/ms];
    D1 = 0;
    sys1 = ss(A,B,C1,D1);
    [yss1,t] = lsim(sys1,input,t);

% for unsprung mass acceleration
    C2 = [ks/mu -(ks+kt)/mu cof/mu -(cof+(1-alp)*(con-cof))/mu];
    D2 = kt/mu;
    sys2 = ss(A,B,C2,D2);
    [yss2,t] = lsim(sys2,input,t);

% For suspension systems responses
    C3 = [1 -1 0 0];
    D3 = 0;
    sys3 = ss(A,B,C3,D3);
    [yss3,t] = lsim(sys3,input,t);

 % For tire responses
    C4 = [0 1 0 0];
    D4 = -1;
    sys4 = ss(A,B,C4,D4);
    [yss4,t] = lsim(sys4,input,t);

    for i=(tss/tstep):max(length(t)) % we start the reading after the system
reach steady state
        if (abs(yss1(i)) > ymax(k,1))
            ymax(k,1) = abs(yss1(i));
        end
        if (abs(yss2(i)) > ymax(k,2))
            ymax(k,2) = abs(yss2(i));
        end
        if (abs(yss3(i)) > ymax(k,3))
            ymax(k,3) = abs(yss3(i));
        end
        if (abs(yss4(i)) > ymax(k,4))
            ymax(k,4) = abs(yss4(i));
        end
    end % for i
end      % for k

         figure(1);loglog(w,ymax(:,1))
        hold on
        figure(2);loglog(w,ymax(:,2))
        hold on
        figure(3);loglog(w,ymax(:,3))
        hold on
        figure(4);loglog(w,ymax(:,4))
        hold on
 end   % for system
```

A.2 H-CAR 4-DOF STEADY STATE TIME-DOMAIN RESPONSE CODE

```
% FILENAME: H4DOF_t_ss_convway.m
% This program is to get the time domain steady state response of the
% model. The equations of motion were derived using usual model, not
% the Chalasani's approach

% Note: The program is based on model derived for the following state
% space representation:
% x1 = sprung mass vertical deflection
% x2 = sprung mass pitch angular deflection
% x3 = front unsprung mass deflection
% x4 = rear unsprung mass deflection

clear all

inputtype = 2; % 1 for heave, 2 for pitch
system = 4; % 1 for passive, 2 for groundhook, 3 for hybrid and 4 for skyhook
figplot = 1;   % 0 if do not want to plot the result, 1 if otherwise

y1max=0; y2max=0; y3max=0; y4max=0; y5max=0; y6max=0; y7max=0; y8max=0;
y1min=0; y2min=0; y3min=0; y4min=0; y5min=0; y6min=0; y7min=0; y8min=0;

% Our parameter values
ms = 730;   % for half car
Iyy = 2460;     % for pitch
ks1 = 19960; ks2 = 17500; % front and rear suspension stiffness
cs1 = 1290; cs2 = 1620;     % front and rear suspension damping coeff
mu1 = 40; mu2 = 35.5;   % front and rear unsprung masses
kt1 = 175500; kt2 = 175500; % front and rear tire stiffness
lf = 1.011; lr = 1.803;    % for pitch

% Based on the parameters above, we found the natural frequencies to be:

if (system == 1)    % natural frequencies for passive system
wn1=5.0955; wn2=7.1128; wn3=69.4906; wn4=72.5727;
end
if (system == 2)    % natural frequencies for groundhook system
wn1=5.0482; wn2=7.0193; wn3=69.9297; wn4=73.7622;
end
if (system == 3)    % natural frequencies for hybrid system
wn1=5.0731; wn2=6.987; wn3=69.9247; wn4=73.7458;
end
if (system == 4)    % natural frequencies for skyhook system
wn1=5.1173; wn2=6.9317; wn3=69.9092; wn4=73.7083;
end

w = wn4

% con and coff for semicative
cof1 = 0.2*cs1; con1 = 2*cs1;
cof2 = 0.2*cs2; con2 = 2*cs2;

if (system == 1)% this is for the passive case
    cof1 = cs1; con1 = cs1;
    cof2 = cs2; con2 = cs2;
    alp = 1;
end
if (system == 2)% this is for the groundhook semi active case
    alp = 0;
end
if (system == 3)% this is for the hybrid semi active case
    alp = 0.5;
end
if (system == 4)% this is for the skyhook semi active casee
    alp = 1;
```

```
end

% My A matrices

a51 = -(ks1 + ks2)/ms; a52 = (ks1*lf - ks2*lr)/ms; a53 = ks1/ms; a54 =
ks2/ms; a55 = -(cof1 + alp*(con1 - cof1) + cof2 + alp*(con2 - cof2))/ms; a56
= ((cof1 + alp*(con1 - cof1))*lf - (cof2 + alp*(con2 - cof2))*lr)/ms; a57 =
cof1/ms; a58 = cof2/ms;
a61 = (ks1*lf - ks2*lr)/Iyy; a62 = -(ks1*lf^2 + ks2*lr^2)/Iyy; a63 = -
ks1*lf/Iyy; a64 = ks2*lr/Iyy; a65 = ((cof1 + alp*(con1 - cof1))*lf - (cof2 +
alp*(con2 - cof2))*lr)/Iyy; a66 = -((cof1 + alp*(con1 - cof1))*lf^2 + (cof2 +
alp*(con2 - cof2))*lr^2)/Iyy; a67 = -cof1*lf/Iyy; a68 = cof2*lr/Iyy;
a71 = ks1/mu1; a72 = -ks1*lf/mu1; a73 = -(ks1 + kt1)/mu1; a74 = 0; a75 =
cof1/mu1;a76 = -cof1*lf/mu1; a77 = -(cof1 + (1 - alp)*(con1 - cof1))/mu1; a78
= 0;
a81 = ks2/mu2; a82 = ks2*lr/mu2; a83 = 0; a84 = -(ks2 + kt2)/mu2; a85 =
cof2/mu2;a86 = cof2*lr/mu2; a87 = 0; a88 = -(cof2 + (1 - alp)*(con2 -
cof2))/mu2;

A1 = [0 0 0 0 1 0 0 0];
A2 = [0 0 0 0 0 1 0 0];
A3 = [0 0 0 0 0 0 1 0];
A4 = [0 0 0 0 0 0 0 1];
A5 = [a51 a52 a53 a54 a55 a56 a57 a58];
A6 = [a61 a62 a63 a64 a65 a66 a67 a68];
A7 = [a71 a72 a73 a74 a75 a76 a77 a78];
A8 = [a81 a82 a83 a84 a85 a86 a87 a88];
A = [A1; A2; A3; A4; A5; A6; A7; A8];

% My B matrix
B = [0 0; 0 0; 0 0; 0 0; 0 0; 0 0; kt1/mu1 0; 0 kt2/mu2];

tstep = 0.01;
tmax = 30;
t = 0:tstep:tmax;

if (inputtype == 1)  % Heave input
%   xin1 = -(1/w)*cos(w*t); xin2 = -(1/w)*cos(w*t); % amplitude 1 m/s
    xin1 = 0.05*sin(w*t); xin2 = 0.05*sin(w*t); % amplitude is 0.05m
end

if (inputtype == 2)  % Pitch input
%   xin1 = -(1/w)*cos(w*t); xin2 = +(1/w)*cos(w*t); % amplitude 1 m/s
    xin1 = 0.05*sin(w*t); xin2 = -0.05*sin(w*t); % amplitude is 0.05m
end

input = [xin1; xin2];

%%%%%%%%%%%%%%%%%%%%%%%%%%%%%%%%
% For sprung mass responses
    C1 = [a51 a52 a53 a54 a55 a56 a57 a58];
    C2 = [a61 a62 a63 a64 a65 a66 a67 a68];
    D1 = 0;
    D2 = 0;
     sys1 = ss(A,B,C1,D1);
    sys2 = ss(A,B,C2,D2);
    [yss1,t1] = lsim(sys1,input,t);% sprung mass heave acceleration
    [yss2,t2] = lsim(sys2,input,t);% sprung mass pitch angular accel.

% For suspension systems responses
    C3 = [1 -lf -1 0 0 0 0 0];
    C4 = [1 lr 0 -1 0 0 0 0];
    D3 = 0;
    D4 = 0;
    sys3 = ss(A,B,C3,D3);
    sys4 = ss(A,B,C4,D4);
    [yss3,t3] = lsim(sys3,input,t); % front suspension deflection
```

```
    [yss4,t4] = lsim(sys4,input,t); % rear suspension deflection

    C5 = [0 0 1 0 0 0 0 0];
    C6 = [0 0 0 1 0 0 0 0];
    D5 = [-1 0];
    D6 = [0 -1];
    sys5 = ss(A,B,C5,D5);
    sys6 = ss(A,B,C6,D6);
    [yss5,t5] = lsim(sys5,input,t); % front tire deflection
    [yss6,t6] = lsim(sys6,input,t); % rear tire deflection

    C7 = [a71 a72 a73 a74 a75 a76 a77 a78];
    C8 = [a81 a82 a83 a84 a85 a86 a87 a88];
    D7 = [kt1/mu1 0];
    D8 = [0 kt2/mu2];
    sys7 = ss(A,B,C7,D7);
    sys8 = ss(A,B,C8,D8);
    [yss7,t7] = lsim(sys7,input,t);% front unsprung mass vert. accel.
    [yss8,t8] = lsim(sys8,input,t);% rear unsprung mass vert. accel.

% *** Now to get the min and max steady state values
    for i=1500:3001 % we start the reading after the system reach steady
state +- after 15 secs
        if (yss1(i) > y1max)
            y1max = yss1(i);
        end
        if (yss2(i) > y2max)
            y2max = yss2(i);
        end
        if (yss3(i) > y3max)
            y3max = yss3(i);
        end
        if (yss4(i) > y4max)
            y4max = yss4(i);
        end
        if (yss5(i) > y5max)
            y5max = yss5(i);
        end
        if (yss6(i) > y6max)
            y6max = yss6(i);
        end
        if (yss7(i) > y7max)
            y7max = yss7(i);
        end
        if (yss8(i) > y8max)
            y8max = yss8(i);
        end
        if (yss1(i) < y1min)
            y1min = yss1(i);
        end
        if (yss2(i) < y2min)
            y2min = yss2(i);
        end
        if (yss3(i) < y3min)
            y3min = yss3(i);
        end
        if (yss4(i) < y4min)
            y4min = yss4(i);
        end
        if (yss5(i) < y5min)
            y5min = yss5(i);
        end
        if (yss6(i) < y6min)
            y6min = yss6(i);
        end
        if (yss7(i) < y7min)
            y7min = yss7(i);
```

```
        end
        if (yss8(i) < y8min)
            y8min = yss8(i);
        end
    end

    if (figplot == 1)   % if we want to plot the results
%%%%%%%%%%%%%%%%%%%%%%%%%%%%%%%%%%%%%%%%%%%%%%%%%%%%%%%%
%  Now, to plot the results
%%%%%%%%%%%%%%%%%%%%%%%%%%%%%%%%%%%%%%%%%%%%%%%%%%%%%%%%
%********** Passive case
if (system == 1)
    figure(11); plot(t1,yss1)% steady state sprung mass accel.
    figure(12); plot(t2,yss2)% steady state sprung mass pitch angular accel.
    figure(13); plot(t3,yss3)% steady state suspension deflection
    figure(14); plot(t4,yss4)% steady state suspension deflection
    figure(15); plot(t5,yss5)% steady state tire deflection
    figure(16); plot(t6,yss6)% steady state tire deflection
    figure(17); plot(t7,yss7)% for front unsprung mass acceleration
    figure(18); plot(t8,yss8)% for rear unsprung mass acceleration
end   % for passive plots

%********* Groundhook case
if (system == 2)
    figure(21); plot(t1,yss1)  % steady state sprung mass accel
    figure(22); plot(t2,yss2)% steady state sprung mass pitch angular accel
    figure(23); plot(t3,yss3)% steady state suspension deflection
    figure(24); plot(t4,yss4)% steady state suspension deflection
    figure(25); plot(t5,yss5)% steady state tire deflection
    figure(26); plot(t6,yss6)% steady state tire deflection
    figure(27); plot(t7,yss7)% steady state front unspr. mass accel.
    figure(28); plot(t8,yss8)% steady state rear unspr. mass accel.
end   % for groundhook plots

%********** Hybrid case
if (system == 3)
    figure(31); plot(t1,yss1)% steady state sprung mass accel
    figure(32); plot(t2,yss2)% steady state sprung mass pitch angular accel
    figure(33); plot(t3,yss3)% steady state suspension deflection
    figure(34); plot(t4,yss4)% steady state suspension deflection
    figure(35); plot(t5,yss5)% steady state tire deflection
    figure(36); plot(t6,yss6)% steady state tire deflection
    figure(37); plot(t7,yss7)% steady state front unspr. mass accel.
    figure(38); plot(t8,yss8)% steady state rear unspr. mass accel.
end   % for hybrid plots

%********** Skyhook case
if (system == 4)
    figure(41); plot(t1,yss1)% steady state sprung mass accel
    figure(42); plot(t2,yss2)% steady state sprung mass pitch
    figure(43); plot(t3,yss3)% steady state suspension deflection
    figure(44); plot(t4,yss4)% steady state suspension deflection
    figure(45); plot(t5,yss5)% steady state tire deflection
    figure(46); plot(t6,yss6)% steady state tire deflection
    figure(47); plot(t7,yss7)% steady state front unspr. mass accel.
    figure(48);   plot(t8,yss8)% steady state rear unspr. mass accel.
end   % for skyhook plots
end   % for if plot
```

A.3 F-CAR 7-DOF TRANSIENT STATE TIME-DOMAIN RESPONSE CODE

```
% FILENAME: F7DOF_t_tr_convway.m
% This program is to get the time domain transient state response of the
model to various input.

clear all
inputtype = 1; % the type of input 1 = heave, 2 = pitch, 3 = roll
system = 1; % 1 = passive, 2 = groundhook, 3 = hybrid and 4 = skyhook
figplot = 1;    % 0 if do not want to plot the result, 1 if otherwise

% Our numerical values
ms = 1460;          % for full car
Iyy = 2460; Ixx = 460;  % for pitch and roll
k1 = 19960; k4 = 19960; % front left and right susp stiffness
k2 = 17500; k3 = 17500; % rear left and right susp stiffness
cs1 = 1290; cs4 = 1290; % front left and right susp damping coeff
cs2 = 1620; cs3 = 1620; % rear left and right susp damping coeff
mu1=40;mu4=40;mu2= 35.5;mu3= 35.5; % front and rear unsprung masses
kt1=175500;kt2=175500;kt3=175500;kt4=175500; % tires' stiffness
lf = 1.011;lr = 1.803; % side dist from front and rear susp to CG
tf = 1.522;tr = 1.51; % frontal dist from right and left susp to CG
kf = 0; kr = 0;       % front and rear anti roll bar stiffness
alf = tf/2; alr = tr/2; arr = tr/2; arf = tf/2;

% con and coff for semiactive
cof1 = 0.2*cs1; cof2 = 0.2*cs2; cof3 = 0.2*cs3; cof4 = 0.2*cs4;
con1 = 2*cs1; con2 = 2*cs2; con3 = 2*cs3; con4 = 2*cs4;

if (system == 1)% this is for the passive case
    cof1 = cs1; con1 = cs1;
    cof2 = cs2; con2 = cs2;
    cof3 = cs3; con3 = cs3;
    cof4 = cs4; con4 = cs4;
    alp = 1;
end
if (system == 2)% this is for the groundhook semi active case
    alp = 0;
end
if (system == 3)% this is for the hybrid semi active case
    alp = 0.5;
end
if (system == 4)% this is for the skyhook semi active casee
    alp = 1;
end


% My matrices
a0101= 0;a0102 = 0;a0103 = 0;a0104 = 0;a0105 = 0;a0106 = 0;a0107 = 0;
a0108= 1;a0109 = 0;a0110 = 0;a0111 = 0;a0112 = 0;a0113 = 0;a0114 = 0;
a0201= 0;a0202 = 0;a0203 = 0;a0204 = 0;a0205 = 0;a0206 = 0;a0207 = 0;
a0208= 0;a0209 = 1;a0210 = 0;a0211 = 0;a0212 = 0;a0213 = 0;a0214 = 0;
a0301= 0;a0302 = 0;a0303 = 0;a0304 = 0;a0305 = 0;a0306 = 0;a0307 = 0;
a0308= 0;a0309 = 0;a0310 = 1;a0311 = 0;a0312 = 0;a0313 = 0;a0314 = 0;
a0401= 0;a0402 = 0;a0403 = 0;a0404 = 0;a0405 = 0;a0406 = 0;a0407 = 0;
a0408= 0;a0409 = 0;a0410 = 0;a0411 = 1;a0412 = 0;a0413 = 0;a0414 = 0;
a0501= 0;a0502 = 0;a0503 = 0;a0504 = 0;a0505 = 0;a0506 = 0;a0507 = 0;
a0508= 0;a0509 = 0;a0510 = 0;a0511 = 0;a0512 = 1;a0513 = 0;a0514 = 0;
a0601= 0;a0602 = 0;a0603 = 0;a0604 = 0;a0605 = 0;a0606 = 0;a0607 = 0;
a0608 = 0;a0609 = 0;a0610 = 0;a0611 = 0;a0612 = 0;a0613= 1;a0614= 0;
a0701= 0;a0702 = 0;a0703 = 0;a0704 = 0;a0705 = 0;a0706 = 0;a0707 = 0;
a0708= 0;a0709 = 0;a0710 = 0;a0711 = 0;a0712 = 0;a0713 = 0;a0714 = 1;
a0801=-(k1+k2+k3+k4)/ms;a0802=(-k1*lf + k2*lr + k3*lr - k4*lf)/ms;
a0803 = (-k1*alf - k2*alr + k3*arr + k4*arf)/ms;
a0804 = k1/ms; a0805 = k2/ms; a0806 = k3/ms; a0807 = k4/ms;
```

```
a0808 = -(cof1 + alp*(con1-cof1) + cof2 + alp*(con2-cof2) + cof3 + alp*(con3-
cof3) + cof4 + alp*(con4-cof4))/ms;
a0809 = (-(cof1 + alp*(con1-cof1))*lf + (cof2 + alp*(con2-cof2))*lr + (cof3 +
alp*(con3-cof3))*lr - (cof4 + alp*(con4-cof4))*lf)/ms;
a0810 = (-(cof1 + alp*(con1-cof1))*alf - (cof2 + alp*(con2-cof2))*alr + (cof3
+ alp*(con3-cof3))*arr + (cof4 + alp*(con4-cof4))*arf)/ms;
a0811 = cof1/ms; a0812 = cof2/ms; a0813 = cof3/ms; a0814 = cof4/ms;

a0901 = (-k1*lf + k2*lr + k3*lr - k4*lf)/Iyy; a0902 = -(k1*lf^2 + k2*lr^2 +
k3*lr^2 + k4*lf^2)/Iyy;
a0903 = (-k1*lf*alf + k2*lr*alr - k3*lr*arr + k4*lf*arf)/Iyy;
a0904=k1*lf/Iyy;a0905=-k2*lr/Iyy;a0906=-k3*lr/Iyy;a0907=k4*lf/Iyy;
a0908 = (-(cof1 + alp*(con1-cof1))*lf + (cof2 + alp*(con2-cof2))*lr + (cof3 +
alp*(con3-cof3))*lr - (cof4 + alp*(con4-cof4))*lf)/Iyy;
a0909 = -((cof1 + alp*(con1-cof1))*lf^2 + (cof2 + alp*(con2-cof2))*lr^2 +
(cof3 + alp*(con3-cof3))*lr^2 + (cof4 + alp*(con4-cof4))*lf^2)/Iyy;
a0910 = (-(cof1 + alp*(con1-cof1))*lf*alf + (cof2 + alp*(con2-cof2))*lr*alr -
(cof3 + alp*(con3-cof3))*lr*arr + (cof4 + alp*(con4-cof4))*lf*arf)/Iyy;
a0911 = cof1*lf/Iyy; a0912 = -cof2*lr/Iyy; a0913 = -cof3*lr/Iyy; a0914 =
cof4*lf/Iyy; %%
a1001 = (-k1*alf - k2*alr + k3*arr + k4*arf)/Ixx;
a1002 = (-k1*lf*alf + k2*lr*alr - k3*lr*arr + k4*lf*arf)/Ixx;
a1003 =  -(k1*alf^2 + k2*alr^2 + k3*arr^2 + k4*arf^2)/Ixx;
a1004 = k1*alf/Ixx; a1005 = k2*alr/Ixx; a1006 = -k3*arr/Ixx; a1007 = -
k4*arf/Ixx;
a1008 = (-(cof1 + alp*(con1-cof1))*alf - (cof2 + alp*(con2-cof2))*alr +(cof3
+ alp*(con3-cof3))*arr + (cof4 + alp*(con4-cof4))*arf)/Ixx;
a1009 = (-(cof1 + alp*(con1-cof1))*lf*alf + (cof2 + alp*(con2-cof2))*lr*alr -
(cof3 + alp*(con3-cof3))*lr*arr + (cof4 + alp*(con4-cof4))*lf*arf)/Ixx;
a1010 = -((cof1 + alp*(con1-cof1))*alf^2 + (cof2 + alp*(con2-cof2))*alr^2
+(cof3 + alp*(con3-cof3))*arr^2 + (cof4 + alp*(con4-cof4))*arf^2)/Ixx;
a1011 = cof1*alf/Ixx; a1012 = cof2*alr/Ixx; a1013 = -cof3*arr/Ixx; a1014 = -
cof4*arf/Ixx;  %%
a1101=k1/mu1;a1102=k1*lf/mu1;a1103=k1*alf/mu1;a1104=-(k1 + kt1)/mu1;
a1105=0; a1106=0; a1107=0; a1108=cof1/mu1; a1109=cof1*lf/mu1;
a1110 = cof1*alf/mu1; a1111 = -(cof1 + (1-alp)*(con1-cof1))/mu1;
a1112 = 0; a1113 = 0; a1114 = 0;  %%
a1201 = k2/mu2; a1202 = -k2*lr/mu2; a1203 = k2*alr/mu2; a1204 = 0;
a1205 = -(k2 + kt2)/mu2; a1206 = 0; a1207 = 0;
a1208 = cof2/mu2; a1209= -cof2*lr/mu2; a1210= cof2*alr/mu2; a1211= 0;
a1212 = -(cof2 + (1-alp)*(con2-cof2))/mu2; a1213 = 0; a1214 = 0;  %%
a1301 = k3/mu3; a1302 = -k3*lr/mu3; a1303 = -k3*arr/mu3; a1304 = 0;
a1305 = 0; a1306 = -(k3 + kt3)/mu3; a1307 = 0;
a1308= cof3/mu3; a1309= -cof3*lr/mu3; a1310= -cof3*arr/mu3; a1311= 0;
a1312 = 0; a1313 = -(cof3 + (1-alp)*(con3-cof3))/mu3; a1314 = 0; %%
a1401 = k4/mu4; a1402 = k4*lf/mu4; a1403 = -k4*arf/mu4; a1404 = 0;
a1405 = 0; a1406 = 0; a1407 = -(k4 + kt4)/mu4;
a1408= cof4/mu4; a1409= cof4*lf/mu4; a1410= -cof4*arf/mu4; a1411= 0;
a1412 = 0; a1413 = 0; a1414 = -(cof4 + (1-alp)*(con4-cof4))/mu4;  %%

A = [a0101 a0102 a0103 a0104 a0105 a0106 a0107 a0108 a0109 a0110 a0111 a0112
a0113 a0114; ...
    a0201 a0202 a0203 a0204 a0205 a0206 a0207 a0208 a0209 a0210 a0211 a0212
a0213 a0214;...
    a0301 a0302 a0303 a0304 a0305 a0306 a0307 a0308 a0309 a0310 a0311 a0312
a0313 a0314;...
    a0401 a0402 a0403 a0404 a0405 a0406 a0407 a0408 a0409 a0410 a0411 a0412
a0413 a0414;...
    a0501 a0502 a0503 a0504 a0505 a0506 a0507 a0508 a0509 a0510 a0511 a0512
a0513 a0514;...
    a0601 a0602 a0603 a0604 a0605 a0606 a0607 a0608 a0609 a0610 a0611 a0612
a0613 a0614;...
    a0701 a0702 a0703 a0704 a0705 a0706 a0707 a0708 a0709 a0710 a0711 a0712
a0713 a0714;...
    a0801 a0802 a0803 a0804 a0805 a0806 a0807 a0808 a0809 a0810 a0811 a0812
a0813 a0814;...
```

```
    a0901 a0902 a0903 a0904 a0905 a0906 a0907 a0908 a0909 a0910 a0911 a0912
a0913 a0914;...
    a1001 a1002 a1003 a1004 a1005 a1006 a1007 a1008 a1009 a1010 a1011 a1012
a1013 a1014;...
    a1101 a1102 a1103 a1104 a1105 a1106 a1107 a1108 a1109 a1110 a1111 a1112
a1113 a1114;...
    a1201 a1202 a1203 a1204 a1205 a1206 a1207 a1208 a1209 a1210 a1211 a1212
a1213 a1214;...
    a1301 a1302 a1303 a1304 a1305 a1306 a1307 a1308 a1309 a1310 a1311 a1312
a1313 a1314;...
    a1401 a1402 a1403 a1404 a1405 a1406 a1407 a1408 a1409 a1410 a1411 a1412
a1413 a1414];

% My B (input) matrix
if (inputtype == 1)  % Heave input
    B = [0; 0; 0; 0; 0; 0; 0; 0; 0; 0; +1*kt1/mu1; +1*kt2/mu2; +1*kt3/mu3;
+1*kt4/mu4];
    D8 = kt1/mu1;
    D9 = kt2/mu2;
    D10 = kt3/mu3;
    D11 = kt4/mu4;
    D12 = -1;
    D13 = -1;
    D14 = -1;
    D15 = -1;
end

if (inputtype == 2)  % Pitch input
    B = [0; 0; 0; 0; 0; 0; 0; 0; 0; 0; +1*kt1/mu1; -1*kt2/mu2; -1*kt3/mu3;
+1*kt4/mu4];
    D8 = kt1/mu1;
    D9 = -kt2/mu2;
    D10 = -kt3/mu3;
    D11 = kt4/mu4;
    D12 = -1;
    D13 = 1;
    D14 = 1;
    D15 = -1;
end

if (inputtype == 3) % Roll input
    B = [0; 0; 0; 0; 0; 0; 0; 0; 0; 0; +1*kt1/mu1; +1*kt2/mu2; -1*kt3/mu3; -
1*kt4/mu4];
    D8 = kt1/mu1;
    D9 = kt2/mu2;
    D10 = -kt3/mu3;
    D11 = -kt4/mu4;
    D12 = -1;
    D13 = -1;
    D14 = 1;
    D15 = 1;
end

%%%%%%%%%%%%%%%%%%%%%%%%%%%%%%%%
% For sprung mass responses

    C1 = [a0801 a0802 a0803 a0804 a0805 a0806 a0807 a0808 a0809 a0810 a0811
a0812 a0813 a0814];
    C2 = [a0901 a0902 a0903 a0904 a0905 a0906 a0907 a0908 a0909 a0910 a0911
a0912 a0913 a0914];
    C3 = [a1001 a1002 a1003 a1004 a1005 a1006 a1007 a1008 a1009 a1010 a1011
a1012 a1013 a1014];
    D1 = 0;
    sys1 = ss(A,B,C1,D1); % For sprung mass heave acceleration
    sys2 = ss(A,B,C2,D1); % for sprung mass pitch angular accel
    sys3 = ss(A,B,C3,D1); % for sprung mass roll angular accel
```

```
% For suspension systems responses

    C4 = [1 lf alf -1 0 0 0 0 0 0 0 0 0 0];
    C5 = [1 -lr alr 0 -1 0 0 0 0 0 0 0 0 0];
    C6 = [1 -lr -arr 0 0 -1 0 0 0 0 0 0 0 0];
    C7 = [1 lf -arf 0 0 0 -1 0 0 0 0 0 0 0];
    D2=0;
    sys4 = ss(A,B,C4,D2); % for front-left suspension deflection, x4
    sys5 = ss(A,B,C5,D2); % for rear-right suspension deflection, x6
    sys6 = ss(A,B,C6,D2); % for rear-left suspension deflection, x5
    sys7 = ss(A,B,C7,D2); % for front-right suspension deflection, x7

% For unsprung mass responses
    C8 = [a1101 a1102 a1103 a1104 a1105 a1106 a1107 a1108 a1109 a1110 a1111
a1112 a1113 a1114];
    C9 = [a1201 a1202 a1203 a1204 a1205 a1206 a1207 a1208 a1209 a1210 a1211
a1212 a1213 a1214];
    C10 = [a1301 a1302 a1303 a1304 a1305 a1306 a1307 a1308 a1309 a1310 a1311
a1312 a1313 a1314];
    C11 = [a1401 a1402 a1403 a1404 a1405 a1406 a1407 a1408 a1409 a1410 a1411
a1412 a1413 a1414];
    sys8 = ss(A,B,C8,D8);    % for FL unsprung mass accel, x4ddot
    sys9 = ss(A,B,C9,D9);    % for RL unsprung mass accel, x5ddot
    sys10 = ss(A,B,C10,D10); % for RR unsprung mass accel, x6ddot
    sys11 = ss(A,B,C11,D11); % for FR unsprung mass accel, x7ddot

    C12 = [0 0 0 1 0 0 0 0 0 0 0 0 0];
    C13 = [0 0 0 0 1 0 0 0 0 0 0 0 0];
    C14 = [0 0 0 0 0 1 0 0 0 0 0 0 0];
    C15 = [0 0 0 0 0 0 1 0 0 0 0 0 0];
    sys12 = ss(A,B,C12,D12); % for F-L tire deflection, x12
    sys13 = ss(A,B,C13,D13); % for R-L tire deflection, x13
    sys14 = ss(A,B,C14,D14); % for R-R tire deflection, x14
    sys15 = ss(A,B,C15,D15); % for F-R tire deflection, x15

    if (figplot == 1)   % if we want to plot the results
%%%%%%%%%%%%%%%%%%%%%%%%%%%%%%%%%%%%%%%%%%%%%%%%%%%%%%%%
%  Now, to plot the results
%%%%%%%%%%%%%%%%%%%%%%%%%%%%%%%%%%%%%%%%%%%%%%%%%%%%%%%%
%********** Passive case

if (system == 1)
    figure(11); step(sys1) % sprung mass heave accel response
    figure(12); step(sys2) % sprung mass pitch angular accel response
    figure(13); step(sys3) % sprung mass roll angular accel response
    figure(14); step(sys4) % F-L suspension deflection response
    figure(15); step(sys5) % R-L suspension deflection response
    figure(16); step(sys6) % R-R suspension deflection response
    figure(17); step(sys7) % F-R suspension deflection response
    figure(18); step(sys8) % F-L unsprung mass acceleration response
    figure(19); step(sys9) % R-L unsprung mass acceleration response
    figure(110); step(sys10) % R-R unsprung mass accel response
    figure(111); step(sys11) % F-R unsprung mass accel response
    figure(112); step(sys12) % F-L tire deflection response
    figure(113); step(sys13) % R-L tire deflection response
    figure(114); step(sys14) % R-R tire deflection response
    figure(115); step(sys15) % F-R tire deflection response
end   % for if system = 1 (passive plot)

%********* Groundhook case
if (system == 2)
    figure(21); step(sys1) % sprung mass heave accel response
    figure(22); step(sys2) % sprung mass pitch angular accel response
    figure(23); step(sys3) % sprung mass roll angular accel response
    figure(24); step(sys4) % F-L suspension deflection response
    figure(25); step(sys5) % R-L suspension deflection response
    figure(26); step(sys6) % R-R suspension deflection response
```

```
    figure(27); step(sys7) % F-R suspension deflection response
    figure(28); step(sys8) % F-L unsprung mass acceleration response
    figure(29); step(sys9) % R-L unsprung mass acceleration response
    figure(210); step(sys10) % R-R unsprung mass accel response
    figure(211); step(sys11) % F-R unsprung mass accel response
    figure(212); step(sys12) % F-L tire deflection response
    figure(213); step(sys13) % R-L tire deflection response
    figure(214); step(sys14) % R-R tire deflection response
    figure(215); step(sys15) % F-R tire deflection response
end % for groundhook plot

%*********** Hybrid case
if (system == 3)
    figure(31); step(sys1) % sprung mass heave accel response
    figure(32); step(sys2) % sprung mass pitch angular accel response
    figure(33); step(sys3) % sprung mass roll angular accel response
    figure(34); step(sys4) % F-L suspension deflection response
    figure(35); step(sys5) % R-L suspension deflection response
    figure(36); step(sys6) % R-R suspension deflection response
    figure(37); step(sys7) % F-R suspension deflection response
    figure(38); step(sys8) % F-L unsprung mass acceleration response
    figure(39); step(sys9) % R-L unsprung mass acceleration response
    figure(310); step(sys10) % R-R unsprung mass accel response
    figure(311); step(sys11) % F-R unsprung mass accel response
    figure(312); step(sys12) % F-L tire deflection response
    figure(313); step(sys13) % R-L tire deflection response
    figure(314); step(sys14) % R-R tire deflection response
    figure(315); step(sys15) % F-R tire deflection response
end % hybrid plot

%********** Skyhook case
if (system == 4)
    figure(41); step(sys1) % sprung mass heave accel response
    figure(42); step(sys2) % sprung mass pitch angular accel response
    figure(43); step(sys3) % sprung mass roll angular accel response
    figure(44); step(sys4) % F-L suspension deflection response
    figure(45); step(sys5) % R-L suspension deflection response
    figure(46); step(sys6) % R-R suspension deflection response
    figure(47); step(sys7) % F-R suspension deflection response
    figure(48); step(sys8) % F-L unsprung mass acceleration response
    figure(49); step(sys9) % R-L unsprung mass acceleration response
    figure(410); step(sys10) % R-R unsprung mass accel response
    figure(411); step(sys11) % F-R unsprung mass accel response
    figure(412); step(sys12) % F-L tire deflection response
    figure(413); step(sys13) % R-L tire deflection response
    figure(414); step(sys14) % R-R tire deflection response
    figure(415); step(sys15) % F-R tire deflection response
end % skyhook plot

end % if figplot
```

APPENDIX B

H-CAR 2-DOF TRANSFER FUNCTIONS

B.1 PASSIVE SYSTEM TRANSFER FUNCTIONS.

All of the transfer functions for passive system are having a common denominator regardless of input type (pitch or heave input), and given as below.

$$\text{Denom} = d_4 s^4 + d_3 s^3 + d_2 s^2 + d_1 s + d_0$$

where

$$d_4 = I_{yy} m_s$$
$$d_3 = c_{s1} I_{yy} + c_{s2} I_{yy} + c_{s1} l_f^{\,2} m_s + c_{s2} l_r^{\,2} m_s$$
$$d_2 = k_{s1} I_{yy} + k_{s2} I_{yy} + c_{s1} c_{s2} \left(l_f + l_r\right)^2 + k_{s1} l_f^{\,2} m_s + k_{s2} l_r^{\,2} m_s$$
$$d_1 = \left(c_{s1} k_{s2} + c_{s2} k_{s1}\right)\left(l_f + l_r\right)^2$$
$$d_0 = k_{s1} k_{s2} \left(l_f + l_r\right)^2$$

The numerators are given below, according to input signal.

B.1.1 Heave Input Signal

The transfer function for the vertical acceleration of the sprung mass is:

$$H_{\dot{x}_1}(s) = \frac{\dot{x}_1}{\dot{v}_{in}} = \frac{s \cdot x_1}{s \cdot v_{in}} = \frac{a_{13} s^3 + a_{12} s^2 + a_{11} s + a_{10}}{\text{Denom}}$$

where

$$a_{13} = \left(c_{s1} + c_{s2}\right) I_{yy}$$
$$a_{12} = k_{s1} I_{yy} + k_{s2} I_{yy} + c_{s1} c_{s2} \left(l_f + l_r\right)^2$$
$$a_{11} = \left(c_{s1} k_{s1} + c_{s2} k_{s2}\right)\left(l_f + l_r\right)^2$$
$$a_{10} = k_{s1} k_{s2} \left(l_f + l_r\right)^2$$

The transfer function for the pitch angular acceleration of the sprung mass is:

$$\mathrm{H}_{\ddot{x}_2}(s) = \frac{\dot{x}_2}{\dot{v}_{in}} = \frac{s \cdot x_2}{s \cdot v_{in}} = \frac{a_{23}s^3 + a_{22}s^2 + a_{21}s + a_{20}}{\text{Denom}}$$

where

$$a_{23} = -\left(c_{s1}l_f + c_{s2}l_r\right)m_s$$
$$a_{22} = -\left(k_{s1}l_f - k_{s2}l_r\right)m_s$$
$$a_{21} = 0$$
$$a_{20} = 0$$

The transfer function for the front suspension deflection of the sprung mass is:

$$\mathrm{H}_{x_3}(s) = \frac{x_3}{\dot{v}_{in}} = \frac{x_3}{s \cdot v_{in}} = \frac{a_{33}s^3 + a_{32}s^2 + a_{31}s + a_{30}}{\text{Denom}}$$

where

$$a_{33} = 0$$
$$a_{32} = -I_{yy}m_s$$
$$a_{31} = -c_{s2}l_r\left(l_f + l_r\right)m_s$$
$$a_{30} = -k_{s2}l_r\left(l_f + l_r\right)m_s$$

The transfer function for the rear suspension deflection of the sprung mass is:

$$\mathrm{H}_{x_4}(s) = \frac{x_4}{\dot{v}_{in}} = \frac{x_4}{s \cdot v_{in}} = \frac{a_{43}s^3 + a_{42}s^2 + a_{41}s + a_{40}}{\text{Denom}}$$

where

$$a_{43} = 0$$
$$a_{42} = -I_{yy}m_s$$
$$a_{41} = -c_{s1}l_f\left(l_f + l_r\right)m_s$$
$$a_{40} = -k_{s1}l_f\left(l_f + l_r\right)m_s$$

B.1.2 Pitch Input Signal

The transfer function for the vertical acceleration of the sprung mass is:

$$H_{\ddot{x}_1}(s) = \frac{\ddot{x}_1}{\dot{v}_{in}} = \frac{s \cdot x_1}{s \cdot v_{in}} = \frac{a_{13}s^3 + a_{12}s^2 + a_{11}s + a_{10}}{\text{Denom}}$$

where

$$a_{13} = (c_{s1} - c_{s2})I_{yy}$$
$$a_{12} = k_{s1}I_{yy} - k_{s2}I_{yy} - c_{s1}c_{s2}l_f^{\,2} + c_{s1}c_{s2}l_r^{\,2}$$
$$a_{11} = -(c_{s2}k_{s1} + c_{s1}k_{s2})(l_f - l_r)(l_f + l_r)$$
$$a_{10} = -k_{s1}k_{s2}(l_f - l_r)(l_f + l_r)$$

The transfer function for the pitch angular acceleration of the sprung mass is:

$$H_{\ddot{x}_2}(s) = \frac{\ddot{x}_2}{\dot{v}_{in}} = \frac{s \cdot x_2}{s \cdot v_{in}} = \frac{a_{23}s^3 + a_{22}s^2 + a_{21}s + a_{20}}{\text{Denom}}$$

where

$$a_{23} = -(c_{s1}l_f + c_{s2}l_r)m_s$$
$$a_{22} = -2c_{s1}c_{s2}l_f - -2c_{s1}c_{s2}l_r - k_{s1}l_f m_s - k_{s2}l_r m_s$$
$$a_{21} = -2(c_{s2}k_{s1} + c_{s1}k_{s2})(l_f + l_r)$$
$$a_{20} = -2k_{s1}k_{s2}(l_f + l_r)$$

The transfer function for the front suspension deflection of the sprung mass is:

$$H_{x_3}(s) = \frac{x_3}{\dot{v}_{in}} = \frac{x_3}{s \cdot v_{in}} = \frac{a_{33}s^3 + a_{32}s^2 + a_{31}s + a_{30}}{\text{Denom}}$$

where

$$a_{33} = 0$$
$$a_{32} = -I_{yy}m_s$$
$$a_{31} = -c_{s2}(2I_{yy} - l_f l_r m_s + l_r^{\,2}m_s)$$
$$a_{30} = -k_{s2}(2I_{yy} - l_f l_r m_s + l_r^{\,2}m_s)$$

The transfer function for the rear suspension deflection of the sprung mass is:

$$H_{x_4}(s) = \frac{x_4}{\dot{v}_{in}} = \frac{x_4}{s \cdot v_{in}} = \frac{a_{43}s^3 + a_{42}s^2 + a_{41}s + a_{40}}{\text{Denom}}$$

where

$$a_{43} = 0$$
$$a_{42} = I_{yy} m_s$$
$$a_{41} = c_{s1}\left(2I_{yy} + {l_f}^2 m_s - l_f l_r m_s\right)$$
$$a_{40} = k_{s1}\left(2I_{yy} + {l_f}^2 m_s - l_f l_r m_s\right)$$

B.2 SEMI-ACTIVE SYSTEM TRANSFER FUNCTIONS.

Similarly, the transfer functions for semi-active system are having a common denominator regardless of input type, however the ones for $H_{\dot{x}_1}$ and $H_{\dot{x}_2}$ are having different root order compared to for H_{x_4} and H_{x_3}. They are given as below. Note that the results are taken from Mathematica notebook file due to its lengthy terms.

$$\text{Denom} = d_5 s^5 + d_4 s^4 + d_3 s^3 + d_2 s^2 + d_1 s + d_0$$

where

```
*** *** *** denominators for Hx1dotH and Hx2dotH only
d4 = Iyy ms
d3 = cof1 Iyy + cof2 Iyy + cof1 lf^2 ms + cof2 lr^2 ms - cof1 Iyy α - cof2 Iyy α + con1 Iyy α +
   con2 Iyy α - cof1 lf^2 ms α + con1 lf^2 ms α - cof2 lr^2 ms α + con2 lr^2 ms α
d2 = Iyy ks1 + Iyy ks2 + cof1 cof2 lf^2 + 2 cof1 cof2 lf lr + cof1 cof2 lr^2 + ks1 lf^2 ms +
   ks2 lr^2 ms - 2 cof1 cof2 lf^2 α + cof2 con1 lf^2 α + cof1 con2 lf^2 α - 4 cof1 cof2 lf lr α +
   2 cof2 con1 lf lr α + 2 cof1 con2 lf lr α - 2 cof1 cof2 lr^2 α + cof2 con1 lr^2 α + cof1 con2 lr^2 α +
   cof1 cof2 lf^2 α^2 - cof2 con1 lf^2 α^2 - cof1 con2 lf^2 α^2 + con1 con2 lf^2 α^2 + 2 cof1 cof2 lf lr α^2 -
   2 cof2 con1 lf lr α^2 - 2 cof1 con2 lf lr α^2 + 2 con1 con2 lf lr α^2 + cof1 cof2 lr^2 α^2 -
   cof2 con1 lr^2 α^2 - cof1 con2 lr^2 α^2 + con1 con2 lr^2 α^2
d1 = -(lf + lr)^2 (-cof2 ks1 - cof1 ks2 + cof2 ks1 α - con2 ks1 α + cof1 ks2 α - con1 ks2 α)
d0 = ks1 ks2 (lf + lr)^2
```

```
** ** ** denominators for Hx3H and Hx4H only
d5 = Iyy ms
d4 = cof1 Iyy + cof2 Iyy + cof1 lf^2 ms + cof2 lr^2 ms - cof1 Iyy α - cof2 Iyy α + con1 Iyy α +
   con2 Iyy α - cof1 lf^2 ms α + con1 lf^2 ms α - cof2 lr^2 ms α + con2 lr^2 ms α
d3 = Iyy ks1 + Iyy ks2 + cof1 cof2 lf^2 + 2 cof1 cof2 lf lr + cof1 cof2 lr^2 + ks1 lf^2 ms +
   ks2 lr^2 ms - 2 cof1 cof2 lf^2 α + cof2 con1 lf^2 α + cof1 con2 lf^2 α - 4 cof1 cof2 lf lr α +
   2 cof2 con1 lf lr α + 2 cof1 con2 lf lr α - 2 cof1 cof2 lr^2 α + cof2 con1 lr^2 α + cof1 con2 lr^2 α +
   cof1 cof2 lf^2 α^2 - cof2 con1 lf^2 α^2 - cof1 con2 lf^2 α^2 + con1 con2 lf^2 α^2 + 2 cof1 cof2 lf lr α^2 -
   2 cof2 con1 lf lr α^2 - 2 cof1 con2 lf lr α^2 + 2 con1 con2 lf lr α^2 + cof1 cof2 lr^2 α^2 -
   cof2 con1 lr^2 α^2 - cof1 con2 lr^2 α^2 + con1 con2 lr^2 α^2
d2 = -(lf + lr)^2 (-cof2 ks1 - cof1 ks2 + cof2 ks1 α - con2 ks1 α + cof1 ks2 α - con1 ks2 α)
d1 = ks1 ks2 (lf + lr)^2
d0 = 0
```

B.2.1 Heave Input Signal

The transfer function for the vertical acceleration of the sprung mass is:

$$H_{\ddot{x}_1}(s) = \frac{\ddot{x}_1}{\dot{v}_{in}} = \frac{s \cdot x_1}{s \cdot v_{in}} = \frac{a_{13}s^3 + a_{12}s^2 + a_{11}s + a_{10}}{\text{Denom}}$$

where

```
** ** ** numerator for Hx1dotH
n14 = 0
n13 = -Iyy (-cof1 - cof2 + 2 cof1 α + 2 cof2 α - 2 con1 α - 2 con2 α)
n12 = Iyy ks1 + Iyy ks2 + cof1 cof2 lf^2 + 2 cof1 cof2 lf lr + cof1 cof2 lr^2 - 3 cof1 cof2 lf^2 α +
   cof2 con1 lf^2 α + 2 cof1 con2 lf^2 α - 6 cof1 cof2 lf lr α + 3 cof2 con1 lf lr α +
   3 cof1 con2 lf lr α - 3 cof1 cof2 lr^2 α + 2 cof2 con1 lr^2 α + cof1 con2 lr^2 α + 2 cof1 cof2 lf^2 α^2 -
   2 cof2 con1 lf^2 α^2 - 2 cof1 con2 lf^2 α^2 + 2 con1 con2 lf^2 α^2 + 4 cof1 cof2 lf lr α^2 -
   4 cof2 con1 lf lr α^2 - 4 cof1 con2 lf lr α^2 + 4 con1 con2 lf lr α^2 + 2 cof1 cof2 lr^2 α^2 -
   2 cof2 con1 lr^2 α^2 - 2 cof1 con2 lr^2 α^2 + 2 con1 con2 lr^2 α^2
n11 =
 -(lf + lr) (-cof2 ks1 lf - cof1 ks2 lf - cof2 ks1 lr - cof1 ks2 lr + 2 cof2 ks1 lf α -
     2 con2 ks1 lf α + cof1 ks2 lf α - con1 ks2 lf α + cof2 ks1 lr α - con2 ks1 lr α +
     2 cof1 ks2 lr α - 2 con1 ks2 lr α)
n10 = ks1 ks2 (lf + lr)^2
```

The transfer function for the pitch angular acceleration of the sprung mass is:

$$H_{\ddot{x}_2}(s) = \frac{\ddot{x}_2}{\dot{v}_{in}} = \frac{s \cdot x_2}{s \cdot v_{in}} = \frac{a_{23}s^3 + a_{22}s^2 + a_{21}s + a_{20}}{\text{Denom}}$$

where

```
** ** ** numerator for Hx2dotH
n24 = 0
n23 = ms (-cof1 lf + cof2 lr + 2 cof1 lf α - 2 con1 lf α - 2 cof2 lr α + 2 con2 lr α)
n22 = -ks1 lf ms + ks2 lr ms - cof2 con1 lf α + cof1 con2 lf α - cof2 con1 lr α + cof1 con2 lr α
n21 = -(cof2 ks1 - con2 ks1 - cof1 ks2 + con1 ks2) (lf + lr) α
n20 = 0
```

The transfer function for the front suspension deflection of the sprung mass is:

$$H_{x_3}(s) = \frac{x_3}{\dot{v}_{in}} = \frac{x_3}{s \cdot v_{in}} = \frac{a_{33}s^3 + a_{32}s^2 + a_{31}s + a_{30}}{\text{Denom}}$$

where

```
** ** ** numerator for Hx3H
n34 = 0
n33 = -Iyy ms
n32 = -cof2 lf lr ms - cof2 lr^2 ms - cof1 Iyy α - cof2 Iyy α + con1 Iyy α + con2 Iyy α -
  cof1 lf^2 ms α + con1 lf^2 ms α + 2 cof2 lf lr ms α - 2 con2 lf lr ms α + cof2 lr^2 ms α - con2 lr^2 ms α
n31 =
 -(lf + lr) (ks2 lr ms + cof1 cof2 lf α - cof2 con1 lf α + cof1 cof2 lr α - cof2 con1 lr α -
    cof1 cof2 lf α^2 + cof2 con1 lf α^2 + cof1 con2 lf α^2 - con1 con2 lf α^2 - cof1 cof2 lr α^2 +
    cof2 con1 lr α^2 + cof1 con2 lr α^2 - con1 con2 lr α^2)
n30 = -(cof1 - con1) ks2 (lf + lr)^2 α
```

The transfer function for the rear suspension deflection of the sprung mass is:

$$H_{x_4}(s) = \frac{x_4}{\dot{v}_{in}} = \frac{x_4}{s \cdot v_{in}} = \frac{a_{43}s^3 + a_{42}s^2 + a_{41}s + a_{40}}{\text{Denom}}$$

where

```
** ** ** numerator for Hx4H
n44 = 0
n43 = -Iyy ms
n42 = -cof1 lf^2 ms - cof1 lf lr ms - cof1 Iyy α - cof2 Iyy α + con1 Iyy α + con2 Iyy α +
  cof1 lf^2 ms α - con1 lf^2 ms α + 2 cof1 lf lr ms α - 2 con1 lf lr ms α - cof2 lr^2 ms α + con2 lr^2 ms α
n41 =
 -(lf + lr) (ks1 lf ms + cof1 cof2 lf α - cof1 con2 lf α + cof1 cof2 lr α - cof1 con2 lr α -
    cof1 cof2 lf α^2 + cof2 con1 lf α^2 + cof1 con2 lf α^2 - con1 con2 lf α^2 - cof1 cof2 lr α^2 +
    cof2 con1 lr α^2 + cof1 con2 lr α^2 - con1 con2 lr α^2)
n40 = -(cof2 - con2) ks1 (lf + lr)^2 α
```

B.2.2 Pitch Input Signal

The transfer function for the vertical acceleration of the sprung mass is:

$$H_{\dot{x}_1}(s) = \frac{\dot{x}_1}{\dot{v}_{in}} = \frac{s \cdot x_1}{s \cdot v_{in}} = \frac{a_{13}s^3 + a_{12}s^2 + a_{11}s + a_{10}}{\text{Denom}}$$

where

```
** ** ** numerator for Hx1dotP
n14 = 0
n13 = -Iyy (-cof1 + cof2 + 2 cof1 α - 2 cof2 α - 2 con1 α + 2 con2 α)
n12 = Iyy ks1 - Iyy ks2 - cof1 cof2 lf^2 + cof1 cof2 lr^2 + 3 cof1 cof2 lf^2 α - cof2 con1 lf^2 α -
   2 cof1 con2 lf^2 α + cof2 con1 lf lr α - cof1 con2 lf lr α - 3 cof1 cof2 lr^2 α + 2 cof2 con1 lr^2 α +
   cof1 con2 lr^2 α - 2 cof1 cof2 lf^2 α^2 + 2 cof2 con1 lf^2 α^2 + 2 cof1 con2 lf^2 α^2 - 2 con1 con2 lf^2 α^2 +
   2 cof1 cof2 lr^2 α^2 - 2 cof2 con1 lr^2 α^2 - 2 cof1 con2 lr^2 α^2 + 2 con1 con2 lr^2 α^2
n11 =
  (lf + lr) (-cof2 ks1 lf - cof1 ks2 lf + cof2 ks1 lr + cof1 ks2 lr + 2 cof2 ks1 lf α -
     2 con2 ks1 lf α + cof1 ks2 lf α - con1 ks2 lf α - cof2 ks1 lr α + con2 ks1 lr α -
     2 cof1 ks2 lr α + 2 con1 ks2 lr α)
n10 = -ks1 ks2 (lf - lr) (lf + lr)
```

The transfer function for the pitch angular acceleration of the sprung mass is:

$$H_{\dot{x}_2}(s) = \frac{\dot{x}_2}{\dot{v}_{in}} = \frac{s \cdot x_2}{s \cdot v_{in}} = \frac{a_{23}s^3 + a_{22}s^2 + a_{21}s + a_{20}}{\text{Denom}}$$

where

```
** ** ** numerator for Hx2dotP
n24 = 0
n23 = ms (-cof1 lf - cof2 lr + 2 cof1 lf α - 2 con1 lf α + 2 cof2 lr α - 2 con2 lr α)
n22 = -2 cof1 cof2 lf - 2 cof1 cof2 lr - ks1 lf ms - ks2 lr ms + 6 cof1 cof2 lf α -
   3 cof2 con1 lf α - 3 cof1 con2 lf α + 6 cof1 cof2 lr α - 3 cof2 con1 lr α - 3 cof1 con2 lr α -
   4 cof1 cof2 lf α^2 + 4 cof2 con1 lf α^2 + 4 cof1 con2 lf α^2 - 4 con1 con2 lf α^2 - 4 cof1 cof2 lr α^2 +
   4 cof2 con1 lr α^2 + 4 cof1 con2 lr α^2 - 4 con1 con2 lr α^2
n21 = (lf + lr) (-2 cof2 ks1 - 2 cof1 ks2 + 3 cof2 ks1 α - 3 con2 ks1 α + 3 cof1 ks2 α - 3 con1 ks2 α)
n20 = -2 ks1 ks2 (lf + lr)
```

The transfer function for the front suspension deflection of the sprung mass is:

$$H_{x_3}(s) = \frac{x_3}{\dot{v}_{in}} = \frac{x_3}{s \cdot v_{in}} = \frac{a_{33}s^3 + a_{32}s^2 + a_{31}s + a_{30}}{\text{Denom}}$$

where

```
** ** ** numerator for Hx3P
n34 = 0
n33 = -Iyy ms
n32 = -2 cof2 Iyy + cof2 lf lr ms - cof2 lr^2 ms - cof1 Iyy α + 3 cof2 Iyy α + con1 Iyy α -
   3 con2 Iyy α - cof1 lf^2 ms α + con1 lf^2 ms α - 2 cof2 lf lr ms α + 2 con2 lf lr ms α +
   cof2 lr^2 ms α - con2 lr^2 ms α
n31 = -2 Iyy ks2 + ks2 lf lr ms - ks2 lr^2 ms - cof1 cof2 lf^2 α + cof2 con1 lf^2 α -
   2 cof1 cof2 lf lr α + 2 cof2 con1 lf lr α - cof1 cof2 lr^2 α + cof2 con1 lr^2 α + cof1 cof2 lf^2 α^2 -
   cof2 con1 lf^2 α^2 - cof1 con2 lf^2 α^2 + con1 con2 lf^2 α^2 + 2 cof1 cof2 lf lr α^2 - 2 cof2 con1 lf lr α^2 -
   2 cof1 con2 lf lr α^2 + 2 con1 con2 lf lr α^2 + cof1 cof2 lr^2 α^2 - cof2 con1 lr^2 α^2 -
   cof1 con2 lr^2 α^2 + con1 con2 lr^2 α^2
n30 = -(cof1 - con1) ks2 (lf + lr)^2 α
```

The transfer function for the rear suspension deflection of the sprung mass is:

$$H_{x_4}(s) = \frac{x_4}{\dot{v}_{in}} = \frac{x_4}{s \cdot v_{in}} = \frac{a_{43}s^3 + a_{42}s^2 + a_{41}s + a_{40}}{\text{Denom}}$$

where

```
** ** ** numerator for Hx4P
n44 = 0
n43 = Iyy ms
n42 = 2 cof1 Iyy + cof1 lf^2 ms - cof1 lf lr ms - 3 cof1 Iyy α + cof2 Iyy α + 3 con1 Iyy α -
   con2 Iyy α - cof1 lf^2 ms α + con1 lf^2 ms α + 2 cof1 lf lr ms α - 2 con1 lf lr ms α +
   cof2 lr^2 ms α - con2 lr^2 ms α
n41 = 2 Iyy ks1 + ks1 lf^2 ms - ks1 lf lr ms + cof1 cof2 lf^2 α - cof1 con2 lf^2 α + 2 cof1 cof2 lf lr α -
   2 cof1 con2 lf lr α + cof1 cof2 lr^2 α - cof1 con2 lr^2 α - cof1 cof2 lf^2 α^2 + cof2 con1 lf^2 α^2 +
   cof1 con2 lf^2 α^2 - con1 con2 lf^2 α^2 - 2 cof1 cof2 lf lr α^2 + 2 cof2 con1 lf lr α^2 +
   2 cof1 con2 lf lr α^2 - 2 con1 con2 lf lr α^2 - cof1 cof2 lr^2 α^2 + cof2 con1 lr^2 α^2 +
   cof1 con2 lr^2 α^2 - con1 con2 lr^2 α^2
n40 = (cof2 - con2) ks1 (lf + lr)^2 α
```

APPENDIX C

H-CAR 2-DOF MEAN SQUARE VALUES

C.1 PASSIVE SYSTEM.

C.1.1 Heave Velocity Input Signal

Mean square of vertical velocity of sprung mass, $\mathrm{E}\left[x_1^{\,2}\right] =$

$$
\begin{aligned}
&-\Big(\big(-(cs2\,ksl + csl\,ks2)\,(lf+lr)^2\,ms\,\big(2\,(csl+cs2)\,Iyy\,(cs2\,ksl+csl\,ks2)\,(lf+lr)^2 - \\
&\quad (Iyy\,(ksl+ks2)+csl\,cs2\,(lf+lr)^2)^2 + Iyy\,ksl\,ks2\,(lf+lr)^2\,ms\big) + (-(csl+cs2)^2\,Iyy\,ksl\,ks2\,(lf+lr)^2 + \\
&\quad ((cs2\,ksl+csl\,ks2)^2\,(lf+lr)^4 - 2\,ksl\,ks2\,(lf+lr)^2\,(Iyy\,(ksl+ks2)+csl\,cs2\,(lf+lr)^2))\,ms) \\
&\quad (csl\,(Iyy+lf^2\,ms)+cs2\,(Iyy+lr^2\,ms)) + (lf+lr)^2 \\
&\quad (Iyy\,(ksl+ks2)+csl\,cs2\,(lf+lr)^2 + (ksl\,lf^2+ks2\,lr^2)\,ms) \\
&\quad ((csl+cs2)^2\,Iyy\,(cs2\,ksl+csl\,ks2)+ksl\,ks2\,ms\,(csl\,(Iyy+lf^2\,ms)+cs2\,(Iyy+lr^2\,ms)))\big)\,\pi\,S0\Big)\Big/ \\
&\Big((lf+lr)^2\,ms\,\big(Iyy\,(cs2\,ksl+csl\,ks2)^2\,(lf+lr)^2\,ms - (cs2\,ksl+csl\,ks2) \\
&\quad (Iyy\,(ksl+ks2)+csl\,cs2\,(lf+lr)^2+(ksl\,lf^2+ks2\,lr^2)\,ms)\,(csl\,(Iyy+lf^2\,ms)+cs2\,(Iyy+lr^2\,ms)) + \\
&\quad ksl\,ks2\,(csl\,(Iyy+lf^2\,ms)+cs2\,(Iyy+lr^2\,ms))^2\big)\Big)
\end{aligned}
$$

Mean square of pitch angular velocity of sprung mass, $\mathrm{E}\left[x_2^{\,2}\right] =$

$$
\begin{aligned}
&-(ms\,(Iyy\,(cs2\,ksl+csl\,ks2)\,(ksl\,lf-ks2\,lr)^2\,ms + \\
&\quad (cs2\,ksl+csl\,ks2)\,(csl\,lf-cs2\,lr)^2\,(Iyy\,(ksl+ks2)+csl\,cs2\,(lf+lr)^2+(ksl\,lf^2+ks2\,lr^2)\,ms) - \\
&\quad ksl\,ks2\,(csl\,lf-cs2\,lr)^2\,(csl\,(Iyy+lf^2\,ms)+cs2\,(Iyy+lr^2\,ms)))\,\pi\,S0)\Big/ \\
&\Big(Iyy\,\big(Iyy\,(cs2\,ksl+csl\,ks2)^2\,(lf+lr)^2\,ms - (cs2\,ksl+csl\,ks2) \\
&\quad (Iyy\,(ksl+ks2)+csl\,cs2\,(lf+lr)^2+(ksl\,lf^2+ks2\,lr^2)\,ms)\,(csl\,(Iyy+lf^2\,ms)+cs2\,(Iyy+lr^2\,ms)) + \\
&\quad ksl\,ks2\,(csl\,(Iyy+lf^2\,ms)+cs2\,(Iyy+lr^2\,ms))^2\big)\Big)
\end{aligned}
$$

Mean square of front suspension deflection, $\mathrm{E}\left[x_3^{\,2}\right] =$

$$
\begin{aligned}
&-(ms\,((cs2\,ksl+csl\,ks2)\,lr\,(lf+lr)\,(-2\,Iyy\,ks2+cs2^2\,lr\,(lf+lr))\,ms + \\
&\quad Iyy\,(cs2\,ksl+csl\,ks2)\,(Iyy\,(ksl+ks2)+csl\,cs2\,(lf+lr)^2+(ksl\,lf^2+ks2\,lr^2)\,ms) + \\
&\quad ks2\,(-Iyy\,ksl+ks2\,lr^2\,ms)\,(csl\,(Iyy+lf^2\,ms)+cs2\,(Iyy+lr^2\,ms)))\,\pi\,S0)\Big/ \\
&\Big(Iyy\,(cs2\,ksl+csl\,ks2)^2\,(lf+lr)^2\,ms - (cs2\,ksl+csl\,ks2) \\
&\quad (Iyy\,(ksl+ks2)+csl\,cs2\,(lf+lr)^2+(ksl\,lf^2+ks2\,lr^2)\,ms)\,(csl\,(Iyy+lf^2\,ms)+cs2\,(Iyy+lr^2\,ms)) + \\
&\quad ksl\,ks2\,(csl\,(Iyy+lf^2\,ms)+cs2\,(Iyy+lr^2\,ms))^2\Big)
\end{aligned}
$$

Mean square of rear suspension deflection, $\mathrm{E}\left[x_4^{\,2}\right] =$

$$
\begin{aligned}
&-(ms\,((cs2\,ksl+csl\,ks2)\,lf\,(lf+lr)\,(-2\,Iyy\,ksl+csl^2\,lf\,(lf+lr))\,ms + \\
&\quad Iyy\,(cs2\,ksl+csl\,ks2)\,(Iyy\,(ksl+ks2)+csl\,cs2\,(lf+lr)^2+(ksl\,lf^2+ks2\,lr^2)\,ms) + \\
&\quad ksl\,(-Iyy\,ks2+ksl\,lf^2\,ms)\,(csl\,(Iyy+lf^2\,ms)+cs2\,(Iyy+lr^2\,ms)))\,\pi\,S0)\Big/ \\
&\Big(Iyy\,(cs2\,ksl+csl\,ks2)^2\,(lf+lr)^2\,ms - (cs2\,ksl+csl\,ks2) \\
&\quad (Iyy\,(ksl+ks2)+csl\,cs2\,(lf+lr)^2+(ksl\,lf^2+ks2\,lr^2)\,ms)\,(csl\,(Iyy+lf^2\,ms)+cs2\,(Iyy+lr^2\,ms)) + \\
&\quad ksl\,ks2\,(csl\,(Iyy+lf^2\,ms)+cs2\,(Iyy+lr^2\,ms))^2\Big)
\end{aligned}
$$

C.1.2 Pitch Velocity Input Signal

Mean square of vertical velocity of sprung mass, $E\left[x_1^2\right] =$

$$-\Big(\Big(-(cs2\,ksl + csl\,ks2)\,(lf+lr)^2\,ms\,\big(-2\,(csl-cs2)\,Iyy\,(cs2\,ksl+csl\,ks2)\,(lf-lr)\,(lf+lr) - (Iyy\,(ksl-ks2)+csl\,cs2\,(-lf^2+lr^2))^2 + Iyy\,ksl\,ks2\,(lf-lr)^2\,ms\big) + (lf+lr)\,(-(csl-cs2)^2\,Iyy\,ksl\,ks2\,(lf+lr) + (lf-lr)\,(2\,Iyy\,ksl\,(ksl-ks2)\,ks2 + (cs2^2\,ksl^2 + csl^2\,ks2^2)\,(lf^2-lr^2))\,ms)\,(csl\,(Iyy+lf^2\,ms)+cs2\,(Iyy+lr^2\,ms)) + (Iyy\,(ksl+ks2)+csl\,cs2\,(lf+lr)^2 + (ksl\,lf^2+ks2\,lr^2)\,ms)\,((csl-cs2)^2\,Iyy\,(cs2\,ksl+csl\,ks2)\,(lf+lr)^2 + ksl\,ks2\,(lf-lr)^2\,ms\,(csl\,(Iyy+lf^2\,ms)+cs2\,(Iyy+lr^2\,ms)))\big)\,\pi\,S0\Big) \Big/ \Big((lf+lr)^2\,ms\,\big(Iyy\,(cs2\,ksl+csl\,ks2)^2\,(lf+lr)^2\,ms - (cs2\,ksl+csl\,ks2)\,(Iyy\,(ksl+ks2)+csl\,cs2\,(lf+lr)^2 + (ksl\,lf^2+ks2\,lr^2)\,ms)\,(csl\,(Iyy+lf^2\,ms)+cs2\,(Iyy+lr^2\,ms)) + ksl\,ks2\,(csl\,(Iyy+lf^2\,ms)+cs2\,(Iyy+lr^2\,ms))^2\big)\Big)$$

Mean square of pitch angular velocity of sprung mass, $E\left[x_2^2\right] =$

$$-\Big((-Iyy\,(cs2\,ksl+csl\,ks2)\,(lf+lr)^2\,(4\,Iyy\,ksl\,ks2\,ms + 4\,(cs2\,ksl+csl\,ks2)\,(lf+lr)\,(csl\,lf+cs2\,lr)\,ms - (2\,csl\,cs2\,(lf+lr)+(ksl\,lf+ks2\,lr)\,ms)^2) + (Iyy\,(ksl+ks2)+csl\,cs2\,(lf+lr)^2 + (ksl\,lf^2+ks2\,lr^2)\,ms)\,((cs2\,ksl+csl\,ks2)\,(lf+lr)^2\,(csl\,lf+cs2\,lr)^2\,ms + 4\,Iyy\,ksl\,ks2\,(csl\,(Iyy+lf^2\,ms)+cs2\,(Iyy+lr^2\,ms))) + (lf+lr)\,(csl\,(Iyy+lf^2\,ms)+cs2\,(Iyy+lr^2\,ms))\,(-ksl\,ks2\,(lf+lr)\,(csl\,lf+cs2\,lr)^2\,ms + 4\,Iyy\,(cs2^2\,ksl^2\,(lf+lr)+ks2\,(csl^2\,ks2\,(lf+lr) - ksl\,(ksl\,lf+ks2\,lr)\,ms))))\,\pi\,S0\Big) \Big/ \Big(Iyy\,(lf+lr)^2\,\big(Iyy\,(cs2\,ksl+csl\,ks2)^2\,(lf+lr)^2\,ms - (cs2\,ksl+csl\,ks2)\,(Iyy\,(ksl+ks2)+csl\,cs2\,(lf+lr)^2 + (ksl\,lf^2+ks2\,lr^2)\,ms)\,(csl\,(Iyy+lf^2\,ms)+cs2\,(Iyy+lr^2\,ms)) + ksl\,ks2\,(csl\,(Iyy+lf^2\,ms)+cs2\,(Iyy+lr^2\,ms))^2\big)\Big)$$

Mean square of front suspension deflection, $E\left[x_3^2\right] =$

$$-\Big((Iyy\,(cs2\,ksl+csl\,ks2)\,(lf+lr)^2\,ms\,(Iyy\,(ksl+ks2)+csl\,cs2\,(lf+lr)^2 + (ksl\,lf^2+ks2\,lr^2)\,ms) + (cs2\,ksl+csl\,ks2)\,(lf+lr)^2\,(2\,Iyy+lr\,(-lf+lr)\,ms)\,(-2\,Iyy\,ks2\,ms + cs2^2\,(2\,Iyy+lr\,(-lf+lr)\,ms)) + ks2\,(csl\,(Iyy+lf^2\,ms)+cs2\,(Iyy+lr^2\,ms))\,(-Iyy\,ksl\,(lf+lr)^2\,ms + ks2\,(2\,Iyy+lr\,(-lf+lr)\,ms)^2)\big)\,\pi\,S0\Big) \Big/ \Big((lf+lr)^2\,\big(Iyy\,(cs2\,ksl+csl\,ks2)^2\,(lf+lr)^2\,ms - (cs2\,ksl+csl\,ks2)\,(Iyy\,(ksl+ks2)+csl\,cs2\,(lf+lr)^2 + (ksl\,lf^2+ks2\,lr^2)\,ms)\,(csl\,(Iyy+lf^2\,ms)+cs2\,(Iyy+lr^2\,ms)) + ksl\,ks2\,(csl\,(Iyy+lf^2\,ms)+cs2\,(Iyy+lr^2\,ms))^2\big)\Big)$$

Mean square of rear suspension deflection, $E\left[x_4^2\right] =$

$$-\Big((Iyy\,(cs2\,ksl+csl\,ks2)\,(lf+lr)^2\,ms\,(Iyy\,(ksl+ks2)+csl\,cs2\,(lf+lr)^2 + (ksl\,lf^2+ks2\,lr^2)\,ms) + (cs2\,ksl+csl\,ks2)\,(lf+lr)^2\,(2\,Iyy+lf\,(lf-lr)\,ms)\,(-2\,Iyy\,ksl\,ms + csl^2\,(2\,Iyy+lf\,(lf-lr)\,ms)) + ksl\,(-Iyy\,ks2\,(lf+lr)^2\,ms + ksl\,(2\,Iyy+lf\,(lf-lr)\,ms)^2)\,(csl\,(Iyy+lf^2\,ms)+cs2\,(Iyy+lr^2\,ms))\big)\,\pi\,S0\Big) \Big/ \Big((lf+lr)^2\,\big(Iyy\,(cs2\,ksl+csl\,ks2)^2\,(lf+lr)^2\,ms - (cs2\,ksl+csl\,ks2)\,(Iyy\,(ksl+ks2)+csl\,cs2\,(lf+lr)^2 + (ksl\,lf^2+ks2\,lr^2)\,ms)\,(csl\,(Iyy+lf^2\,ms)+cs2\,(Iyy+lr^2\,ms)) + ksl\,ks2\,(csl\,(Iyy+lf^2\,ms)+cs2\,(Iyy+lr^2\,ms))^2\big)\Big)$$

C.2 SEMI-ACTIVE SYSTEM.

C.2.1 Heave Velocity Input Signal

Mean square of vertical velocity of sprung mass, $\mathrm{E}\left[x_1^{\,2}\right] =$

$$
\begin{aligned}
&-\Big(\pi\, S0\, \Big((Iyy\,(ksl+ks2)+ksl\,lf^2\,ms+ks2\,lr^2\,ms+cof2\,conl\,lf^2\,\alpha+2\,cof2\,conl\,lf\,lr\,\alpha+cof2\,conl\,lr^2\,\alpha-cof2\,conl\,lf^2\,\alpha^2+\\
&\quad conl\,con2\,lf^2\,\alpha^2-2\,cof2\,conl\,lf\,lr\,\alpha^2+2\,conl\,con2\,lf\,lr\,\alpha^2-cof2\,conl\,lr^2\,\alpha^2+conl\,con2\,lr^2\,\alpha^2+\\
&\quad cofl\,(lf+lr)^2\,(-1+\alpha)\,(cof2\,(-1+\alpha)-con2\,\alpha))\,(-Iyy\,(cofl+cof2-2\,cofl\,\alpha-2\,cof2\,\alpha+2\,(conl+con2)\,\alpha)^2+\\
&\quad (cof2\,ksl\,(-1+\alpha)+cofl\,ks2\,(-1+\alpha)-(con2\,ksl+conl\,ks2)\,\alpha)+ksl\,ks2\,ms\,(-cofl\,(Iyy+lf^2\,ms)\,(-1+\alpha)-\\
&\quad cof2\,(Iyy+lr^2\,ms)\,(-1+\alpha)+(conl\,Iyy+con2\,Iyy+conl\,lf^2\,ms+con2\,lr^2\,ms)\,\alpha))+\\
&\quad ms\,(cof2\,ksl\,(-1+\alpha)+cofl\,ks2\,(-1+\alpha)-(con2\,ksl+conl\,ks2)\,\alpha)\,\big(Iyy\,ksl\,ks2\,(lf+lr)^2\,ms+2\,Iyy\,(lf+lr)\\
&\quad (-2\,(conl+con2)\,\alpha+cofl\,(-1+2\,\alpha)+cof2\,(-1+2\,\alpha))\,(-(con2\,ksl\,(2\,lf+lr)+conl\,ks2\,(lf+2\,lr))\,\alpha+\\
&\quad cof2\,ksl\,(lr\,(-1+\alpha)+lf\,(-1+2\,\alpha))+cofl\,ks2\,(lf\,(-1+\alpha)+lr\,(-1+2\,\alpha)))-\\
&\quad (Iyy\,(ksl+ks2)+(lf+lr)\,(conl\,\alpha\,(2\,con2\,(lf+lr)\,\alpha+cof2\,(lf+2\,lr-2\,lf\,\alpha-2\,lr\,\alpha))+\\
&\quad cofl\,(con2\,\alpha\,(2\,lf+lr-2\,lf\,\alpha-2\,lr\,\alpha)+cof2\,(lf+lr)\,(1-3\,\alpha+2\,\alpha^2))))^2\big)+\\
&\quad (-cofl\,(Iyy+lf^2\,ms)\,(-1+\alpha)-cof2\,(Iyy+lr^2\,ms)\,(-1+\alpha)+(conl\,Iyy+con2\,Iyy+conl\,lf^2\,ms+con2\,lr^2\,ms)\,\alpha)\\
&\quad (-Iyy\,ksl\,ks2\,(cofl+cof2-2\,cofl\,\alpha-2\,cof2\,\alpha+2\,(conl+con2)\,\alpha)^2+\\
&\quad ms\,((-(con2\,ksl\,(2\,lf+lr)+conl\,ks2\,(lf+2\,lr))\,\alpha+\\
&\quad cof2\,ksl\,(lr\,(-1+\alpha)+lf\,(-1+2\,\alpha))+cofl\,ks2\,(lf\,(-1+\alpha)+lr\,(-1+2\,\alpha)))^2-\\
&\quad 2\,ksl\,ks2\,(Iyy\,(ksl+ks2)+(lf+lr)\,(conl\,\alpha\,(2\,con2\,(lf+lr)\,\alpha+cof2\,(lf+2\,lr-2\,lf\,\alpha-2\,lr\,\alpha))+\\
&\quad cofl\,(con2\,\alpha\,(2\,lf+lr-2\,lf\,\alpha-2\,lr\,\alpha)+cof2\,(lf+lr)\,(1-3\,\alpha+2\,\alpha^2)))))\Big)\Big)\Big/\\
&\Big(ms\,\Big(Iyy\,(lf+lr)^2\,ms\,(cof2\,ksl\,(-1+\alpha)+cofl\,ks2\,(-1+\alpha)-(con2\,ksl+conl\,ks2)\,\alpha)^2+ksl\,ks2\\
&\quad (cofl\,(Iyy+lf^2\,ms)\,(-1+\alpha)+cof2\,(Iyy+lr^2\,ms)\,(-1+\alpha)-(conl\,Iyy+con2\,Iyy+conl\,lf^2\,ms+con2\,lr^2\,ms)\,\alpha)^2+\\
&\quad (cof2\,ksl\,(-1+\alpha)+cofl\,ks2\,(-1+\alpha)-(con2\,ksl+conl\,ks2)\,\alpha)\\
&\quad (-cofl\,(Iyy+lf^2\,ms)\,(-1+\alpha)-cof2\,(Iyy+lr^2\,ms)\,(-1+\alpha)+(conl\,Iyy+con2\,Iyy+conl\,lf^2\,ms+con2\,lr^2\,ms)\,\alpha)\\
&\quad (Iyy\,(ksl+ks2)+ksl\,lf^2\,ms+ks2\,lr^2\,ms+cof2\,conl\,lf^2\,\alpha+2\,cof2\,conl\,lf\,lr\,\alpha+\\
&\quad cof2\,conl\,lr^2\,\alpha-cof2\,conl\,lf^2\,\alpha^2+conl\,con2\,lf^2\,\alpha^2-2\,cof2\,conl\,lf\,lr\,\alpha^2+2\,conl\,con2\,lf\,lr\,\alpha^2-\\
&\quad cof2\,conl\,lr^2\,\alpha^2+conl\,con2\,lr^2\,\alpha^2+cofl\,(lf+lr)^2\,(-1+\alpha)\,(cof2\,(-1+\alpha)-con2\,\alpha))\Big)\Big)
\end{aligned}
$$

Mean square of pitch angular velocity of sprung mass, $\mathrm{E}\left[x_2^{\,2}\right] =$

$$
\begin{aligned}
&-(\pi\, S0\,(-ms\,(cof2\,ksl\,(-1+\alpha)+cofl\,ks2\,(-1+\alpha)-(con2\,ksl+conl\,ks2)\,\alpha)\,(Iyy\,(ksl+ks2)+ksl\,lf^2\,ms+ks2\,lr^2\,ms+\\
&\quad cof2\,conl\,lf^2\,\alpha+2\,cof2\,conl\,lf\,lr\,\alpha+cof2\,conl\,lr^2\,\alpha-cof2\,conl\,lf^2\,\alpha^2+conl\,con2\,lf^2\,\alpha^2-2\,cof2\,conl\,lf\,lr\,\alpha^2+\\
&\quad 2\,conl\,con2\,lf\,lr\,\alpha^2-cof2\,conl\,lr^2\,\alpha^2+conl\,con2\,lr^2\,\alpha^2+cofl\,(lf+lr)^2\,(-1+\alpha)\,(cof2\,(-1+\alpha)-con2\,\alpha))\\
&\quad (-2\,conl\,lf\,\alpha+2\,con2\,lr\,\alpha+cofl\,lf\,(-1+2\,\alpha)+cof2\,(lr-2\,lr\,\alpha))^2-\\
&\quad Iyy\,(cof2\,ksl\,(-1+\alpha)+cofl\,ks2\,(-1+\alpha)-(con2\,ksl+conl\,ks2)\,\alpha)\\
&\quad ((ksl\,lf\,ms-ks2\,lr\,ms+(cof2\,conl-cofl\,con2)\,(lf+lr)\,\alpha)^2-2\,(cof2\,ksl-con2\,ksl+(-cofl+conl)\,ks2)\\
&\quad (lf+lr)\,ms\,\alpha\,(2\,(conl\,lf-con2\,lr)\,\alpha+cof2\,lr\,(-1+2\,\alpha)+cofl\,(lf-2\,lf\,\alpha)))+\\
&\quad (-cofl\,(Iyy+lf^2\,ms)\,(-1+\alpha)-cof2\,(Iyy+lr^2\,ms)\,(-1+\alpha)+(conl\,Iyy+con2\,Iyy+conl\,lf^2\,ms+con2\,lr^2\,ms)\,\alpha)\\
&\quad (Iyy\,(cof2\,ksl-con2\,ksl+(-cofl+conl)\,ks2)^2\,\alpha^2-\\
&\quad ksl\,ks2\,ms\,(-2\,conl\,lf\,\alpha+2\,con2\,lr\,\alpha+cofl\,lf\,(-1+2\,\alpha)+cof2\,(lr-2\,lr\,\alpha))^2)))\Big/\\
&\Big(Iyy\,\Big(Iyy\,(lf+lr)^2\,ms\,(cof2\,ksl\,(-1+\alpha)+cofl\,ks2\,(-1+\alpha)-(con2\,ksl+conl\,ks2)\,\alpha)^2+ksl\,ks2\\
&\quad (cofl\,(Iyy+lf^2\,ms)\,(-1+\alpha)+cof2\,(Iyy+lr^2\,ms)\,(-1+\alpha)-(conl\,Iyy+con2\,Iyy+conl\,lf^2\,ms+con2\,lr^2\,ms)\,\alpha)^2+\\
&\quad (cof2\,ksl\,(-1+\alpha)+cofl\,ks2\,(-1+\alpha)-(con2\,ksl+conl\,ks2)\,\alpha)\\
&\quad (-cofl\,(Iyy+lf^2\,ms)\,(-1+\alpha)-cof2\,(Iyy+lr^2\,ms)\,(-1+\alpha)+(conl\,Iyy+con2\,Iyy+conl\,lf^2\,ms+con2\,lr^2\,ms)\,\alpha)\\
&\quad (Iyy\,(ksl+ks2)+ksl\,lf^2\,ms+ks2\,lr^2\,ms+cof2\,conl\,lf^2\,\alpha+2\,cof2\,conl\,lf\,lr\,\alpha+\\
&\quad cof2\,conl\,lr^2\,\alpha-cof2\,conl\,lf^2\,\alpha^2+conl\,con2\,lf^2\,\alpha^2-2\,cof2\,conl\,lf\,lr\,\alpha^2+2\,conl\,con2\,lf\,lr\,\alpha^2-\\
&\quad cof2\,conl\,lr^2\,\alpha^2+conl\,con2\,lr^2\,\alpha^2+cofl\,(lf+lr)^2\,(-1+\alpha)\,(cof2\,(-1+\alpha)-con2\,\alpha))\Big)\Big)
\end{aligned}
$$

Mean square of front suspension deflection, $\mathrm{E}\left[x_3^{\,2}\right] =$

$$-\Big(\pi\, S0\, \Big((Iyy\,(ksl+ks2)+ksl\,lf^2\,ms+ks2\,lr^2\,ms+cof2\,conl\,lf^2\,\alpha+2\,cof2\,conl\,lf\,lr\,\alpha+ cof2\,conl\,lr^2\,\alpha-cof2\,conl\,lf^2\,\alpha^2+conl\,con2\,lf^2\,\alpha^2-2\,cof2\,conl\,lf\,lr\,\alpha^2+2\,conl\,con2\,lf\,lr\,\alpha^2- cof2\,conl\,lr^2\,\alpha^2+conl\,con2\,lr^2\,\alpha^2+cofl\,(lf+lr)^2\,(-1+\alpha)\,(cof2\,(-1+\alpha)-con2\,\alpha))\,(-Iyy\,ksl\,ms\,(cof2\,ksl\,(-1+\alpha)+cofl\,ks2\,(-1+\alpha)-(con2\,ksl+conl\,ks2)\,\alpha)+(cofl-conl)^2\,ks2\,\alpha^2\,(-cofl\,(Iyy+lf^2\,ms)\,(-1+\alpha)-cof2\,(Iyy+lr^2\,ms)\,(-1+\alpha)+(conl\,Iyy+con2\,Iyy+conl\,lf^2\,ms+con2\,lr^2\,ms)\,\alpha))+ksl\,(-cofl\,(Iyy+lf^2\,ms)\,(-1+\alpha)-cof2\,(Iyy+lr^2\,ms)\,(-1+\alpha)+(conl\,Iyy+con2\,Iyy+conl\,lf^2\,ms+con2\,lr^2\,ms)\,\alpha)\,(-Iyy\,ksl\,ks2\,ms+(ks2\,lr\,ms-(cofl-conl)\,(lf+lr)\,\alpha\,(cof2\,(-1+\alpha)-con2\,\alpha))^2-2\,(cofl-conl)\,ks2\,\alpha\,((cofl\,(Iyy+lf^2\,ms)-conl\,(Iyy+lf^2\,ms)-con2\,(Iyy-lr\,(2\,lf+lr)\,ms))\,\alpha+cof2\,(lf\,lr\,ms\,(1-2\,\alpha)+Iyy\,\alpha+lr^2\,(ms-ms\,\alpha))))+(cof2\,ksl\,(-1+\alpha)+cofl\,ks2\,(-1+\alpha)-(con2\,ksl+conl\,ks2)\,\alpha)\,\Big((cofl-conl)^2\,Iyy\,ks2\,(lf+lr)^2\,ms\,\alpha^2-ksl\,\Big(2\,Iyy\,(lf+lr)\,ms\,(-ks2\,lr\,ms+(cofl-conl)\,(lf+lr)\,\alpha\,(cof2\,(-1+\alpha)-con2\,\alpha))+((-cofl\,(Iyy+lf^2\,ms)+conl\,(Iyy+lf^2\,ms)+con2\,(Iyy-lr\,(2\,lf+lr)\,ms))\,\alpha+cof2\,(lr^2\,ms\,(-1+\alpha)-Iyy\,\alpha+lf\,lr\,ms\,(-1+2\,\alpha)))^2\Big)\Big)\Big)\Big)\Big/\Big(ksl\,\Big(Iyy\,(lf+lr)^2\,ms\,(cof2\,ksl\,(-1+\alpha)+cofl\,ks2\,(-1+\alpha)-(con2\,ksl+conl\,ks2)\,\alpha)^2+ksl\,ks2\,(cofl\,(Iyy+lf^2\,ms)\,(-1+\alpha)+cof2\,(Iyy+lr^2\,ms)\,(-1+\alpha)-(conl\,Iyy+con2\,Iyy+conl\,lf^2\,ms+con2\,lr^2\,ms)\,\alpha)^2+(cof2\,ksl\,(-1+\alpha)+cofl\,ks2\,(-1+\alpha)-(con2\,ksl+conl\,ks2)\,\alpha)\,(-cofl\,(Iyy+lf^2\,ms)\,(-1+\alpha)-cof2\,(Iyy+lr^2\,ms)\,(-1+\alpha)+(conl\,Iyy+con2\,Iyy+conl\,lf^2\,ms+con2\,lr^2\,ms)\,\alpha)\,(Iyy\,(ksl+ks2)+ksl\,lf^2\,ms+ks2\,lr^2\,ms+cof2\,conl\,lf^2\,\alpha+2\,cof2\,conl\,lf\,lr\,\alpha+cof2\,conl\,lr^2\,\alpha-cof2\,conl\,lf^2\,\alpha^2+conl\,con2\,lf^2\,\alpha^2-2\,cof2\,conl\,lf\,lr\,\alpha^2+2\,conl\,con2\,lf\,lr\,\alpha^2-cof2\,conl\,lr^2\,\alpha^2+conl\,con2\,lr^2\,\alpha^2+cofl\,(lf+lr)^2\,(-1+\alpha)\,(cof2\,(-1+\alpha)-con2\,\alpha))\Big)\Big)$$

Mean square of rear suspension deflection, $\mathrm{E}\left[x_4^{\,2}\right]=$

$$-\Big(\pi\, S0\, \Big((Iyy\,(ksl+ks2)+ksl\,lf^2\,ms+ks2\,lr^2\,ms+cof2\,conl\,lf^2\,\alpha+2\,cof2\,conl\,lf\,lr\,\alpha+ cof2\,conl\,lr^2\,\alpha-cof2\,conl\,lf^2\,\alpha^2+conl\,con2\,lf^2\,\alpha^2-2\,cof2\,conl\,lf\,lr\,\alpha^2+2\,conl\,con2\,lf\,lr\,\alpha^2- cof2\,conl\,lr^2\,\alpha^2+conl\,con2\,lr^2\,\alpha^2+cofl\,(lf+lr)^2\,(-1+\alpha)\,(cof2\,(-1+\alpha)-con2\,\alpha))\,(-Iyy\,ks2\,ms\,(cof2\,ksl\,(-1+\alpha)+cofl\,ks2\,(-1+\alpha)-(con2\,ksl+conl\,ks2)\,\alpha)+(cof2-con2)^2\,ksl\,\alpha^2\,(-cofl\,(Iyy+lf^2\,ms)\,(-1+\alpha)-cof2\,(Iyy+lr^2\,ms)\,(-1+\alpha)+(conl\,Iyy+con2\,Iyy+conl\,lf^2\,ms+con2\,lr^2\,ms)\,\alpha))+ks2\,(-cofl\,(Iyy+lf^2\,ms)\,(-1+\alpha)-cof2\,(Iyy+lr^2\,ms)\,(-1+\alpha)+(conl\,Iyy+con2\,Iyy+conl\,lf^2\,ms+con2\,lr^2\,ms)\,\alpha)\,(-Iyy\,ksl\,ks2\,ms+(ksl\,lf\,ms-(cof2-con2)\,(lf+lr)\,\alpha\,(cofl\,(-1+\alpha)-conl\,\alpha))^2-2\,(cof2-con2)\,ksl\,\alpha\,((cof2\,(Iyy+lr^2\,ms)-con2\,(Iyy+lr^2\,ms)-conl\,(Iyy-lf\,(lf+2\,lr)\,ms))\,\alpha+cofl\,(lf\,lr\,ms\,(1-2\,\alpha)+Iyy\,\alpha+lf^2\,(ms-ms\,\alpha))))+(cof2\,ksl\,(-1+\alpha)+cofl\,ks2\,(-1+\alpha)-(con2\,ksl+conl\,ks2)\,\alpha)\,\Big((cof2-con2)^2\,Iyy\,ksl\,(lf+lr)^2\,ms\,\alpha^2-ks2\,\Big(-2\,Iyy\,(lf+lr)\,ms\,(ksl\,lf\,ms-(cof2-con2)\,(lf+lr)\,\alpha\,(cofl\,(-1+\alpha)-conl\,\alpha))+((-cof2\,(Iyy+lr^2\,ms)+con2\,(Iyy+lr^2\,ms)+conl\,(Iyy-lf\,(lf+2\,lr)\,ms))\,\alpha+cofl\,(lf^2\,ms\,(-1+\alpha)-Iyy\,\alpha+lf\,lr\,ms\,(-1+2\,\alpha)))^2\Big)\Big)\Big)\Big)\Big/\Big(ks2\,\Big(Iyy\,(lf+lr)^2\,ms\,(cof2\,ksl\,(-1+\alpha)+cofl\,ks2\,(-1+\alpha)-(con2\,ksl+conl\,ks2)\,\alpha)^2+ksl\,ks2\,(cofl\,(Iyy+lf^2\,ms)\,(-1+\alpha)+cof2\,(Iyy+lr^2\,ms)\,(-1+\alpha)-(conl\,Iyy+con2\,Iyy+conl\,lf^2\,ms+con2\,lr^2\,ms)\,\alpha)^2+(cof2\,ksl\,(-1+\alpha)+cofl\,ks2\,(-1+\alpha)-(con2\,ksl+conl\,ks2)\,\alpha)\,(-cofl\,(Iyy+lf^2\,ms)\,(-1+\alpha)-cof2\,(Iyy+lr^2\,ms)\,(-1+\alpha)+(conl\,Iyy+con2\,Iyy+conl\,lf^2\,ms+con2\,lr^2\,ms)\,\alpha)\,(Iyy\,(ksl+ks2)+ksl\,lf^2\,ms+ks2\,lr^2\,ms+cof2\,conl\,lf^2\,\alpha+2\,cof2\,conl\,lf\,lr\,\alpha+cof2\,conl\,lr^2\,\alpha-cof2\,conl\,lf^2\,\alpha^2+conl\,con2\,lf^2\,\alpha^2-2\,cof2\,conl\,lf\,lr\,\alpha^2+2\,conl\,con2\,lf\,lr\,\alpha^2-cof2\,conl\,lr^2\,\alpha^2+conl\,con2\,lr^2\,\alpha^2+cofl\,(lf+lr)^2\,(-1+\alpha)\,(cof2\,(-1+\alpha)-con2\,\alpha))\Big)\Big)$$

C.2.2 Pitch Velocity Input Signal

Mean square of vertical velocity of sprung mass, $\mathrm{E}\left[x_1^{\,2}\right]=$

$$-\Big(\pi S0\ \Big((Iyy\ (ksl+ks2)+ksl\ lf^2\ ms+ks2\ lr^2\ ms+cof2\ conl\ lf^2\ \alpha+2\ cof2\ conl\ lf\ lr\ \alpha+ cof2\ conl\ lr^2\ \alpha-cof2\ conl\ lf^2\ \alpha^2+conl\ con2\ lf^2\ \alpha^2-2\ cof2\ conl\ lf\ lr\ \alpha^2+2\ conl\ con2\ lf\ lr\ \alpha^2- cof2\ conl\ lr^2\ \alpha^2+conl\ con2\ lr^2\ \alpha^2+cofl\ (lf+lr)^2\ (-l+\alpha)\ (cof2\ (-l+\alpha)-con2\ \alpha))\ (ksl\ ks2\ (lf-lr)^2\ ms\ (-cofl\ (Iyy+lf^2\ ms)\ (-l+\alpha)-cof2\ (Iyy+lr^2\ ms)\ (-l+\alpha)+ (conl\ Iyy+con2\ Iyy+conl\ lf^2\ ms+con2\ lr^2\ ms)\ \alpha)-Iyy\ (lf+lr)^2\ (cof2\ ksl\ (-l+\alpha)+ cofl\ ks2\ (-l+\alpha)-(con2\ ksl+conl\ ks2)\ \alpha)\ (cof2-2\ cof2\ \alpha+2\ (-conl+con2)\ \alpha+cofl\ (-l+2\alpha))^2)+ (lf+lr)^2\ ms\ (cof2\ ksl\ (-l+\alpha)+cofl\ ks2\ (-l+\alpha)-(con2\ ksl+conl\ ks2)\ \alpha)\ \Big(Iyy\ ksl\ ks2\ (lf-lr)^2\ ms-2\ Iyy\ (lf+lr)\ (cof2-2\ cof2\ \alpha+2\ (-conl+con2)\ \alpha+cofl\ (-l+2\alpha))\ ((-conl\ ks2\ (lf-2\ lr)+con2\ ksl\ (-2\ lf+lr))\ \alpha+ cofl\ ks2\ (lr+lf\ (-l+\alpha)-2\ lr\ \alpha)+cof2\ ksl\ (lr-lr\ \alpha+lf\ (-l+2\alpha)))- (Iyy\ (ksl-ks2)-(lf+lr)\ (conl\ \alpha\ (2\ con2\ (lf-lr)\ \alpha+cof2\ (lf+2\ lr\ (-l+\alpha)-2\ lf\ \alpha))+ cofl\ (-con2\ \alpha\ (lr+2\ lf\ (-l+\alpha)-2\ lr\ \alpha)+cof2\ (lf-lr)\ (1-3\alpha+2\alpha^2))))^2)+(lf+lr) (-cofl\ (Iyy+lf^2\ ms)\ (-l+\alpha)-cof2\ (Iyy+lr^2\ ms)\ (-l+\alpha)+(conl\ Iyy+con2\ Iyy+conl\ lf^2\ ms+con2\ lr^2\ ms)\ \alpha) (-Iyy\ ksl\ ks2\ (lf+lr)\ (cof2-2\ cof2\ \alpha+2\ (-conl+con2)\ \alpha+cofl\ (-l+2\alpha))^2+ ms\ ((lf+lr)\ ((-conl\ ks2\ (lf-2\ lr)+con2\ ksl\ (-2\ lf+lr))\ \alpha+ cofl\ ks2\ (lr+lf\ (-l+\alpha)-2\ lr\ \alpha)+cof2\ ksl\ (lr-lr\ \alpha+lf\ (-l+2\alpha)))^2+2\ ksl\ ks2\ (lf-lr) (Iyy\ (ksl-ks2)-(lf+lr)\ (conl\ \alpha\ (2\ con2\ (lf-lr)\ \alpha+cof2\ (lf+2\ lr\ (-l+\alpha)-2\ lf\ \alpha))+ cofl\ (-con2\ \alpha\ (lr+2\ lf\ (-l+\alpha)-2\ lr\ \alpha)+cof2\ (lf-lr)\ (1-3\alpha+2\alpha^2)))))\Big)\Big/ \Big((lf+lr)^2\ ms\ \Big(Iyy\ (lf+lr)^2\ ms\ (cof2\ ksl\ (-l+\alpha)+cofl\ ks2\ (-l+\alpha)-(con2\ ksl+conl\ ks2)\ \alpha)^2+ ksl\ ks2 (cofl\ (Iyy+lf^2\ ms)\ (-l+\alpha)+cof2\ (Iyy+lr^2\ ms)\ (-l+\alpha)-(conl\ Iyy+con2\ Iyy+conl\ lf^2\ ms+con2\ lr^2\ ms)\ \alpha)^2+ (cof2\ ksl\ (-l+\alpha)+cofl\ ks2\ (-l+\alpha)-(con2\ ksl+conl\ ks2)\ \alpha) (-cofl\ (Iyy+lf^2\ ms)\ (-l+\alpha)-cof2\ (Iyy+lr^2\ ms)\ (-l+\alpha)+(conl\ Iyy+con2\ Iyy+conl\ lf^2\ ms+con2\ lr^2\ ms)\ \alpha) (Iyy\ (ksl+ks2)+ksl\ lf^2\ ms+ks2\ lr^2\ ms+cof2\ conl\ lf^2\ \alpha+2\ cof2\ conl\ lf\ lr\ \alpha+ cof2\ conl\ lr^2\ \alpha-cof2\ conl\ lf^2\ \alpha^2+conl\ con2\ lf^2\ \alpha^2-2\ cof2\ conl\ lf\ lr\ \alpha^2+2\ conl\ con2\ lf\ lr\ \alpha^2- cof2\ conl\ lr^2\ \alpha^2+conl\ con2\ lr^2\ \alpha^2+cofl\ (lf+lr)^2\ (-l+\alpha)\ (cof2\ (-l+\alpha)-con2\ \alpha))\Big)\Big)$$

Mean square of pitch angular velocity of sprung mass, $\mathrm{E}\left[x_2^{\,2}\right]=$

$$-\Big(\pi S0\ \Big((Iyy\ (ksl+ks2)+ksl\ lf^2\ ms+ks2\ lr^2\ ms+cof2\ conl\ lf^2\ \alpha+2\ cof2\ conl\ lf\ lr\ \alpha+ cof2\ conl\ lr^2\ \alpha-cof2\ conl\ lf^2\ \alpha^2+conl\ con2\ lf^2\ \alpha^2-2\ cof2\ conl\ lf\ lr\ \alpha^2+2\ conl\ con2\ lf\ lr\ \alpha^2- cof2\ conl\ lr^2\ \alpha^2+conl\ con2\ lr^2\ \alpha^2+cofl\ (lf+lr)^2\ (-l+\alpha)\ (cof2\ (-l+\alpha)-con2\ \alpha))\ (4\ Iyy\ ksl\ ks2\ (-cofl\ (Iyy+lf^2\ ms)\ (-l+\alpha)-cof2\ (Iyy+lr^2\ ms)\ (-l+\alpha)+ (conl\ Iyy+con2\ Iyy+conl\ lf^2\ ms+con2\ lr^2\ ms)\ \alpha)-(lf+lr)^2\ ms\ (cof2\ ksl\ (-l+\alpha)+cofl\ ks2\ (-l+\alpha)- (con2\ ksl+conl\ ks2)\ \alpha)\ (2\ (conl\ lf+con2\ lr)\ \alpha+cofl\ (lf-2\ lf\ \alpha)+cof2\ (lr-2\ lr\ \alpha))^2)+ Iyy\ (lf+lr)^2\ (cof2\ ksl\ (-l+\alpha)+cofl\ ks2\ (-l+\alpha)-(con2\ ksl+conl\ ks2)\ \alpha)\ \Big(4\ Iyy\ ksl\ ks2\ ms+2\ (lf+lr)\ ms\ (cof2\ ksl\ (2-3\alpha)+cofl\ ks2\ (2-3\alpha)+3\ (con2\ ksl+conl\ ks2)\ \alpha) (2\ (conl\ lf+con2\ lr)\ \alpha+cofl\ (lf-2\ lf\ \alpha)+cof2\ (lr-2\ lr\ \alpha))- (ksl\ lf\ ms+ks2\ lr\ ms+3\ cof2\ conl\ lf\ \alpha+3\ cof2\ conl\ lr\ \alpha-4\ cof2\ conl\ lf\ \alpha^2+4\ conl\ con2\ lf\ \alpha^2- 4\ cof2\ conl\ lr\ \alpha^2+4\ conl\ con2\ lr\ \alpha^2+cofl\ (lf+lr)\ (con2\ (3-4\alpha)\ \alpha+cof2\ (2-6\alpha+4\alpha^2)))^2\Big)+(lf+lr) (-cofl\ (Iyy+lf^2\ ms)\ (-l+\alpha)-cof2\ (Iyy+lr^2\ ms)\ (-l+\alpha)+(conl\ Iyy+con2\ Iyy+conl\ lf^2\ ms+con2\ lr^2\ ms)\ \alpha) (-ksl\ ks2\ (lf+lr)\ ms\ (2\ (conl\ lf+con2\ lr)\ \alpha+cofl\ (lf-2\ lf\ \alpha)+cof2\ (lr-2\ lr\ \alpha))^2+ Iyy\ ((lf+lr)\ (-3\ (con2\ ksl+conl\ ks2)\ \alpha+cof2\ ksl\ (-2+3\alpha)+cofl\ ks2\ (-2+3\alpha))^2- 4\ ksl\ ks2\ (ksl\ lf\ ms+ks2\ lr\ ms+3\ cof2\ conl\ lf\ \alpha+3\ cof2\ conl\ lr\ \alpha-4\ cof2\ conl\ lf\ \alpha^2+4\ conl\ con2\ lf\ \alpha^2-4 cof2\ conl\ lr\ \alpha^2+4\ conl\ con2\ lr\ \alpha^2+cofl\ (lf+lr)\ (con2\ (3-4\alpha)\ \alpha+cof2\ (2-6\alpha+4\alpha^2)))))\Big)\Big/ \Big(Iyy\ (lf+lr)^2\ \Big(Iyy\ (lf+lr)^2\ ms\ (cof2\ ksl\ (-l+\alpha)+cofl\ ks2\ (-l+\alpha)-(con2\ ksl+conl\ ks2)\ \alpha)^2+ksl\ ks2 (cofl\ (Iyy+lf^2\ ms)\ (-l+\alpha)+cof2\ (Iyy+lr^2\ ms)\ (-l+\alpha)-(conl\ Iyy+con2\ Iyy+conl\ lf^2\ ms+con2\ lr^2\ ms)\ \alpha)^2+ (cof2\ ksl\ (-l+\alpha)+cofl\ ks2\ (-l+\alpha)-(con2\ ksl+conl\ ks2)\ \alpha) (-cofl\ (Iyy+lf^2\ ms)\ (-l+\alpha)-cof2\ (Iyy+lr^2\ ms)\ (-l+\alpha)+(conl\ Iyy+con2\ Iyy+conl\ lf^2\ ms+con2\ lr^2\ ms)\ \alpha) (Iyy\ (ksl+ks2)+ksl\ lf^2\ ms+ks2\ lr^2\ ms+cof2\ conl\ lf^2\ \alpha+2\ cof2\ conl\ lf\ lr\ \alpha+ cof2\ conl\ lr^2\ \alpha-cof2\ conl\ lf^2\ \alpha^2+conl\ con2\ lf^2\ \alpha^2-2\ cof2\ conl\ lf\ lr\ \alpha^2+2\ conl\ con2\ lf\ lr\ \alpha^2- cof2\ conl\ lr^2\ \alpha^2+conl\ con2\ lr^2\ \alpha^2+cofl\ (lf+lr)^2\ (-l+\alpha)\ (cof2\ (-l+\alpha)-con2\ \alpha))\Big)\Big)$$

Mean square of front suspension deflection, $\mathrm{E}\left[x_3^{\,2}\right]=$

$$-\Big(\pi\, S0\, \Big((lf+lr)^2\,(Iyy\,(ksl+ks2)+ksl\,lf^2\,ms+ks2\,lr^2\,ms+cof2\,conl\,lf^2\,\alpha+2\,cof2\,conl\,lf\,lr\,\alpha+ cof2\,conl\,lr^2\,\alpha-cof2\,conl\,lf^2\,\alpha^2+conl\,con2\,lf^2\,\alpha^2-2\,cof2\,conl\,lf\,lr\,\alpha^2+2\,conl\,con2\,lf\,lr\,\alpha^2- cof2\,conl\,lr^2\,\alpha^2+conl\,con2\,lr^2\,\alpha^2+cofl\,(lf+lr)^2\,(-1+\alpha)\,(cof2\,(-1+\alpha)-con2\,\alpha))\,(-Iyy\,ksl\,ms\,(cof2\,ksl\,(-1+\alpha)+cofl\,ks2\,(-1+\alpha)-(con2\,ksl+conl\,ks2)\,\alpha)+(cofl-conl)^2\,ks2\,\alpha^2\,(-cofl\,(Iyy+lf^2\,ms)\,(-1+\alpha)-cof2\,(Iyy+lr^2\,ms)\,(-1+\alpha)+(conl\,Iyy+con2\,Iyy+conl\,lf^2\,ms+con2\,lr^2\,ms)\,\alpha))+ ksl\,(-cofl\,(Iyy+lf^2\,ms)\,(-1+\alpha)-cof2\,(Iyy+lr^2\,ms)\,(-1+\alpha)+(conl\,Iyy+con2\,Iyy+conl\,lf^2\,ms+con2\,lr^2\,ms)\,\alpha)\,\Big(-Iyy\,ksl\,ks2\,(lf+lr)^2\,ms+(2\,Iyy\,ks2+ks2\,lr\,(-lf+lr)\,ms-(cofl-conl)\,(lf+lr)^2\,\alpha\,(cof2\,(-1+\alpha)-con2\,\alpha))^2-2\,(cofl-conl)\,ks2\,(lf+lr)^2\,\alpha\,((cofl\,(Iyy+lf^2\,ms)-conl\,(Iyy+lf^2\,ms)+con2\,(3\,Iyy+lr\,(-2\,lf+lr)\,ms))\,\alpha+ cof2\,(Iyy\,(2-3\,\alpha)+lr\,ms\,(lr-lr\,\alpha+lf\,(-1+2\,\alpha))))\Big)+(lf+lr)^2\,(cof2\,ksl\,(-1+\alpha)+cofl\,ks2\,(-1+\alpha)-(con2\,ksl+conl\,ks2)\,\alpha)\,\Big((cofl-conl)^2\,Iyy\,ks2\,(lf+lr)^2\,ms\,\alpha^2-ksl\,\Big(-2\,Iyy\,ms\,(2\,Iyy\,ks2+ks2\,lr\,(-lf+lr)\,ms-(cofl-conl)\,(lf+lr)^2\,\alpha\,(cof2\,(-1+\alpha)-con2\,\alpha))+((-cofl\,(Iyy+lf^2\,ms)+conl\,(Iyy+lf^2\,ms)-con2\,(3\,Iyy+lr\,(-2\,lf+lr)\,ms))\,\alpha+ cof2\,(Iyy\,(-2+3\,\alpha)+lr\,ms\,(lf+lr\,(-1+\alpha)-2\,lf\,\alpha)))^2\Big)\Big)\Big)\Big/ \Big(ksl\,(lf+lr)^2\,\Big(Iyy\,(lf+lr)^2\,ms\,(cof2\,ksl\,(-1+\alpha)+cofl\,ks2\,(-1+\alpha)-(con2\,ksl+conl\,ks2)\,\alpha)^2+ksl\,ks2\,(cofl\,(Iyy+lf^2\,ms)\,(-1+\alpha)+cof2\,(Iyy+lr^2\,ms)\,(-1+\alpha)-(conl\,Iyy+con2\,Iyy+conl\,lf^2\,ms+con2\,lr^2\,ms)\,\alpha)^2+ (cof2\,ksl\,(-1+\alpha)+cofl\,ks2\,(-1+\alpha)-(con2\,ksl+conl\,ks2)\,\alpha)\,(-cofl\,(Iyy+lf^2\,ms)\,(-1+\alpha)-cof2\,(Iyy+lr^2\,ms)\,(-1+\alpha)+(conl\,Iyy+con2\,Iyy+conl\,lf^2\,ms+con2\,lr^2\,ms)\,\alpha)\,(Iyy\,(ksl+ks2)+ksl\,lf^2\,ms+ks2\,lr^2\,ms+cof2\,conl\,lf^2\,\alpha+2\,cof2\,conl\,lf\,lr\,\alpha+ cof2\,conl\,lr^2\,\alpha-cof2\,conl\,lf^2\,\alpha^2+conl\,con2\,lf^2\,\alpha^2-2\,cof2\,conl\,lf\,lr\,\alpha^2+2\,conl\,con2\,lf\,lr\,\alpha^2- cof2\,conl\,lr^2\,\alpha^2+conl\,con2\,lr^2\,\alpha^2+cofl\,(lf+lr)^2\,(-1+\alpha)\,(cof2\,(-1+\alpha)-con2\,\alpha))\Big)\Big)$$

Mean square of rear suspension deflection, $\mathrm{E}\left[x_4^{\,2}\right] =$

$$-\Big(\pi\, S0\, \Big((lf+lr)^2\,(Iyy\,(ksl+ks2)+ksl\,lf^2\,ms+ks2\,lr^2\,ms+cof2\,conl\,lf^2\,\alpha+2\,cof2\,conl\,lf\,lr\,\alpha+ cof2\,conl\,lr^2\,\alpha-cof2\,conl\,lf^2\,\alpha^2+conl\,con2\,lf^2\,\alpha^2-2\,cof2\,conl\,lf\,lr\,\alpha^2+2\,conl\,con2\,lf\,lr\,\alpha^2- cof2\,conl\,lr^2\,\alpha^2+conl\,con2\,lr^2\,\alpha^2+cofl\,(lf+lr)^2\,(-1+\alpha)\,(cof2\,(-1+\alpha)-con2\,\alpha))\,(-Iyy\,ks2\,ms\,(cof2\,ksl\,(-1+\alpha)+cofl\,ks2\,(-1+\alpha)-(con2\,ksl+conl\,ks2)\,\alpha)+(cof2-con2)^2\,ksl\,\alpha^2\,(-cofl\,(Iyy+lf^2\,ms)\,(-1+\alpha)-cof2\,(Iyy+lr^2\,ms)\,(-1+\alpha)+(conl\,Iyy+con2\,Iyy+conl\,lf^2\,ms+con2\,lr^2\,ms)\,\alpha))+ ks2\,(-cofl\,(Iyy+lf^2\,ms)\,(-1+\alpha)-cof2\,(Iyy+lr^2\,ms)\,(-1+\alpha)+(conl\,Iyy+con2\,Iyy+conl\,lf^2\,ms+con2\,lr^2\,ms)\,\alpha)\,\Big(-Iyy\,ksl\,ks2\,(lf+lr)^2\,ms+(2\,Iyy\,ksl+ksl\,lf\,(lf-lr)\,ms-(cof2-con2)\,(lf+lr)^2\,\alpha\,(cofl\,(-1+\alpha)-conl\,\alpha))^2-2\,(cof2-con2)\,ksl\,(lf+lr)^2\,\alpha\,((conl\,(3\,Iyy+lf\,(lf-2\,lr)\,ms)+cof2\,(Iyy+lr^2\,ms)-con2\,(Iyy+lr^2\,ms))\,\alpha+ cofl\,(Iyy\,(2-3\,\alpha)+lf\,ms\,(lf-lf\,\alpha+lr\,(-1+2\,\alpha))))\Big)+(lf+lr)^2\,(cof2\,ksl\,(-1+\alpha)+cofl\,ks2\,(-1+\alpha)-(con2\,ksl+conl\,ks2)\,\alpha)\,\Big((cof2-con2)^2\,Iyy\,ksl\,(lf+lr)^2\,ms\,\alpha^2-ks2\,\Big(-2\,Iyy\,ms\,(2\,Iyy\,ksl+ksl\,lf\,(lf-lr)\,ms-(cof2-con2)\,(lf+lr)^2\,\alpha\,(cofl\,(-1+\alpha)-conl\,\alpha))+((conl\,(3\,Iyy+lf\,(lf-2\,lr)\,ms)+cof2\,(Iyy+lr^2\,ms)-con2\,(Iyy+lr^2\,ms))\,\alpha+ cofl\,(Iyy\,(2-3\,\alpha)+lf\,ms\,(lf-lf\,\alpha+lr\,(-1+2\,\alpha))))^2\Big)\Big)\Big)\Big/ \Big(ks2\,(lf+lr)^2\,\Big(Iyy\,(lf+lr)^2\,ms\,(cof2\,ksl\,(-1+\alpha)+cofl\,ks2\,(-1+\alpha)-(con2\,ksl+conl\,ks2)\,\alpha)^2+ksl\,ks2\,(cofl\,(Iyy+lf^2\,ms)\,(-1+\alpha)+cof2\,(Iyy+lr^2\,ms)\,(-1+\alpha)-(conl\,Iyy+con2\,Iyy+conl\,lf^2\,ms+con2\,lr^2\,ms)\,\alpha)^2+ (cof2\,ksl\,(-1+\alpha)+cofl\,ks2\,(-1+\alpha)-(con2\,ksl+conl\,ks2)\,\alpha)\,(-cofl\,(Iyy+lf^2\,ms)\,(-1+\alpha)-cof2\,(Iyy+lr^2\,ms)\,(-1+\alpha)+(conl\,Iyy+con2\,Iyy+conl\,lf^2\,ms+con2\,lr^2\,ms)\,\alpha)\,(Iyy\,(ksl+ks2)+ksl\,lf^2\,ms+ks2\,lr^2\,ms+cof2\,conl\,lf^2\,\alpha+2\,cof2\,conl\,lf\,lr\,\alpha+ cof2\,conl\,lr^2\,\alpha-cof2\,conl\,lf^2\,\alpha^2+conl\,con2\,lf^2\,\alpha^2-2\,cof2\,conl\,lf\,lr\,\alpha^2+2\,conl\,con2\,lf\,lr\,\alpha^2- cof2\,conl\,lr^2\,\alpha^2+conl\,con2\,lr^2\,\alpha^2+cofl\,(lf+lr)^2\,(-1+\alpha)\,(cof2\,(-1+\alpha)-con2\,\alpha))\Big)\Big)$$

APPENDIX D

VITA

Sany Izan Ihsan was born in Kuching, in the state of Sarawak, Malaysia on November 9th, 1971. His parents are Mr. Ihsan Hj. Awang and Mrs. Aisah Abdullah.

He attended primary and secondary school at Sek. Men. Raja Ali (SEMERA) in Kuala Lumpur, Malaysia and high school in Shah Alam, Malaysia under a special preparatory program to pursue his study abroad. He obtained his Bachelor of Science degree in Mechanical Engineering from the University of Wisconsin at Madison on May 1995 and received his Master of Science degree in Aerospace Engineering from the University of Tennessee Space Institute, Tullahoma, USA in May 1999. In September 2003 he joined the International Islamic University Malaysia (IIUM) for PhD program.

He has joined the International Islamic University Malaysia as an assistant lecturer in January 1996 and currently holding a lecturer position on study leave.

He is married to Mrs. Suriza Ahmad Zabidi and they are currently blessed with four children – Muhammad (11), Zubair (10), Muaz (7) and Sofwan (4).